IOWA STATE UNIVERSITY
Digital Repository

1968

A mechanistic investigation of the photochemistry of 4,4-dimethyl-2-cyclohexenone

Tad Harbison Koch

Iowa State University

KOCH, Tad Harbison, 1943-
A MECHANISTIC INVESTIGATION OF THE
PHOTOCHEMISTRY OF 4,4-DIMETHYL-2-
CYCLOHEXENONE.

Iowa State University, Ph.D., 1968
Chemistry, organic

A MECHANISTIC INVESTIGATION OF THE

PHOTOCHEMISTRY OF 4,4-DIMETHYL-2-CYCLOHEXENONE

by

Tad Harbison Koch

A Dissertation Submitted to the

Graduate Faculty in Partial Fulfillment of

The Requirements for the Degree of

DOCTOR OF PHILOSOPHY

Major Subject: Organic Chemistry

Approved:

In Charge of Major Work

Head of Major Department

Dean of Graduate College

Iowa State University
Of Science and Technology
Ames, Iowa

1968

TABLE OF CONTENTS

LIST OF FIGURES

LIST OF TABLES

VITA

The author was born to Dr. and Mrs. Justin L. Koch in Mt. Vernon, Ohio on January 1, 1943. He graduated from Mt. Vernon High School, valedictorian, in June 1960. After attending Ohio Wesleyan University for one year, he transferred to Ohio State University and continued his undergraduate education majoring in mathematics. In June 1964, he was granted the Bachelor of Science degree, *summa cum laude*. The author entered Iowa State University as a graduate student in organic chemistry in July 1964. Initial research under the supervision of Professor O. L. Chapman led to a publication describing a synthesis of 4,5-trimethylenetropone. Research for this thesis was conducted during the years 1966 to 1968 also under the supervision of Professor O. L. Chapman. During his graduate education, the author was a National Science Foundation Cooperative Fellow from July 1964 to June 1966 and a National Science Foundation Graduate Fellow from July 1966 to June 1968. After receiving the Doctor of Philosophy degree in August 1968, the author continued his academic career as Assistant Professor of Chemistry at the University of Colorado.

We see a little, presume a great deal, and so jump to a conclusion.

John Locke

INTRODUCTION

In his early studies of the photodimerization of 2-cyclopentenone and the photocycloaddition of 2-cyclopentenone to olefins, Eaton (1) emphasized the synthetic utility of the photocycloaddition reaction. The importance of the reaction was elegantly demonstrated by Corey (2) with a three step synthesis of α-carophylene alcohol (I). The initial step of the synthesis was the photoaddition of 3-methyl-2-cyclohexenone to 3,3-dimethylcyclopentene. Three cycloadducts are formed. The *cis-anti-cis* adduct II was the major product (74%) and was used in the synthesis of α-carophylene alcohol (I).
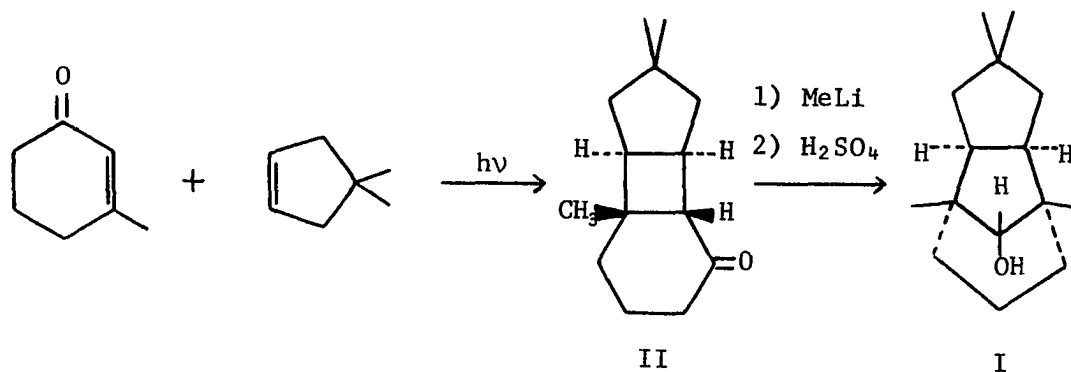
Guthrie *et al.* (3) have employed the photocycloaddition reaction in a synthesis of a precursor of the alkaloid atisine. An important intermediate step in the synthesis was the photocycloaddition of cyclohexenone III to allene yielding the required methylene cyclobutane IV.

III   IV
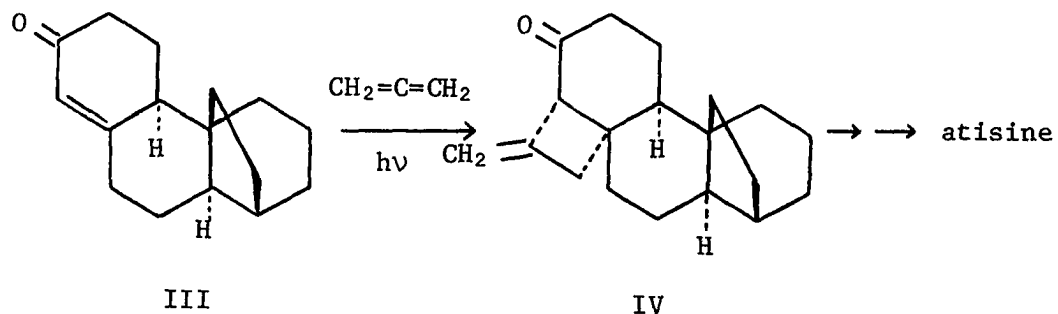
Since photocycloaddition is among the most important photochemical reactions from a synthetic point of view, an investigation of the mechanism was undertaken. In an extensive study of photocycloaddition of α,β-unsaturated cyclic ketones to olefins, Corey and co-workers found that the mode of addition is a complex function of the ketone and the olefin. From their qualitative study, one can often predict the orientation and stereochemistry of the photocycloadducts from the starting ketone and olefin structures. The investigation presented here attempts to quantitatively relate the mode of addition to the electronic nature of the excited ketone.

The system chosen for the investigation was the photocycloaddition of 4,4-dimethyl-2-cyclohexenone to 1,1-dimethoxyethylene. In addition to the photocycloaddition reaction illustrated above, 4,4-dimethyl-2-cyclohexenone also photochemically rearranges, forms oxetanes, and is reduced. Since 4,4-dimethyl-2-cyclohexenone undergoes most of the photoreactions of cyclic α,β-unsaturated ketones, it provides a good example for study.

All four photochemical reactions are initiated by populating the n-π^* singlet state of 4,4-dimethyl-2-cyclohexenone. This study is then concerned with the electronic changes from the n-π^* singlet state taking place before or during reaction. Since one cannot see these changes with the naked eye or even with sophisticated electronic equipment in some cases, the changes are determined indirectly by observing the effect of small environmental changes on the efficiency of product formation.

REVIEW OF LITERATURE

Photochemical Reactions of Some

Pertinent Cyclic α,β-Unsaturated Ketones

The photoreactions of cyclopentenones and cyclohexenones are numerous and complex. They include dimerization, olefin cycloaddition to the double bond, oxetane formation, rearrangement, solvent addition, and, reduction. The electronic and geometric requirements of each reaction are not well understood.

Dimerization

Eaton (1, 4, 5) reports that 2-cyclopentenone (3 M in benzene) photo-dimerizes to give the head-to-head (V) and head-to-tail (VI) *cis-anti-cis* dimers with a quantum yield of 0.27. The ratio of dimeric products (V:VI) is influenced by the concentration of 2-cyclopentenone and solvent. Polar
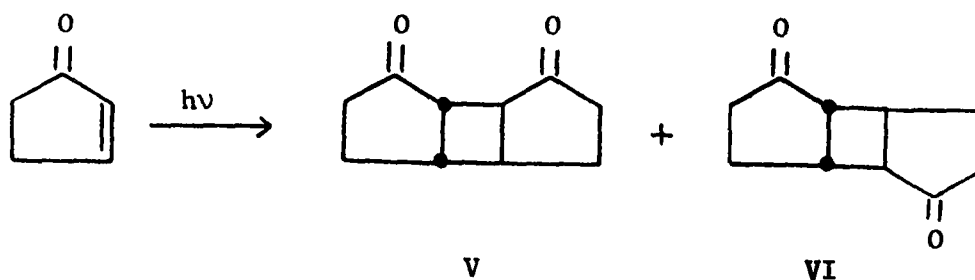
solvents and high concentrations of 2-cyclopentenone favor formation of the more polar head-to-head dimer (V). The concentration effect is a manifestation of the solvent effect, high concentrations of 2-cyclo-pentenone increasing the polarity of non-polar solvents. Dimerization is

sensitized by xanthone (triplet energy, 74.2 kcal./mole; with xanthone absorbing 91% of the light ϕ_{sens}/ϕ_o = 0.86) and quenched by piperylene giving a linear Stern-Volmer plot (slope, 5.25 ℓ/mole for 3 M 2-cyclopentenone). Eaton concludes that the dimerization arises entirely from a triplet state.

Ruhlen and Leermakers (6, 7) estimate the first triplet state of 2-cyclopentenone to be 61±1 kcal./mole above ground state by a Saltiel plot for *cis*- and *trans*-piperylenes and the photostationary state mixture of *cis*- and *trans*-piperylenes with 2-cyclopentenone as a sensitizer. They observe that the intersystem crossing efficiency, measured with Hammond's triplet counting procedure with *cis*-piperylene, is a function of *cis*-piperylene concentration. Hence, the rate of dimerization must be competitive with energy transfer. This interpretation is consistent with the reactive lifetime of 2-cyclopentenone (5×10^{-10} sec.) calculated from Eaton's Stern-Volmer plot.

Ruhlen and Leermakers (6, 7) find that xanthone (E_T = 74.2 kcal./mole) and acetophenone (E_T = 73.6 kcal./mole) sensitize 2-cyclopentenone dimerization ($\phi_{sens}/\phi_o \sim 1.0$), but benzophenone ($E_T$ = 69 kcal./mole) quenches the reaction by light absorption. P. deMayo and co-workers (8) report a similar observation for the photocycloaddition of 2-cyclopentenone to cyclohexene (*vide infra*).

Hammond and co-workers (9) have studied the photodimerization of 2-cyclohexenone. Four products are reported. Two are identified as the *cis-anti-cis* head-to-head (VII) and the head-to-tail (VIII) dimers. The other two minor products are not identified but are thought to be dimeric by g.l.p.c. retention time.

VII   VIII
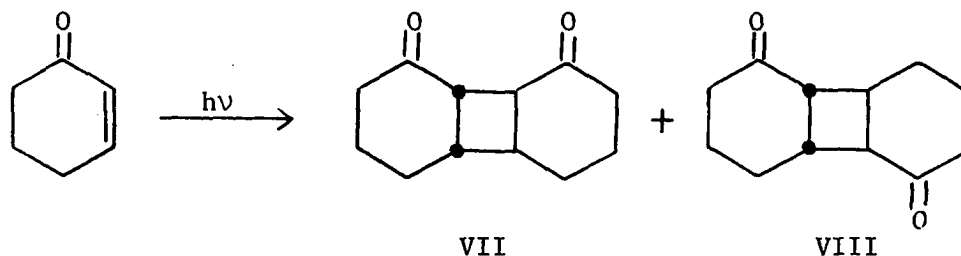
Saltiel plots for sensitized isomerization of stilbenes, 1,2-diphenylpropenes, and 2,3-diphenyl-2-butenes all suggest that the triplet energy of 2-cyclohexenone is 61 ± 1 kcal./mole. The maximum in the n-π^* absorption spectrum places the singlet energy at 85 kcal./mole. Since there is a large singlet triplet energy difference (24 kcal./mole), Hammond believes that the lowest triplet has π-π^* configuration and that there is a higher energy n-π^* triplet above the 61 kcal./mole triplet. Attempts to intercept a high energy triplet with 2,3-diphenyl-2-butene failed.

The ratio of dimers (VII:VIII) and the rate of dimerization are dependent on concentration and solvent. A plot of reciprocal of quantum yield versus reciprocal of 2-cyclohexenone concentration deviates from linearity. Linear extrapolation from high 2-cyclohexenone to low 2-cyclohexenone concentrations yields larger quantum yields than observed experimentally. Again the concentration effect is a manifestation of the solvent effect. Studies of isophorone photodimerization (10) suggest that a plot of reciprocal of quantum yield versus reciprocal of 2-cyclohexenone concentration would probably be linear if a highly polar solvent such as aqueous acetic acid were used (*vide infra*).

The dimerization of 2-cyclohexenone is sensitized by acetophenone (E_T = 73 kcal./mole), benzophenone (E_T = 69 kcal./mole), thioxanthone (E_T = 65.5 kcal./mole), and naphthalene (E_T = 61 kcal./mole). Quenching with piperylene gives a linear Stern-Volmer plot with slope, 13.5 ℓ/mole (1.0 M 2-cyclohexenone, ϕ_o = 0.28). The presence of piperylene had no effect on the dimer composition.

Triplet counting with 2-cyclohexenone as a sensitizer for isomerization of 0.05 M 1,2-diphenylpropenes gives 0.33 for the intersystem crossing efficiency of 2-cyclohexenone. Extrapolation of the plot of reciprocal of quantum yield versus reciprocal of 2-cyclohexenone concentration to infinite 2-cyclohexenone concentration places the magnitude of the intersystem crossing efficiency between 0.5 and 0.8. Hammond was not able to resolve the discrepancy between these two determinations of the intersystem crossing efficiency of 2-cyclohexenone. As with 2-cyclopentenone, the intersystem crossing efficiency measured by the triplet counting technique may be a function of 1,2-diphenylpropene concentration. The triplet lifetime of 2-cyclohexenone is short (7 × 10^{-10} sec.), and Hammond used only 0.05 M 1,2-diphenylpropene. The details of this proposal will be described in the Results and Discussion Section.

Hammond proposes the following one triplet mechanism to account for the formation of all dimers of 2-cyclohexenone.

$$K + h\nu \longrightarrow {}^1K^*$$
$${}^1K^* \longrightarrow {}^3K^*$$
$${}^3K^* \longrightarrow K$$
$${}^1K^* \longrightarrow K$$
$${}^3K^* + K \xrightarrow{k_r} KK \text{ (dimers)}$$

K ≡
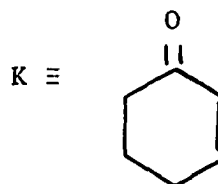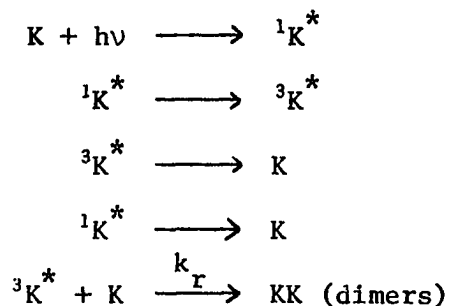
He concludes that k_r, the rate constant for dimerization, must be solvent dependent.

Chapman *et al.* (10) have investigated the photodimerization of isophorone (IX). Irradiation of isophorone (IX) yields three dimers, a *cis-cis* head-to-head dimer (X) and the *cis-syn-cis* (XI) and *cis-anti-cis* (XII) head-to-tail dimers. The product composition is strongly dependent
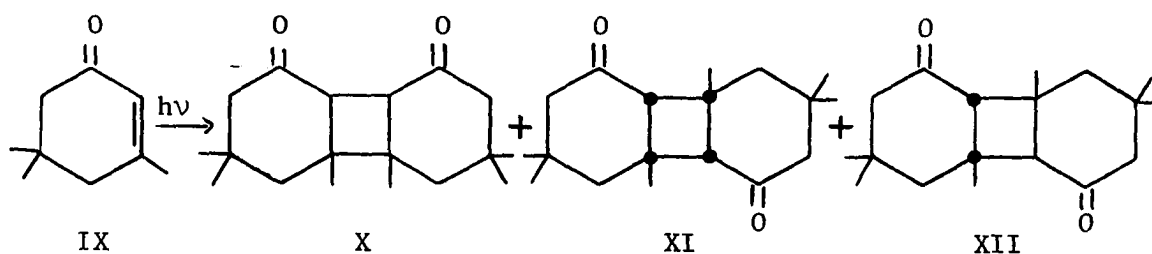
on solvent, polar solvents favoring head-to-head dimerization. Plots of reciprocal of quantum yield versus reciprocal of isophorone concentration in acetic acid are linear for formation of the head-to-head (X) and the two head-to-tail dimers (XI and XII). Quenching by isoprene and ferric acetonyl acetonate gives linear Stern-Volmer plots with slopes 143 and 1170 ℓ/mole, respectively. All dimers are quenched equally by both quenchers. Benzophenone absorbing 32% of the light sensitizes formation of head-to-head dimer (X) 40% more than the head-to-tail dimers (XI and XII), ϕ_{sens}/ϕ_o = 3.43 and 2.40, respectively.

With this data in mind Chapman and Trecker propose the following minimum mechanism.

$$K + h\nu \longrightarrow K^* \qquad \phi_{ic} = 0.04$$

$$K + h\nu \longrightarrow K^{1*} \qquad \phi_{ic} = 0.29$$

$$K^* \xrightarrow{k_d} K \qquad k_d = 5.7 \times 10^6 \text{ sec}^{-1}$$

$$K^{1*} \xrightarrow{k_d'} K \qquad k_d' = 4.9 \times 10^6 \text{ sec}^{-1}$$

$$K^* + K \xrightarrow{k_r} \text{head to tail dimers (XI and XII)}$$

$$k_r = 7.6 \times 10^5 \text{ } \ell/\text{mole}/\text{sec}$$

$$[\text{Isophorone}] = 1.0 \text{ M}$$

$$K^{1*} + K \xrightarrow{k_r'} \text{head to head dimer (X)}$$

$$k_r' = 1.5 \times 10^6 \text{ } \ell/\text{mole}/\text{sec}$$

$$[\text{Isophorone}] = 1.0 \text{ M}$$

K ≡
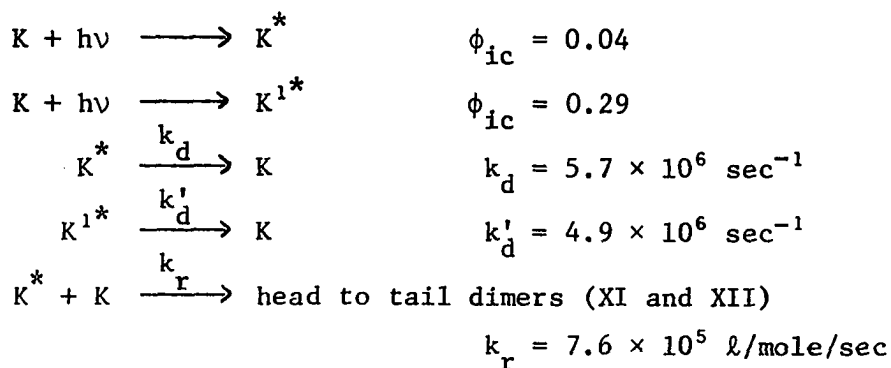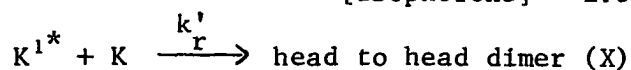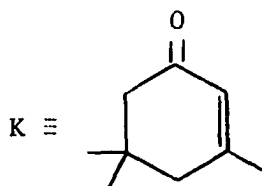
The two reactive states K^* and K'^* are triplets of unspecified con-figuration and geometry. The rate constants and intersystem crossing efficiencies (ϕ_{ic} and ϕ_{ic}') were calculated from the slope of the ferric acetonyl acetonate Stern-Volmer plot and the plots of reciprocal of quantum yield versus reciprocal of isophorone concentration.

Yates and co-workers (11, 12) have recently reported that 3-phenyl, 3-p-anisyl, and 3-p-nitrophenyl-2-cyclohexenones photodimerize to give only the *cis-anti-cis* head to head dimer (XIII).
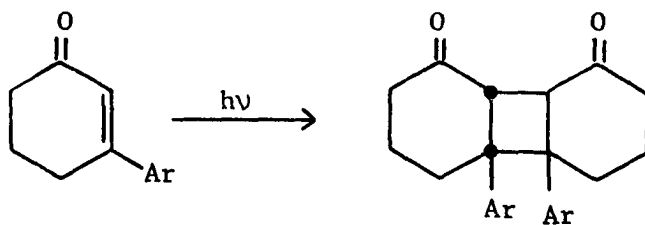
XIII

(-) Piperitone (XIV) photodimerizes to give three head-to-head photodimers, one of which has at least one *trans* ring junction (13). The complete stereochemistry has been established for only one of the dimers (XV).

XIV   XV
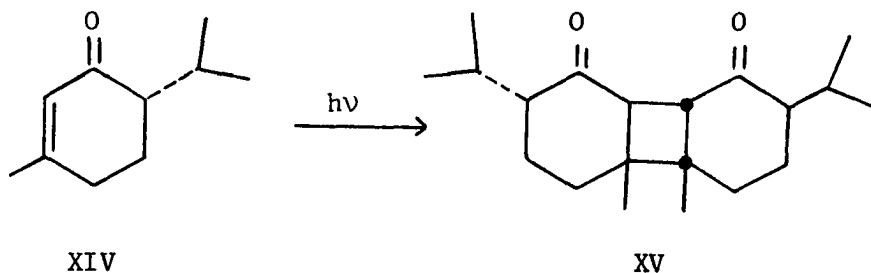
Olefin cycloaddition

Corey *et al.* (14) qualitatively examined the photoaddition of excited α,β-unsaturated cyclic ketones to determine the mode of addition as a function of ketone and olefin structure.

2-Cyclohexenone cleanly adds to 1,1-dimethoxyethylene to give *cis*- and *trans*-7,7-dimethoxybicyclo[4.2.0]octan-2-ones (XVI and XVII) in 21 and 49% yields, respectively. Benzyl vinyl ether, methyl vinyl ether, and

XVI   XVII
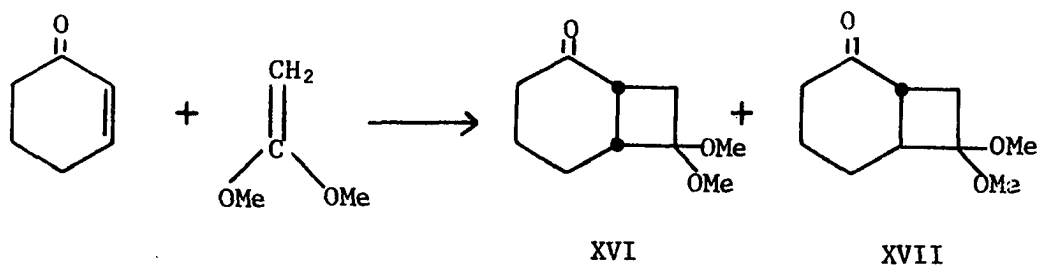
vinyl acetate also add to excited 2-cyclohexenone to give *cis*- and *trans*-7-substituted bicyclo[4.2.0]octan-2-ones. 2-Cyclohexenone reacts with isobutylene with less orientational specificity, yielding 6.5% *cis*-7,7-dimethylbicyclo[4.2.0]octan-2-one (XVIII), 26.5% *trans*-7,7-dimethylbicyclo-[4.2.0]octan-2-one (XIX), 6% 8,8-dimethylbicyclo[4.2.0]octan-2-one (XX), 2-(β-methylallyl)-cyclohexanone (XXI), and 3-(β-methylallyl)-cyclohexanone (XXII).
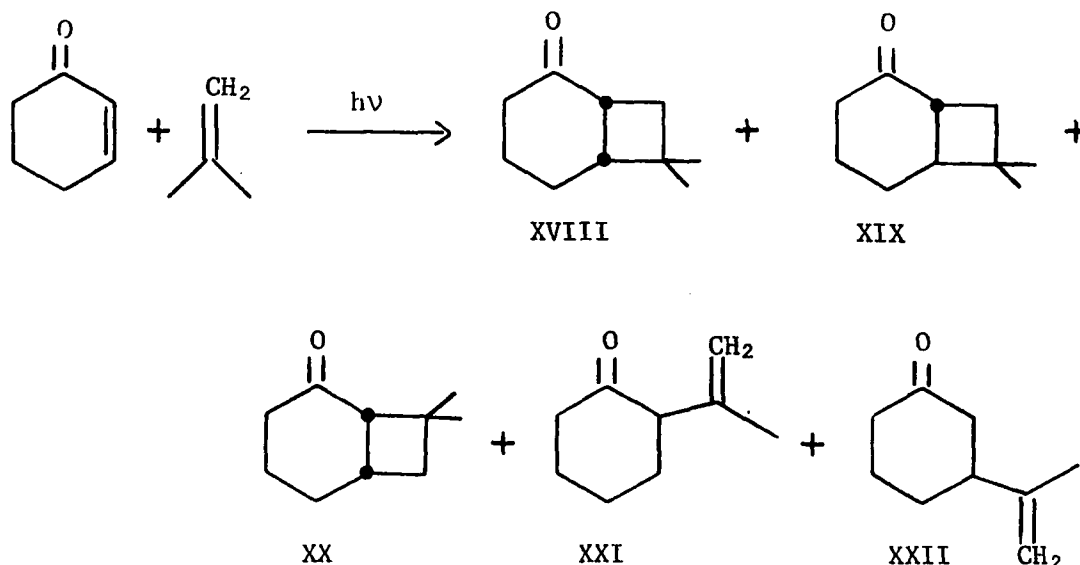
Some olefins add to excited 2-cyclohexenones to give predominantly the 8-substituted bicyclo[4.2.0]octan-2-ones. Allene reacts to give a 55% yield of 8-methylenebicyclo[4.2.0]octan-2-one (XXIII) and acrylonitrile gives predominantly 8-cyanobicyclo[4.2.0]octan-2-ones (XXIV). In all cases in which the 8-substituted product is formed, the bridgehead stereochemistry is *cis*.
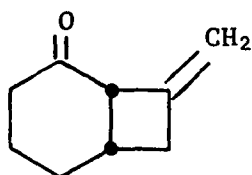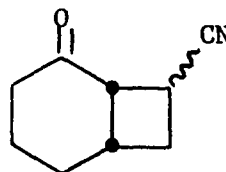
XXIII   XXIV

The order of reactivities of various substituted olefins with

2-cyclohexenones is given by 1,1-dimethoxyethylene >> methoxyethylene >

cyclopentene > allene >> acrylonitrile. Electron rich 1,1-dimethoxy-

ethylene adds about twenty times faster than allene.

Corey has suggested a general mechanism for the photocycloaddition

of 2-cyclohexenone to olefins.

$$K^* + 0 \rightleftharpoons \text{oriented } \pi \text{ complex} \rightleftharpoons \text{diradical}$$
$$[K^{*\delta-} \quad 0^{\delta+}]$$

cycloaddition product
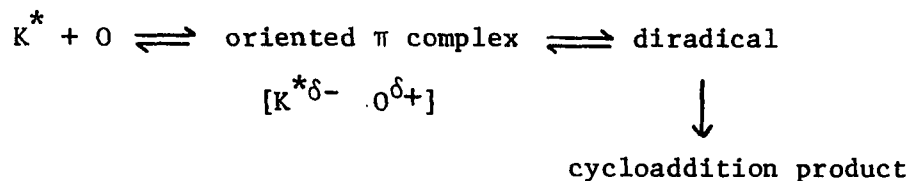
In this mechanism orientational specificity and reactivity are thought

to be governed by complex formation and stereochemistry is thought to be

controlled by closure of the diradical. The mechanism is illustrated as

follows with 2-cyclohexenone reacting with 1,1-dimethoxyethylene.

XXV

XXVI   XXVII   XVI   XVII
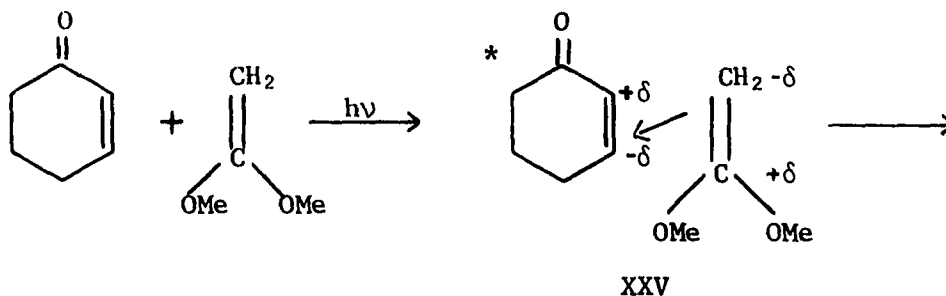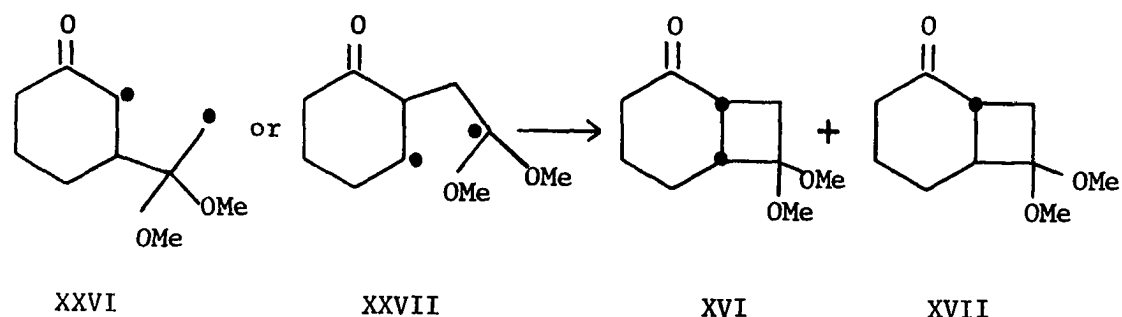
The complex XXV is a four-center π-complex of 2-cyclohexenone in its

n-π* state and 1,1-dimethoxyethylene in its ground state. The complex

undergoes bond formation to give either biradical XXVI or XXVII followed

by ring closure. Corey suggests that *trans*-cycloadducts result from ring

closure of highly energetic biradicals.

The biradical intermediate was proposed to explain formation of open

chain products (XXI and XXII) and the complete lack of stereospecificity

in reaction of *cis*- and *trans*-2-butenes with 2-cyclohexenone. *Cis*- and

trans-2-butenes react with excited 2-cyclohexenone to give the same three

cycloadducts. The n.m.r. and i.r. spectra of the crude irradiation mixtures

in each case were essentially identical. Furthermore, under the reaction

conditions *cis*-2-butene does not isomerize to *trans*-2-butene. Unfortunately,

the adduct structures from this critical experiment are not known.

Irradiation of 3-methylcyclohexenone with isobutylene (14) gives *cis*-

6,8,8-trimethylbicyclo[4.2.0]octan-2-one (XXVIII) as the major product.

Isophorone, however, reacts with 1,1-dimethoxyethylene (15) to give *cis*- and

trans-4,4,6-trimethyl-7,7-dimethoxybicyclo[4.2.0]octan-2-ones (XXIX and XXX)

in the ratio of about 2:1 in benzene. The orientation specificities of

XXVIII

IX   XXIX   XXX
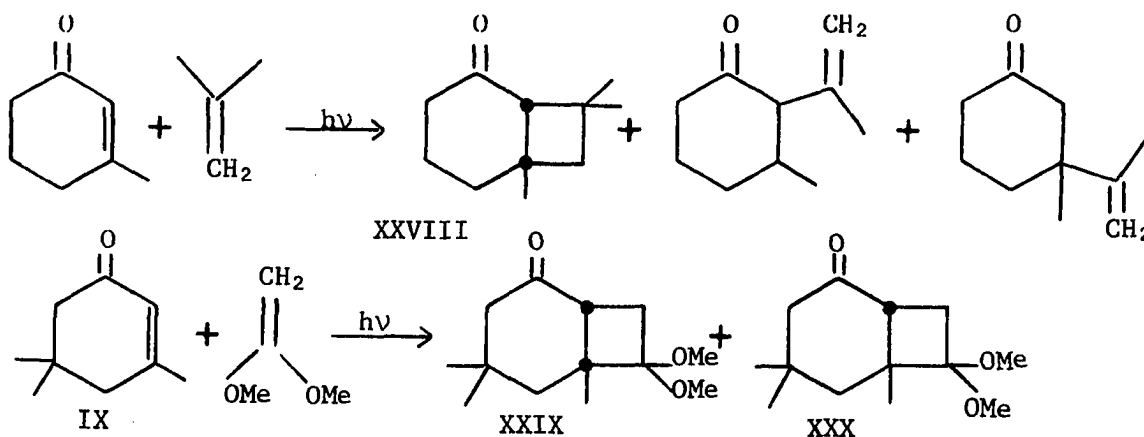
cycloaddition to 3-methyl-2-cyclohexenones can be explained by consideration of both electronic and steric factors in formation of the complex and biradical.

Other ring systems have also been investigated. Excited 2-cyclopentenone reacts with 1,1-dimethoxyethylene (14) to give a single adduct, *cis*-6,6-dimethoxybicyclo[3.2.0]heptan-2-one (XXXI). However, deMayo *et al.* (16) report that two products are formed from the photolysis of 1,1-dimethoxyethylene and 2-cyclopentenone. The structure of the second product is not known. Eaton (17) reports that 2-cyclopentenone adds to allene to give 90% 7-methylenebicyclo[3.2.0]heptane-2-one (XXXII) and 10% 6-methylenebicyclo[3.2.0]heptan-2-one (XXXIII).
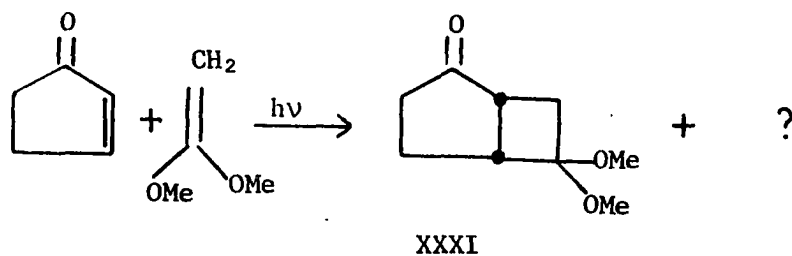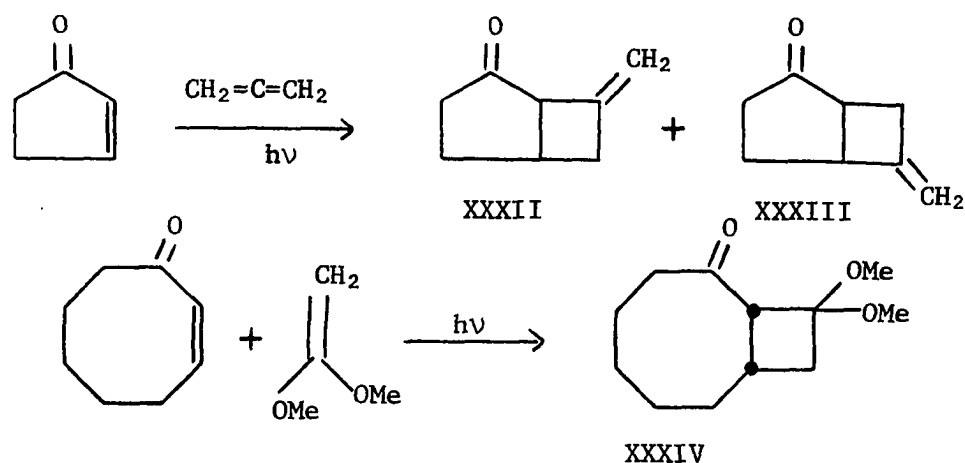
XXXI

Corey finds that 2-cycloheptenone irradiated with 1,1-dimethoxy ethylene

does not lead to isolable quantities of cycloaddition product; however,

2-cyclooctenone gives *cis*-10,10-dimethoxybicyclo[6.2.0]decan-2-one (XXXIV).

The latter reaction is thought to involve ground state addition of 1,1-

dimethoxyethylene to *trans*-2-cyclooctenone. Eaton and Lin (18) have

demonstrated that 2-cyclooctenone undergoes photochemical *cis-trans*

isomerization, and Eaton and Lin (19) and Corey *et al.* (20) have observed

the photochemical *cis-trans* isomerization of 2-cycloheptenone.

T. A. Rettig (21) found that 1,1-diphenylethylene reacts with 4,4-

dimethyl-2-cyclohexenone (XXXV) to give *trans*-5,5-dimethyl-7,7-diphenyl-

bicyclo[4.2.0]octan-2-one (XXXVI). The reaction is not sensitized by

benzophenone or quenched by oxygen, piperylene, or dipivaloyl methane.
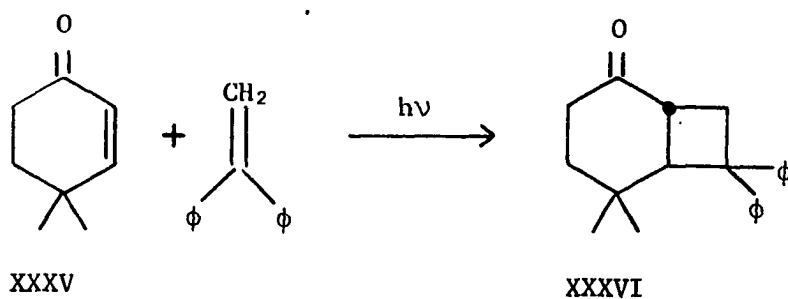
Furthermore, when benzophenone is absorbing all of the light in a sensi-

tization experiment, 4,4-dimethyl-2-cyclohexenone (XXXV) and 1,1-diphenyl-

ethylene in *l*-butyl alcohol are photostable, giving no photoadducts or

rearrangement products (*vide infra*). Rettig concludes that the photo-

cycloaddition occurs from either the n-π^* singlet state of 4,4-dimethyl-

2-cyclohexenone or the π-π^* singlet state of 1,1-diphenylethylene.

Tetramethylethylene adds to excited 4,4-dimethyl-2-cyclohexenone

(XXXV) to give an oxetane (XXXVII) and *trans*-cyclobutane (XXXVIII).[1]

XXXV   XXXVII   XXXVIII
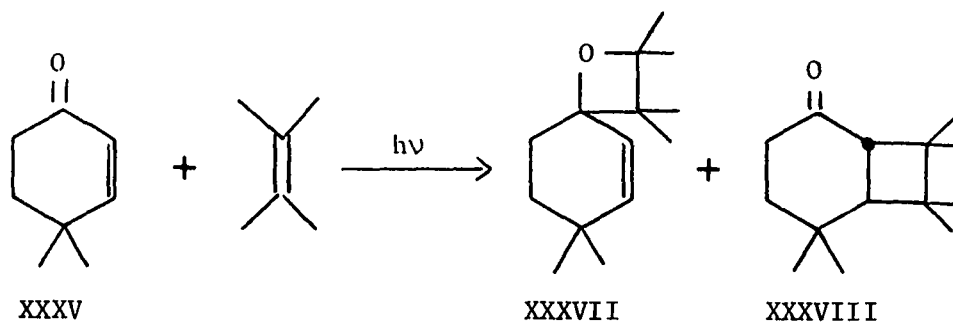
Oxetane formation

Excited ketones and aldehydes often react with olefins to give

oxetanes. The reaction is commonly called the Paterno-Büchi reaction (22, 23,

24). The mechanism is generally thought to involve initial electrophyllic

attack on the olefin by the n-orbital of the ketone or aldehyde in its

n-π^* triplet state. Orientational specificity of addition is controlled

---

[1]O. L. Chapman, P. J. Nelson, and D. Ostrem, Department of Chemistry, Iowa State University of Science and Technology, Ames, Iowa. Private communication. 1968.
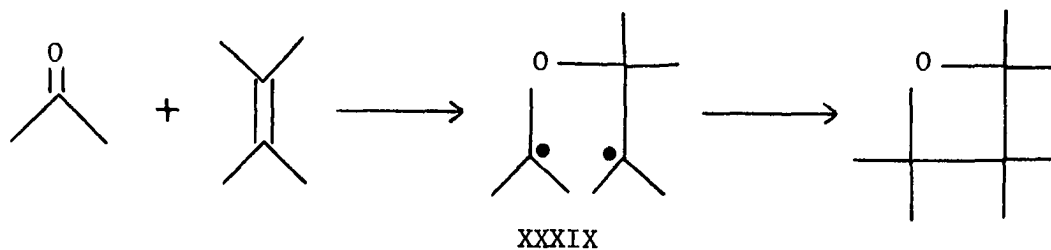
XXXIX

by the stability of the intermediate biradical (Büchi Rule). The biradical

(XXXIX) can cyclize to give oxetane or decompose to starting materials (23,

25) sometimes with isomerization of the olefin (26). Ketones and aldehydes

with lowest π-π^* triplet states do not generally react with olefins to give

oxetanes (24, 27).

Unsaturated ketones sometimes give oxetane products. Patel and

Schuster (28) have shown that irradiation of 4-methyl-4-trichloromethyl-

cyclohexadienone (XL) with isobutylene at low temperature yields among

other products an oxetane (XLI).

XL   XLI
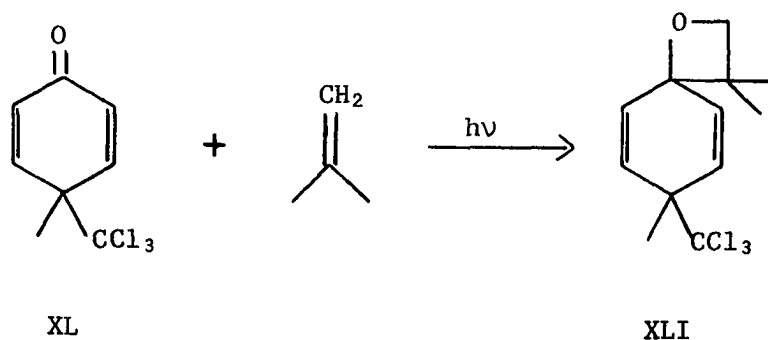
As a result of recent investigations by Yang *et al.* (29, 30) (*vide*

infra) and Turro and co-workers (31), there is some reason to believe that

states other than the n-π^* triplet state are important in the Paterno-Büchi

reaction. Turro observes that electron deficient olefins such as 1,2-di-

cycanoethylene react stereospecifically with excited ketones in their n-π^*

singlet states. The reaction involves a nucleophilic attack by the electron

rich π system of the ketone on the electron poor olefin.

Rearrangement

In t-butyl alcohol 4,4-dimethyl-2-cyclohexenone (XXXV) photo-

rearranges (21, 32) to give 6,6-dimethylbicyclo[3.1.0]hexan-2-one (XLII)

and 3-isopropyl-2-cyclopentenone (XLIII). In acetic acid solution two

additional products are formed, XLIV and XLV. Rearrangement in t-butyl

alcohol is sensitized by benzophenone and quenched by oxygen. Rettig
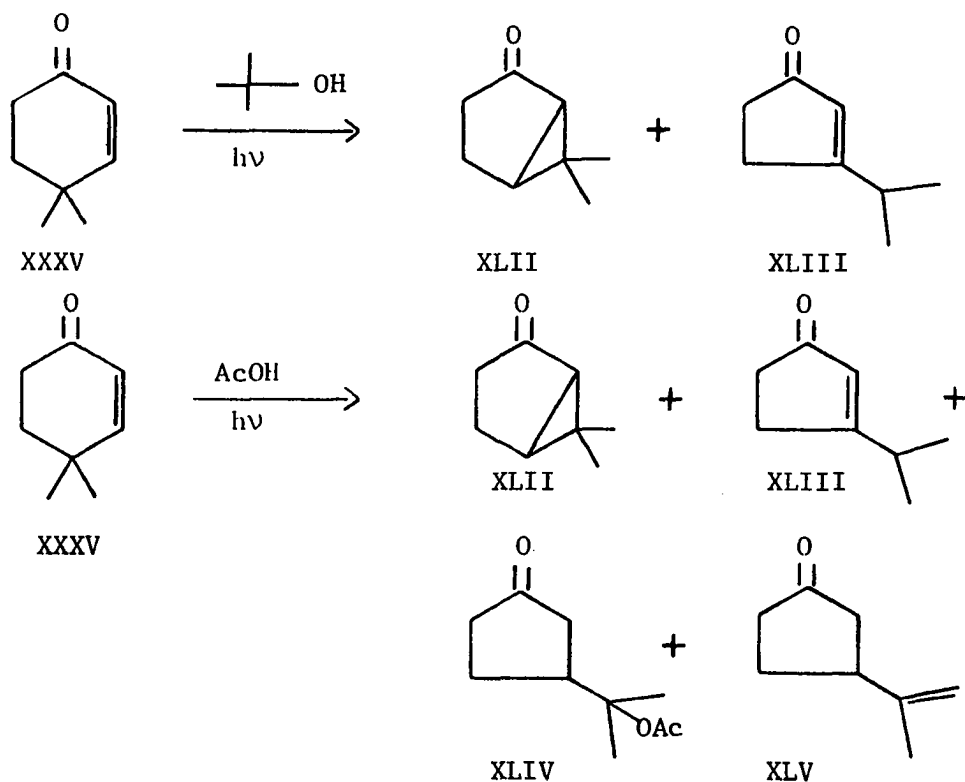
believes that rearrangement in *t*-butyl alcohol results from 4,4-dimethyl-

2-cyclohexenone in the n-π^* singlet state and the lowest triplet state.

Rearrangement from the n-π^* singlet is invoked to account for rearrange-

ment in the presence of 1,1-diphenylethylene which supposedly quenches all

4,4-dimethyl-2-cyclohexenone triplets.

Zimmerman and co-workers have made a comprehensive study of the photo-

rearrangement of 4,4-disubstituted-2-cyclohexenones to establish a general

mechanism. They (33, 34) find that both 4a-methyl-4,4a,9,10-tetrahydro-

2(3H)phenanthrone (XLVI) and $\Delta^{1,9}$-10-methyl-2-octalone (XLVII) rearrange

to lumiproducts XLVIII and XLIX, respectively.

$$\phi = 0.0084$$

XLVI   XLVIII

$$\phi = 0.0038$$

XLVII   XLIX
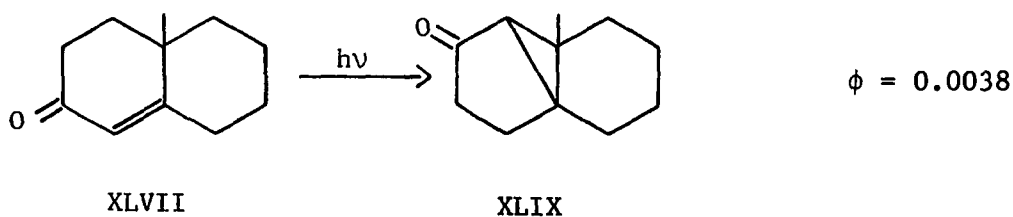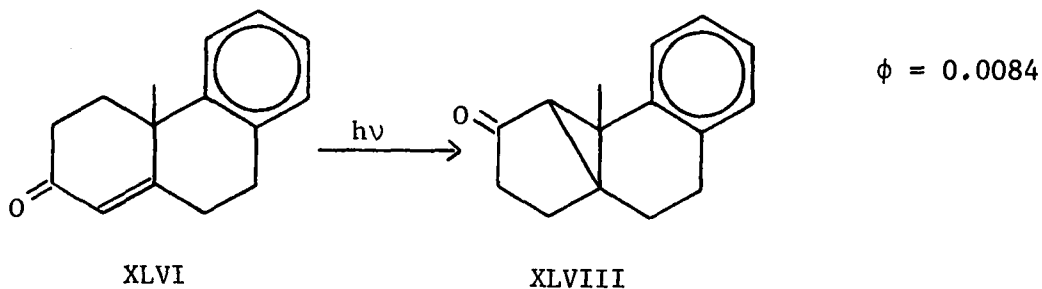
The rearrangements were studied in both benzene and t-butyl alcohol. Solvent appears to have little effect on the quantum efficiencies. In t-butyl alcohol the quantum yield for formation at XLVIII was 0.0084 and for formation of XLIX, 0.0038. Both reactions are sensitized by aceto-phenone giving ϕ_{sens}/ϕ_o equal to 1.0 and 2.0 for rearrangement of XLVI and XLVII, respectively. The rearrangement of phenanthrone (XLVI) in t-butyl alcohol was quenched equally by naphthalene and di-t-butyl nitroxide, both quenchers giving the same linear Stern-Volmer plot (slope, 55 ℓ/mole.

Zimmerman suggests the following kinetic scheme for the rearrange-ment of phenanthrone (XLVI) and octalone (XLVII).

$$K + h\nu \longrightarrow K^* \qquad K \equiv \text{phenanthrone (XLVI)}$$

$$^1K^* \longrightarrow {}^3K^* \qquad \phi_{ic} \quad 1.0$$

$$^3K^* \xrightarrow{k_r} \text{Lumiproduct (XLVIII)} \qquad k_r = 2.9 \times 10^5 \text{ sec}^{-1}$$

$$^3K^* \xrightarrow{k_d'} K \qquad k_d' = 3.9 \times 10^7 \text{ sec}^{-1}$$

$$^3K^* + Q \xrightarrow{k_q} K + Q^* \qquad k_q = 2 \times 10^9 \text{ } \ell/\text{mole/sec}$$
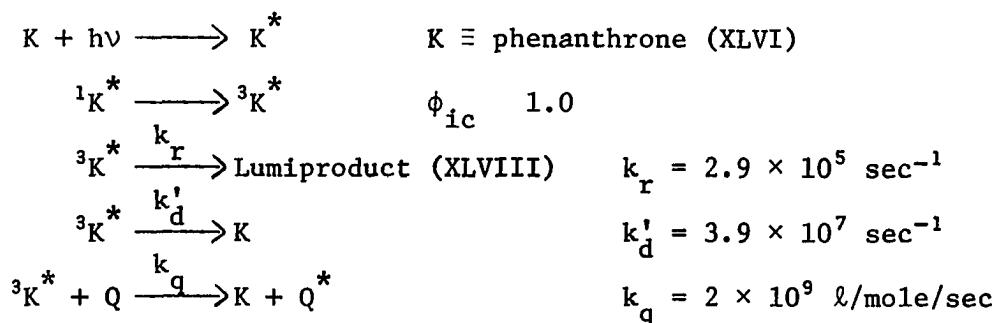
The rate constants were calculated for phenanthrone (XLVI) rearrangement from the slope of the Stern-Volmer plot, the quantum yield, and the assumptions that the intersystem crossing efficiency is unity and the quenching rate is diffusion controlled. The intersystem crossing efficiency is assumed to be unity as a result of the sensitization experiment.

Chapman, Sieja, and Welstead (35) have observed that optically active phenanthrone (XLVI) photorearranges to lumiproduct (XLVII) in t-butyl alcohol with at least 95% retention of optical activity. They conclude that rearrangements of this type must involve a stereospecific 1-10 bond

migration.

Zimmerman (34) feels the rearrangement results from an n-π* or π-π* triplet state. Because of the phosphorescence emission spectrum of the phenanthrone (XLVI), he favors the n-π* state and suggests the following mechanism using the o, •, y notation.

XLVI

XLIX

XLVIII
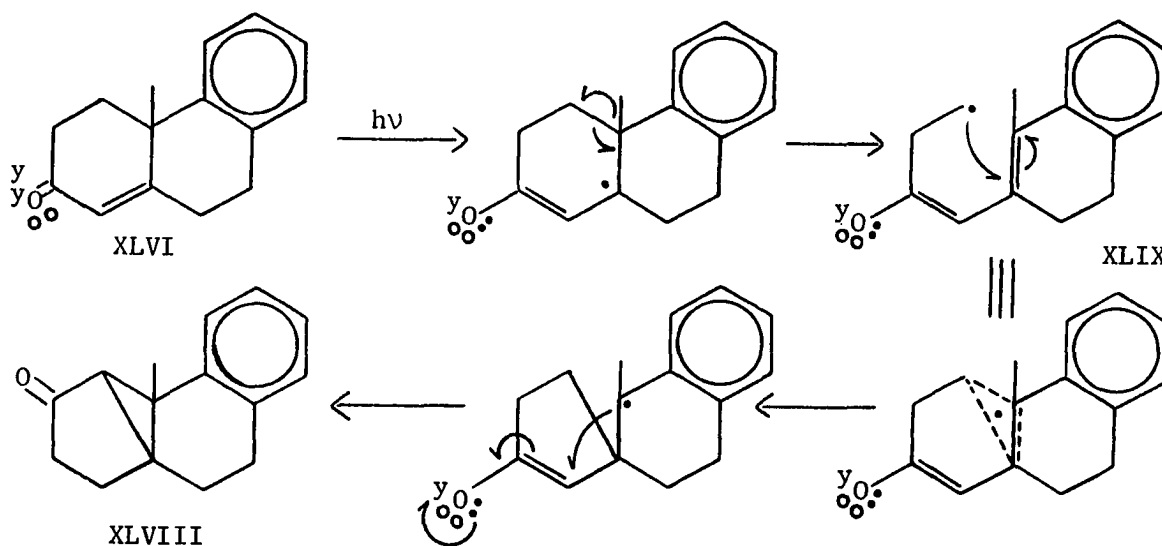
Biradical (XLIX) is pictured as a delocalized π-system to explain the stereospecificity observed by Chapman and co-workers.

Labeling experiments by Zimmerman and Sam (36) demonstrate that 4,5-diphenyl-2-cyclohexenone (L) undergoes 4,5-bond migration upon photolysis. 4,5-Diphenyl-2-cyclohexenone labeled with carbon-14 in position 3 gives 4,6-diphenylbicyclo[3.1.0]hexan-2-one (LI) with carbon-14 in the 5-position. Acetophenone sensitizes formation of both products (LI and LII) without change in product composition. Zimmerman suggests that the mechanism for
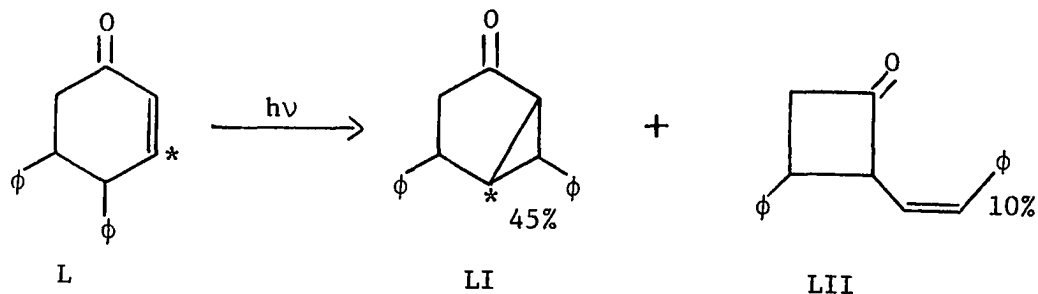
rearrangement of 4,5-diphenyl-2-cyclohexenone (L) is formally the same as proposed for rearrangement of phenanthrone (XLVI). Formation of cyclo-butanone (LII) indicates that the intermediate biradical analogous to XLIX may have more freedom.

In order to gain some idea of the electron distribution in the excited C=C-C=O chromophore, Zimmerman and co-workers studied the photorearrangement of some 4,4-diaryl-substituted 2-cyclohexenones. Irradiation of 4,4-diphenyl-2-cyclohexenone (37) results in phenyl migration yielding *cis*- and *trans*-5,6-diphenylbicyclo[3.1.0]hexan-2-one (LIII and LIV). Photolysis
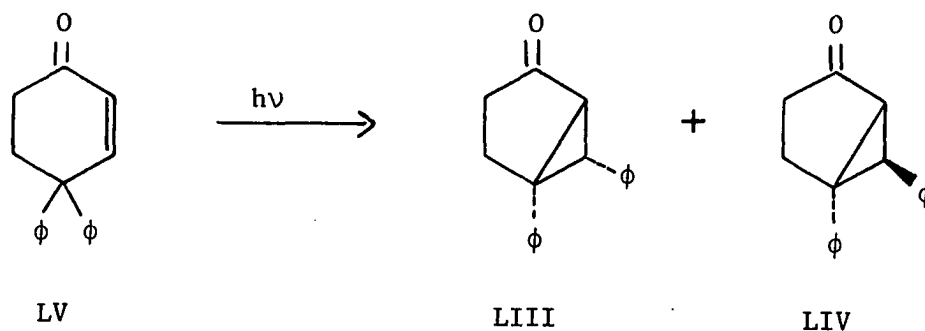
of 4-phenyl-4-p-cyanophenyl-2-cyclohexenone and 4-phenyl-4-p-methoxyphenyl-2-cyclohexenone (38) gives a preferential migration of the substituted

phenyl group (preference factors: 14±2.5 for p-cyanophenyl, 12.5±2.5 for

p-methoxyphenyl). In all aryl migrations the product with *trans* stereo-

chemistry is strongly favored. These migratory aptitudes indicate that
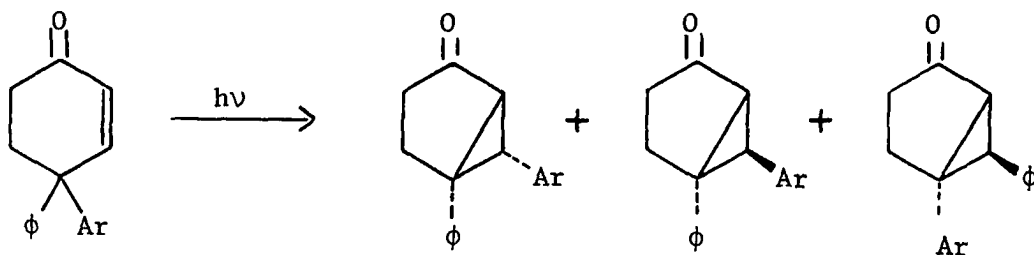
Ar = p-cyanophenyl

= p-methoxyphenyl

the best representation of the excited C=C-C=O chromophore of 4,4-diaryl-

2-cyclohexenones is Ċ-C=C-Ȯ. A positively charged β-carbon would have

favored phenyl migration over p-cyanophenyl migration, and a negatively

charged β-carbon would have favored phenyl migration over p-methoxyphenyl

migration.

Both Zimmerman and Dauben have found that the methylene analogs of

4,4-disubstituted-2-cyclohexenones behave differently. In contrast to

4,4-diphenyl-2-cyclohexenone (LV), the benzophenone sensitized irradiation

of 1-methylene-4,4-diphenylcyclohex-2-ene (39) gives no monomeric products.

However, direct irradiation yields the *cis*- and *trans*-5,6-diphenyl-2-

methylenebicyclo[3.1.0]hexenes (LVI and LVII). The triphenylene sensitized

irradiation of 1-methylene-4,4-dimethylcyclohex-2-ene (40) gives no mono-

meric products. Furthermore, direct irradiation in pentane gives no mono-

meric products. When methanol is used as a solvent in a direct irradiation

LVI   LVII
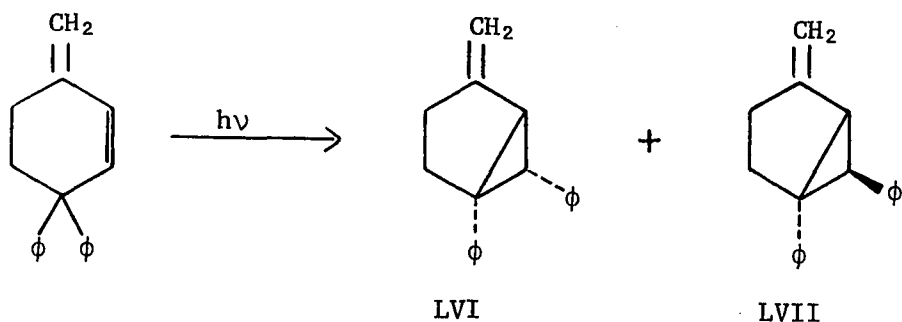
only solvent addition products LVIII and LIX are obtained. Dauben proposes

ground state addition of methanol to an intermediate bicyclobutane (LX).

LX   LVIII   LIX
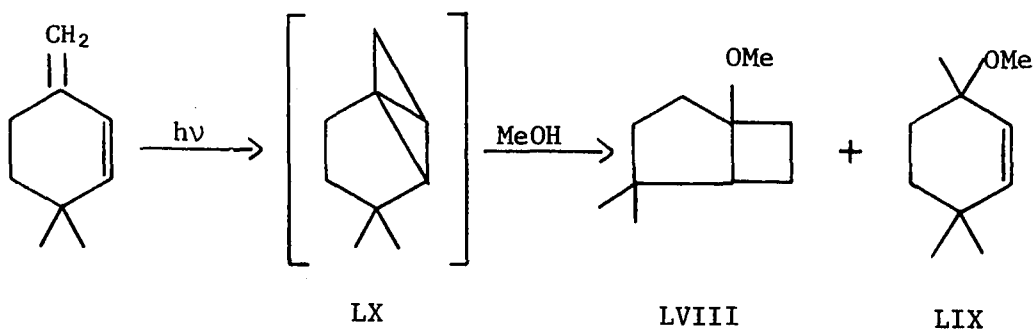
The photochemical reactions of these two dienes result from a $\pi-\pi^*$

state. It is not known whether the rearrangement reactions of the

corresponding enones are $n-\pi^*$ or $\pi-\pi^*$ reactions. Since the photochemical

reactions of these dienes and the corresponding enones are different, the

enone rearrangements may be occurring from an $n-\pi^*$ state. This reasoning

is only suggestive and does not prove the electronic configuration of the

state responsible for enone rearrangements. One must also consider the

electronic differences between dienes and enones. The oxygen atom of the

enone chromophore may provide enough perturbation of the $\pi-\pi^*$ state to

cause the enone rearrangement reactions.

Photoreactions of some α,β-unsaturated ketones with solvent

Irradiation of α,β-unsaturated cyclic ketones in solution often leads to reaction with solvent. Solvent addition by a polar mechanisms as well as free radical reactions to give pinacols, solvent adducts, and double bond reduction have been reported.

Δ^4-Androsten-2-one (LXI) when irradiated in hexane (41) gives pinacol formation (LXII) in addition to lumiandrostenone (LXIII).

LXI   LXII   LXIII
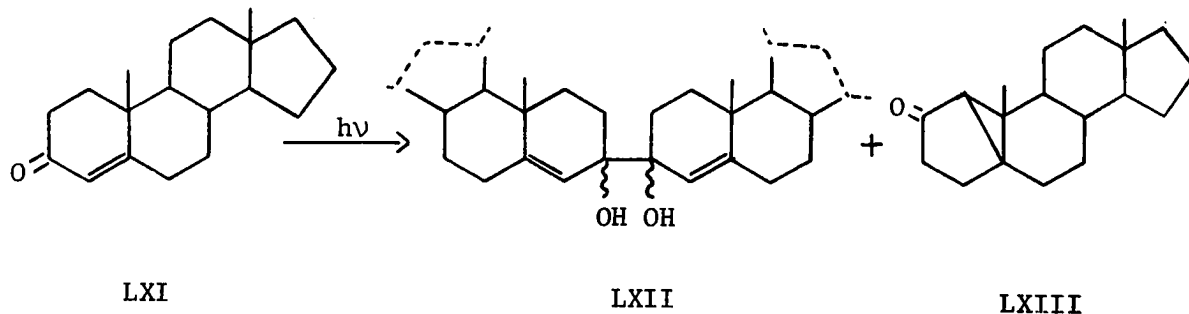
Jeger and co-workers (42) report that irradiation of testosterone (LXIV) in ether solution yields 2% cyclobutane type dimer, 30% pinacols (LXV), and 15% of two diethyl ether solvent adducts.

LXIV   LXV

+ ether adducts
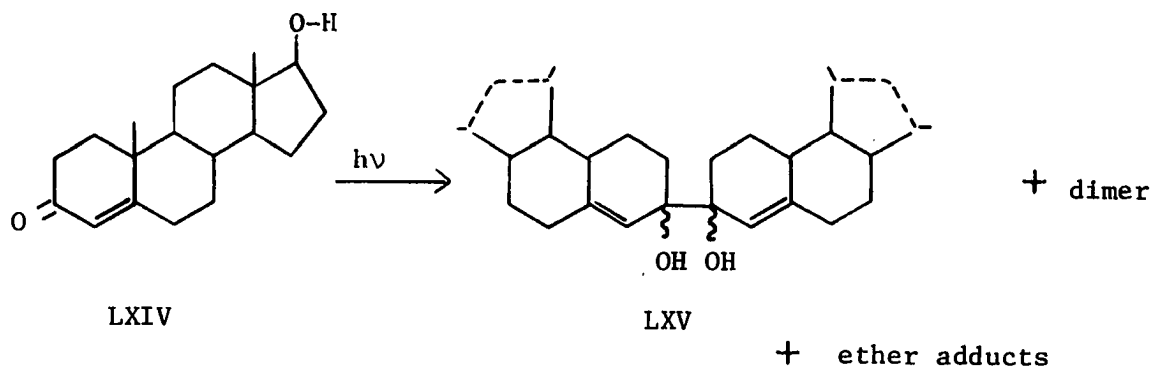
In isopropyl alcohol photolysis of phenanthrone (XLVI)(33) yields

pinacol (LXVI) and lumi product (XLVIII) in the ratio of 1 to 5. Zimmerman
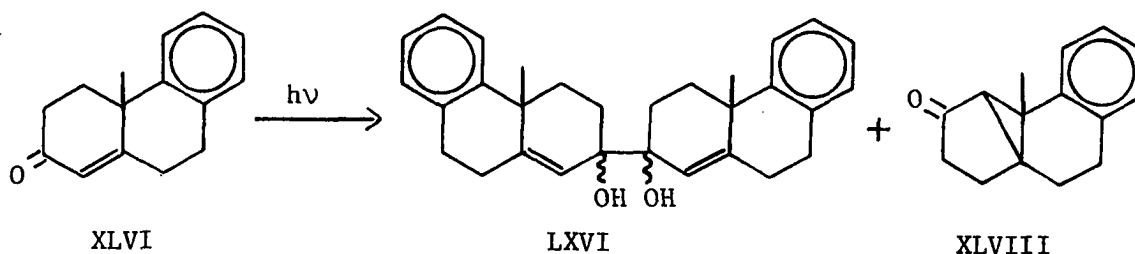
estimates the bimolecular rate constant for hydrogen abstraction from

isopropyl alcohol to be 3×10^3 ℓ/mole/sec, about 100 times smaller than

the rate constant for hydrogen abstraction by acetophenone.

Pfau and co-workers (43) report that irradiation of 2-cyclopentenone

in isopropyl alcohol in the presence of benzophenone gives an isopropyl

alcohol solvent adduct (LXVII); where as isophorone (IX) under the same

conditions yields an adduct with benzophenone (LXVIII). Irradiation of

4,4-dimethyl-2-cyclohexenone (XXXV) in isopropyl alcohol in the presence

of benzophenone gave neither product.
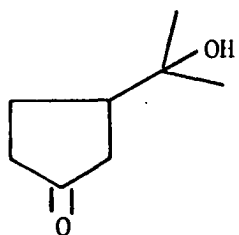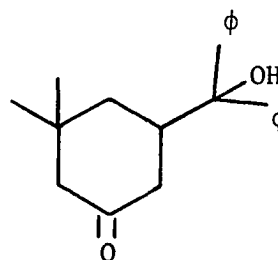
In contrast Chapman *et al.* (10) report that isophorone (IX) in addition to dimerizing (*vide supra*) photoreduces to 3,3,5-trimethylcyclo-hexanone in nonpolar, hydrogen donating solvents. No reduction products were detected in polar, protic solvents including isopropyl alcohol.

Leermakers and Ruhlen (7) find that 2-cyclopentenone forms a solvent addition product (LXIX) when irradiated in cyclohexane. Acetophenone sensitizes formation of the solvent adduct with ϕ_{sens}/ϕ_o equal to about 9.0 for 0.12 M 2-cyclopentenone in cyclohexane.

LXIX
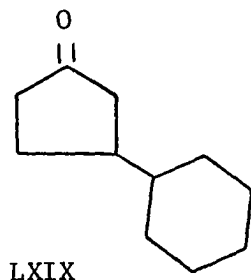
Irradiation of 3β-acetoxypregna-5,16-dien-20-one (LXX) in methyl, ethyl, isopropyl, and cyclohexyl alcohols (44, 45) gives double bond reduction of LXX and solvent adduct formation. In methyl alcohol the yield

LXX
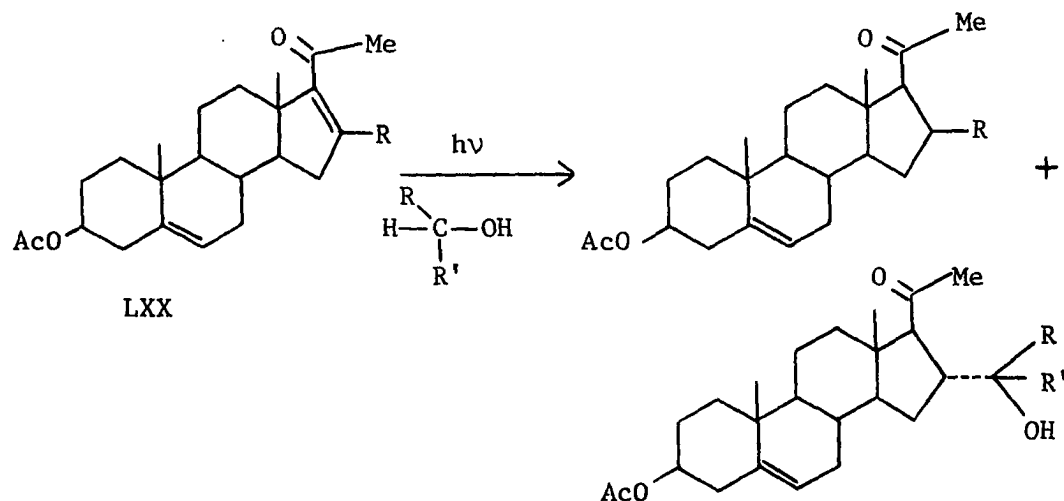
of solvent adduct was very low. Photolysis of 7,11-didehydrohecogenin acetate (LXXI) in ethyl alcohol or dioxane (44,45) gives strictly double bond reduction. No substantial change in the yields of products resulted
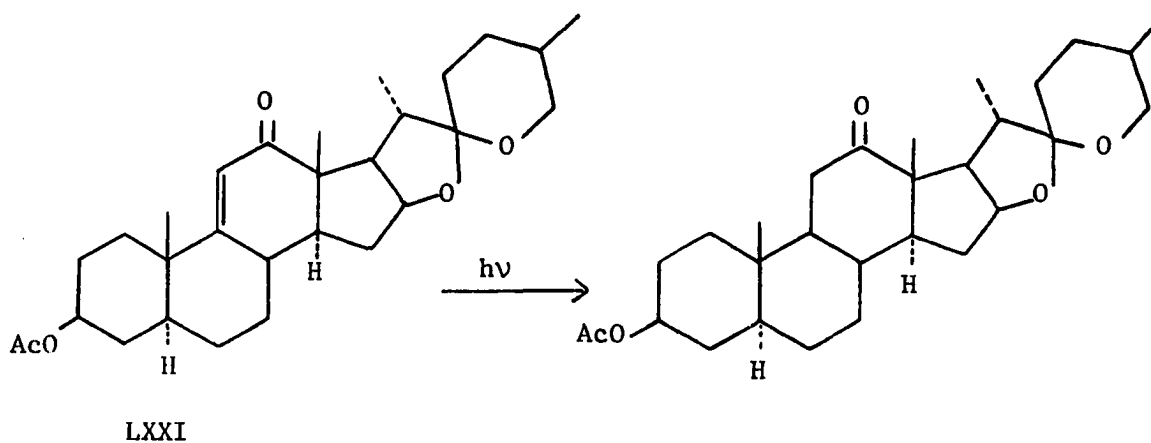
LXXI

from the inclusion of benzophenone in the irradiation of either LXX or LXXI.

Matsuura and Ogura (46) have found that irradiation of Pummerer's ketone (LXXII) in methyl alcohol gives an adduct (LXXIII) in 79% yield. In less acidic isopropyl alcohol the yield is only 37%. Rearrangement to LXXIV accounts for the remainder of the reaction in each case.

LXXII   LXXIII   LXXIV
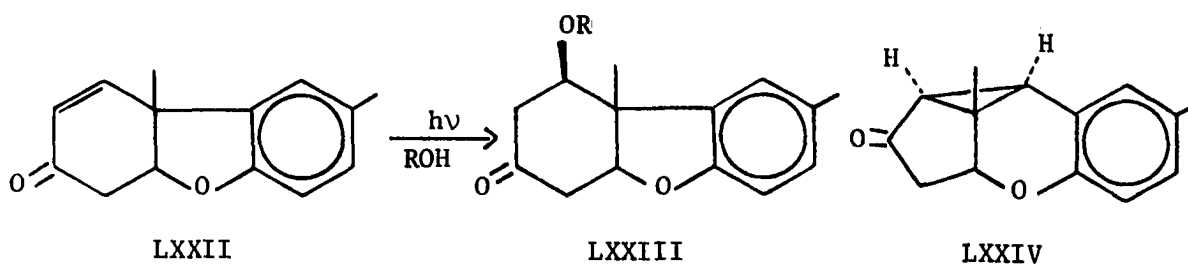
Irradiation of phenanthrone (XLVI) in aqueous acetic acid (75%)

gives, in addition to lumiproduct (XLVIII), two new primary photoproducts

(LXXV and LXXVI) in 1 and 3% yield, respectively.
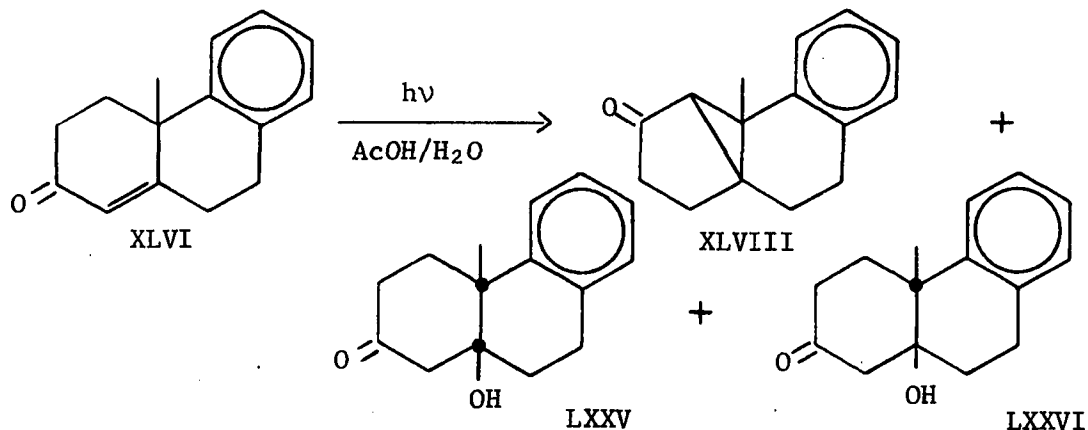
Photolysis of 1-acetylcyclohexene (47) in methyl, ethyl, and *t*-butyl

alcohols yields the *cis*- and *trans*-alkoxides (LXXVII and LXXVIII). The

cis-alkoxide is always the predominant product. The reaction is not

quenched by oxygen or piperylene but is sensitized by acetophenone. The
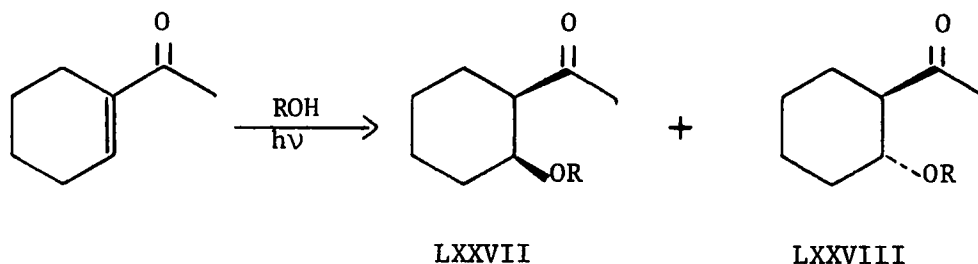
sensitization and quenching results are reminescent of *cis-trans*

isomerization.

Nozaki *et al.* (48) report that 2-cycloheptenone undergoes solvent

addition to give an ether adduct (LXXIX) upon photolysis in methyl, ethyl,

isopropyl and *t*-butyl alcohols. Dimers are also products in the less

acidic solvents. The solvent adduct probably results from ground state

addition of solvent to *trans*-2-cycloheptenone.

LXXIX
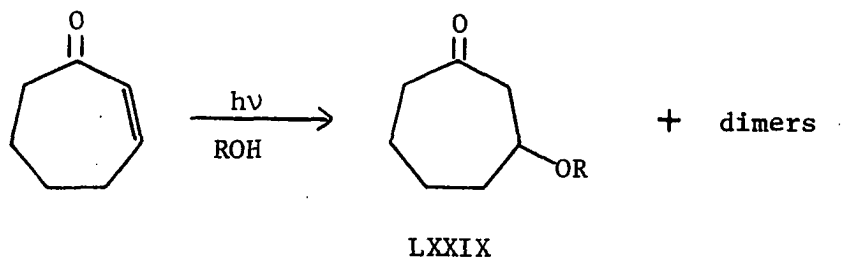
Chapman and Barber[1] have shown that excited $\Delta^{1,7}$-bicyclo[5.3.0]decen-

2-one does not add methanol.
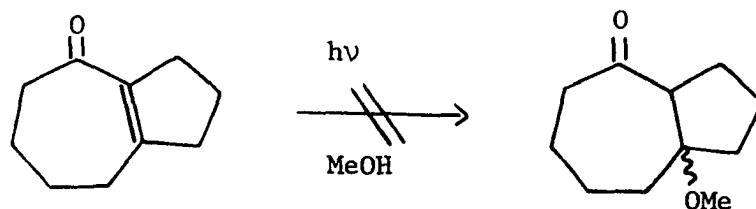
In this case *cis-trans* isomerization of the double bond is sterically

forbidden.

_____

[1]O. L. Chapman and L. L. Barber, Department of Chemistry, Iowa State University of Science and Technology, Ames, Iowa. Private communication. 1968.

Recent Reports of Photochemical Processes

Resulting from Upper Excited States

A number of research groups have recently reported evidence
indicating that upper excited states may be important in energy transfer
and in several non-dissociative photochemical reactions. Upper excited
states are defined as singlet states above the first excited singlet state
(S_2, S_3, etc.) and triplet states above the first excited triplet state
(T_2, T_3, etc.). Non-dissociative photochemical reactions from upper
excited states was previously thought to be improbable if not impossible
because of very short lifetimes. Reactions from upper excited states have
to compete with internal conversion. The rates of internal conversion
from S_2, S_3, S_4, etc. to S_1 are known to be of the order of 10^{11} to 10^{13}
sec.$^{-1}$(49).

DeMayo *et al.* (16, 50) have recently looked at the mechanism of
photoaddition of 2-cyclopentenone to olefins, especially cyclohexene.
2-Cyclopentenone adds to cyclohexene to give four photoproducts, at least
one is presumed to be a cyclobutane type adduct. The actual structures
of the adducts have not been established. The quantum yield of formation
in neat cyclohexene is 0.49.

Other neat olefins including cyclopentene, *cis*-dichloroethylene,
trans-3-hexene, and 1,1-dimethoxyethylene react with excited 2-cyclo-
pentenone to give photoadducts with quantum yields at 0.32, 0.24, 0.22,
and 0.34, respectively. It is interesting to contrast the reactivity of
2-cyclopentenone with the reactivity of 2-cyclohexenone toward various
olefins. 2-Cyclohexenone reacts with 1,1-dimethoxyethylene 20 times

faster than with isobutylene. 2-Cyclopentenone, however, reacts with most olefins at about the same rate. Like 2-cyclohexenone, 2-cyclopentenone does not add stereospecifically to *cis*- and *trans*-olefins.

Cycloaddition to cyclohexene was quenched by acenaphthene giving a linear Stern-Volmer plot (slope, 11.1 ℓ/mole for 2.2 M cyclohexene). The slope of the Stern-Volmer plot indicates that the reactive lifetime is 1.1×10^{-9} sec.

Sensitizers with triplet energies of 71.2 kcal./mole or greater sensitize the photoaddition of 2-cyclopentenone to cyclohexene. Benzophenone (triplet energy, 69 kcal./mole) does not sensitize photoaddition but does sensitize isopropyl alcohol solvent addition (*vide infra*). DeMayo *et al.* propose that photoaddition to olefins results from the second triplet state T_2 and solvent addition comes from the first triplet state T_1.

To substantiate that excited benzophenone transfers energy to 2-cyclopentenone, deMayo and co-workers have shown that 2-cyclopentenone quenches benzophenone photoreduction at close to a diffusion controlled rate. The quenching data is represented by a linear Stern-Volmer plot.

Using the triplet counting procedure for 2-cyclopentenone with *trans*-piperylene as the acceptor, deMay *et al.* find that the measured intersystem crossing efficiency of 2-cyclopentenone is a function of piperylene concentration. This observation is also reported by Ruhlen and Leermakers (7). An intersystem crossing efficiency close to unity is found in neat piperylene. The triplet counting experiment indicates that the rate of decay of reactive triplet is competitive with the rate of energy transfer to *trans*-piperylene. If energy transfer occurs at a diffusion controlled rate, then the rate constant for triplet decay must be very large.

The quantum yield for photoaddition of 2-cyclopentenone to cyclo-hexene is independent of cyclohexene concentration over a range from 10 M to 0.16 M. A plot of reciprocal of quantum yield versus reciprocal of olefin concentration has almost zero slop (less than 0.02 ℓ/mole) and intercept 2.1. A similar plot for photoaddition of 2-cyclopentenone to *trans*-2-hexene has slope 0.57 ℓ/mole and intercept 4.8. A simple bi-molecular mechanism involving triplet 2-cyclopentenone demands that both intercepts be the same. DeMayo *et al.* invoke a rather vaguely defined complex formation to explain the intercept discrepancy and concentration data.

A mechanism consistent with deMayo's data for the addition of excited 2-cyclopentenone to olefins is as follows, where $^3K_1^*$ and $^3K_2^*$ represent the first and second triplet states of 2-cyclopentenone.

$$K + h\nu \longrightarrow {}^1K^*$$

$$^1K^* \longrightarrow {}^3K_2^* \quad \phi_{ic}$$

$$^3K_2^* \xrightarrow{k_d} {}^3K_1^*$$

$$^3K_1^* + \text{isopropanol} \longrightarrow \text{solvent adduct} \qquad 0 \equiv \text{olefin}$$

$$^3K_2^* + 0 \xrightarrow{k_c} [{}^3K_2^* \cdots 0]$$

$$[{}^3K_2^* \cdots 0] \xrightarrow{k_r} \text{photoadducts}$$

$$[{}^3K_2^* \cdots 0] \xrightarrow{k_d'} K + 0$$

$$^3K_2^* + Q \xrightarrow{k_q} K + {}^3Q^*$$

$K \equiv$
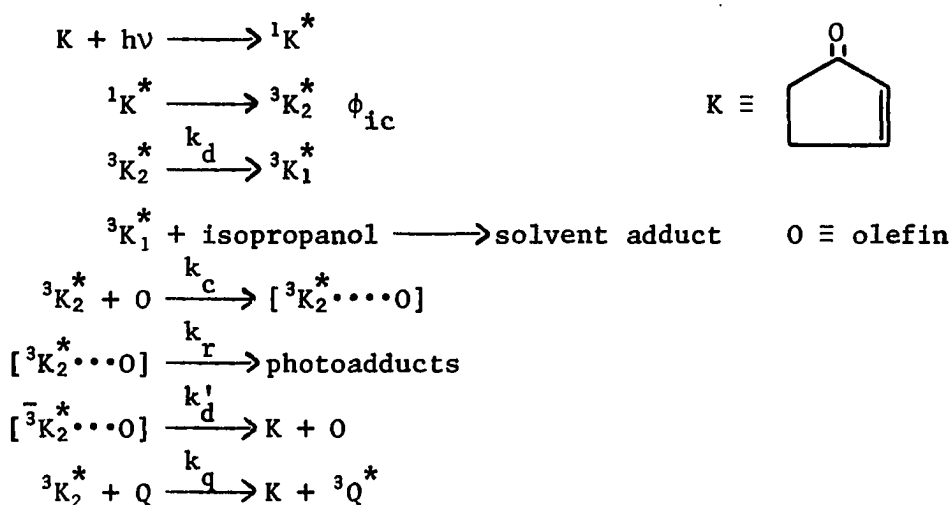
From the experimental data, one can assign an order of magnitude to some of the rate constants. From the triplet counting experiment k_d must be about 10^9 sec.$^{-1}$ Since the quantum yield of photoaddition is reasonably independent of olefin concentration, k_c must be 10^{10} ℓ/mole/sec., close

to diffusion controlled. Complex formation is necessary to explain the intercept discrepancy and to account for the high rate constant (k_c). A steady state treatment of this mechanism gives the following expression of reciprocal of quantum yield.

$$\frac{1}{\phi} = \frac{1}{\phi_{ic}} \left[1 + \frac{k_d'}{k_r} + \frac{k_d(k_r + k_d')}{k_r k_c [O]} \right]$$

The expression indicates that the intercept of a plot of reciprocal of quantum versus reciprocal of olefin concentration is dependent on olefin. Decay of the complex to ground state enone and ground state olefin may be an example of what Hammond has described as quenching by vibrational energy transfer (51, 52).

N. C. Yang *et al.* (29, 30) have recently looked at the mechanism of photoaddition of 9-anthraldehyde to olefins. Although 9-anthraldehyde has a low lying $\pi-\pi^*$ triplet state, it reacts with simple olefins to form oxetanes in appreciable quantum yield. Wavelength and sensitization studies indicate that oxetane formation results from a high energy excited state. If light of wavelength shorter than 400 mμ is used oxetane is the major product; while the dimer of 9-anthraldehyde is the major product with light longer than 410 mμ. The lowest triplet state of 9-anthraldehyde is estimated at 41 kcal./mole (24). However, only sensitizers with triplet energy greater than 59 kcal./mole sensitize oxetane formation. Hence oxetane formation must come from an upper singlet or triplet excited state while dimerization must come from a lower singlet or triplet excited state.

A Stern-Volmer plot for quenching photoaddition of 9-anthraldehyde to trimethylethylene by di-*t*-butyl nitroxide indicates that two reactive states

of lifetimes of 3×10^{-10} sec. and 1×10^{-9} sec. are involved in oxetane

formation. Yang concludes that two of the following three states result

in oxetane formation: n-π^* singlet state, n-π^* triplet state, and an

upper π-π^* triplet state. These states are shown in an energy diagram in

Figure 1.

Liu *et al.* (53, 54, 55) have looked at the possibility of energy

transfer from upper triplet states. Initially looking at sensitized

isomerization of rigid systems such as 2,3-bis(perfluoromethyl)bicyclo-

[2.2.2]octa-2,5,7-triene (LXXX), they find that anthracenes transfer

energy to LXXX from their second excited triplet states (T$_2$ states).
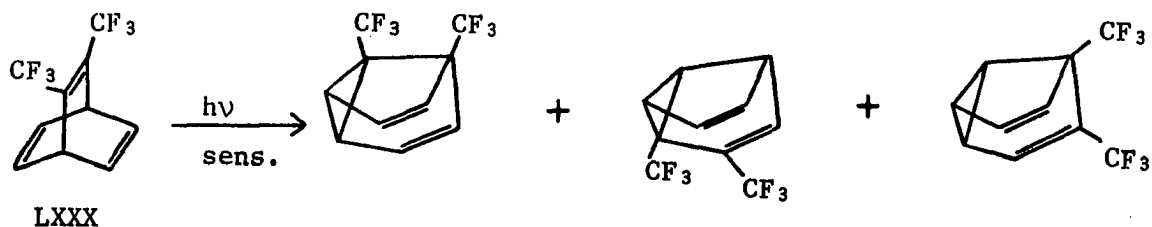
LXXX

The energy diagram of anthracene is shown in Figure 1. The lowest

triplet state lies 42.5 kcal./mole above ground state, and the second

triplet state, 74.4 kcal./mole above ground state (56, 57). The triplet

energy of barrelene (LXXX) lies between 59 and 68 kcal./mole (53). 9,10-

Dibromoanthracene (lowest triplet 40.2 kcal./mole) sensitizes rearrange-

ment of LXXX much better than 9-fluorenone (triplet energy 51 kcal./mole).

Liu and co-workers conclude that anthracenes must transfer energy to

barrelene (LXXX) from their T$_2$ states.

To prove that the T$_1$ state of anthracenes are not transferring

Figure 1. Energy level diagrams

        Top - 9-anthraldehyde (the T_1 energy estimated in reference 30)

        Bottom - anthracene (energy values taken from references 56 and 57)
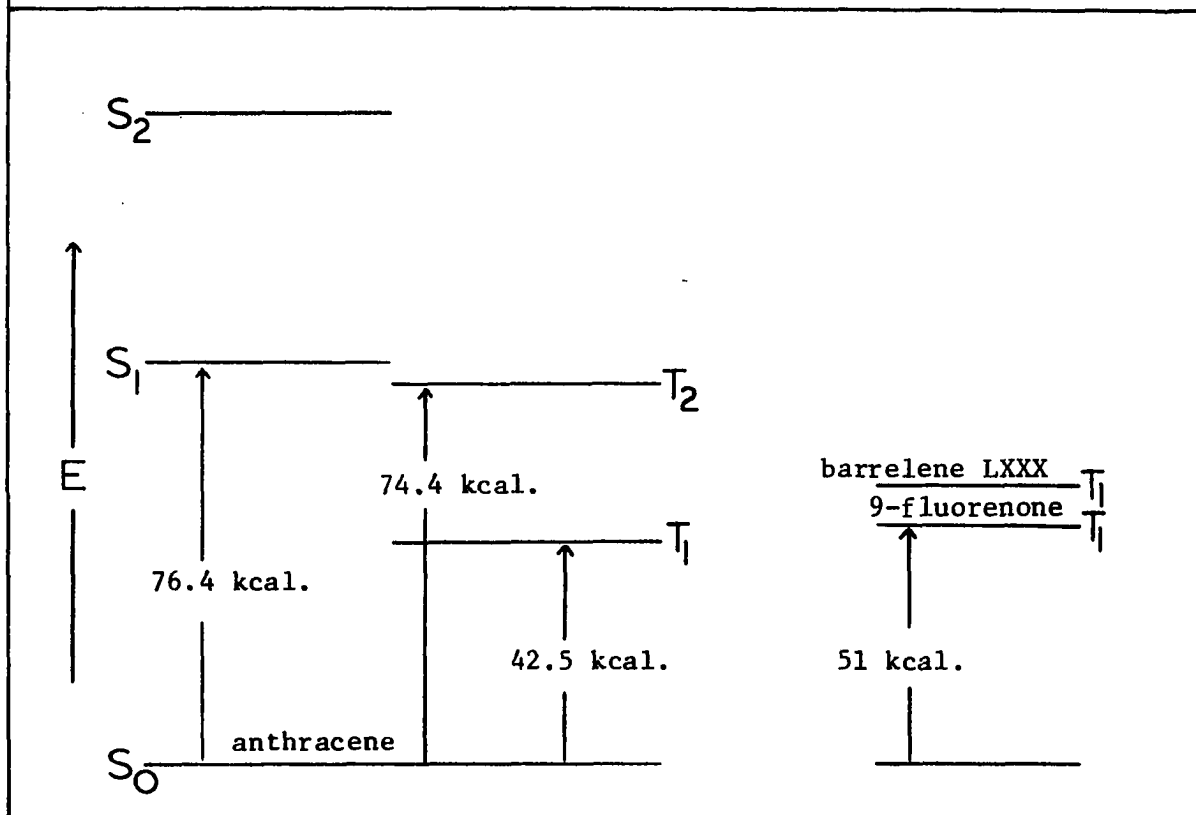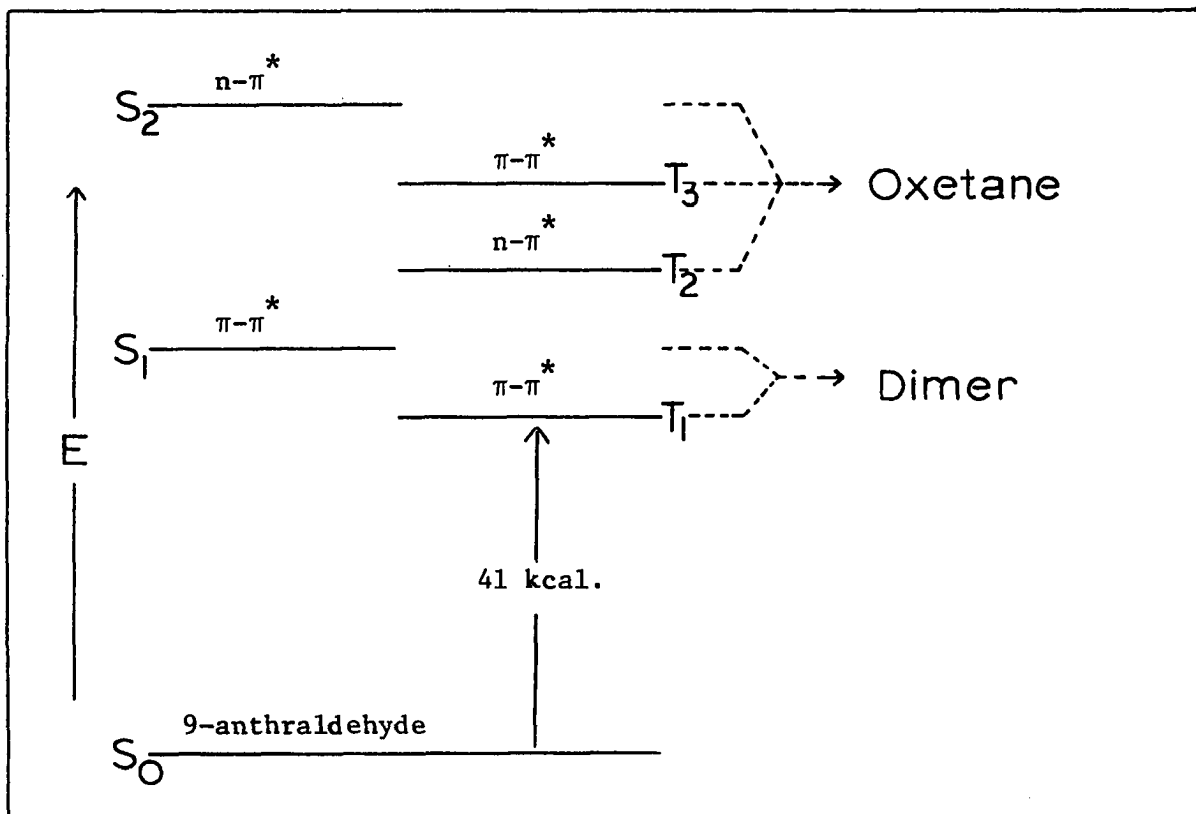
energy to LXXX, Liu and Edman did a cleaver double sensitization experiment. 9-Fluorenone does not sensitize rearrangement of barralene LXXX very well but should transfer energy to 9,10-dibromoanthracene, populating the T_1 state. Using this technique to heavily populate the T_1 state of 9,10-dibromoanthracene in the presence of barrelene LXXX, Liu and Edman find no significant amount of rearrangment.

The following kinetic scheme has been proposed.

$$A_{S_0} \xrightarrow{h\nu} A_{S_1}$$

$$A_{S_1} \xrightarrow{} A_{T_2} \quad \text{efficiency = a}$$

$$A_{T_2} \xrightarrow{k_{it}} A_{T_1} \xrightarrow{} A_{S_0}$$

$$A_{T_2} + B \xrightarrow{k_t} A_{S_0} + B_{T_1}$$

$$B_{T_1} \xrightarrow{} \text{products} \quad \text{efficiency = b}$$

$A \equiv$ anthracene

$B \equiv$ barrelene LXXX

$$\frac{1}{\phi} = \frac{1}{ab}\left[1 + \frac{k_{it}}{k_t[B]}\right]$$
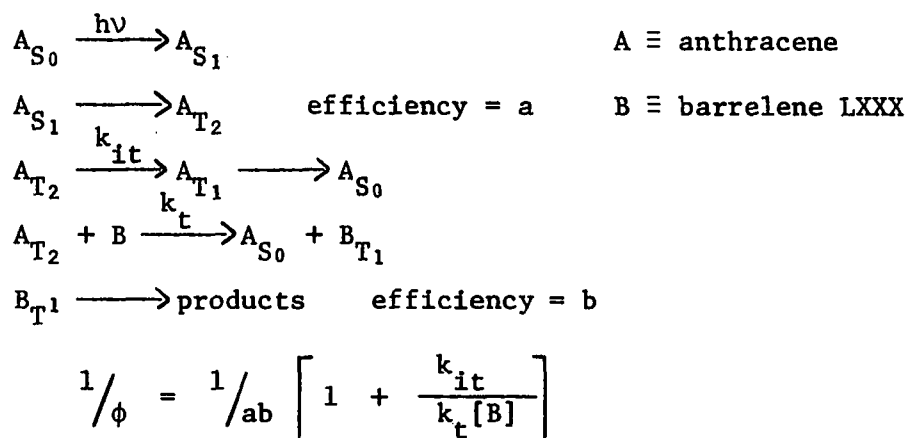
From the slope and intercept of the linear plot of reciprocal of quantum yield of sensitized isomerization of LXXX versus reciprocal of barrelene (LXXX) concentration, Liu and Edman estimate the rate constant for internal conversion from T_2 to T_1 at 5×10^{10} ℓ/mole/sec. Liu's neglect of quenching of A_{T_2} by A_{S_0} in the kinetic scheme may negate the calculation of the rate constant for internal conversion (k_{it}). The validity of the expression relating reciprocal of quantum to reciprocal of barrelene (LXXX) concentration is dependent on the concentration of 9,10-dibromoanthracene. If the concentration of 9,10-dibromoanthracene were of the same order of magnitude as the concentration of barrelene (LXXX), then energy transfer from A_{T_2} to A_{S_0} would be competive with energy transfer to barrelene (LXXX).

Including the quenching of A_{T_2} by A_{S_0} in the kinetic scheme leads to a more complex expression for the reciprocal of quantum yield of barrelene (LXXX) rearrangement. With this expression the rate constant for internal conversion (k_{it}) cannot be calculated from the slope and intercept of the plot of reciprocal of quantum yield versus reciprocal of barrelene (LXXX) concentration. Since Liu did not specify the concentration of 9,10-dibromoanthracene the validity of the calculation of k_{it} cannot be assessed.

Liu *et al.* (54, 55) also observed that anthracenes sensitize from their T_2 states the dimerization of butadiene [triplet energy 59.6 kcal./mole (58)] and acrylonitrile [triplet energy 62 kcal./mole (59)] and the isomerization of piperylenes [triplet energy, *cis*-piperylene 56.9 kcal./mole, *trans*-piperylene 58.8 kcal./mole (60)] and stilbenes [triplet energy, *cis*-stilbene 57 kcal./mole, *trans*-stilbene 51 kcal./mole (61)].

Kearns *et al.* (62, 63) have studied the mechanism of dye-sensitized photooxygenation of cholest-4-en-3β-ol (LXXXI). Two products are formed, an epoxy-ketone (LXXXII) and an enone (LXXXIII). The ratio of epoxy-ketone LXXXII to enone LXXXIII is dependent on sensitizer energy and

LXXXI   LXXXII   LXXXIII
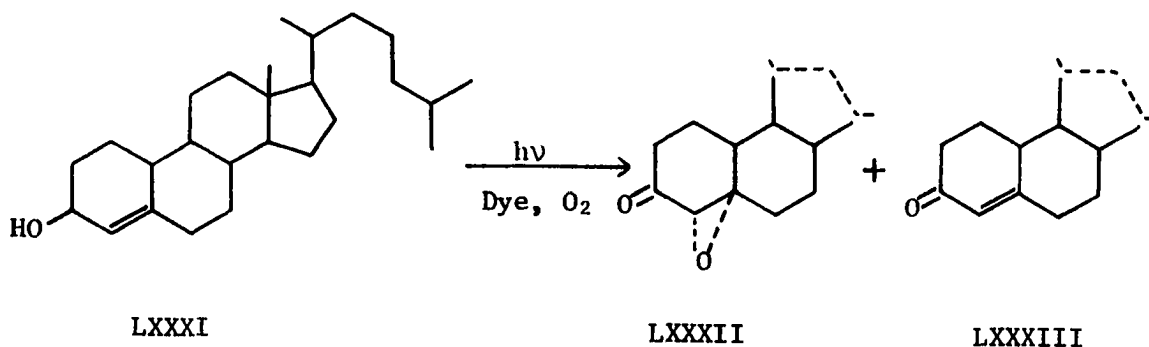
cholestenol (LXXXI) concentration. Kearns and co-workers find that both

the $^1\Sigma_g^+$ (37.7 kcal./mole above ground state) and the $^1\Delta_g$ (22 kcal.) states

of oxygen are involved as reaction intermediates and that the observed

variation in product distribution with sensitizer energy results from

variation in the relative amounts of $^1\Sigma_g^+$ and $^1\Delta_g$ generated. High energy

sensitizers ($E_T > 50$) favor formation of the $^1\Sigma_g^+$ state of oxygen and enone

(LXXXIII) product. Low energy sensitizers ($E_T > 38$ kcal.) generate only

the $^1\Delta_g$ state of oxygen and favor formation of epoxy-ketone product

(LXXXII). The lifetime of the high energy $^1\Sigma_g^+$ state of oxygen is short.

As a result the ratio of epoxy-ketone (LXXXII) to enone (LXXXIII) is

dependent on cholestenol (LXXXI) concentration. Low concentrations of

cholestenol (LXXXI) favor formation of epoxy-ketone (LXXXII) even with high

energy sensitizers because the short lived $^1\Sigma_g^+$ state decays to the $^1\Delta_g$

state before it can react.

RESULTS AND DISCUSSION

The purpose of this investigation was to understand the mechanism of
photocycloaddition of 4,4-dimethyl-2-cyclohexenone to olefins and its
relation to the photochemical rearrangement of 4,4-dimethyl-2-cyclohexenone.
Corey *et al.* (14) have provided an extensive study of photoaddition of 2-
cyclohexenone to olefins with emphasis on reactivity and product structures
as a function of olefin structure. Of the olefins investigated, they find
that 1,1-dimethoxyethylene is the most reactive. 2-Cyclohexenone cleanly
photoadds to 1,1-dimethoxyethylene to give *cis-* and *trans*-7,7-dimethoxy-
bicyclo[4.2.0]-octan-2-ones (XVI and XVII). At about the same time,
Chapman *et al.* (32) were investigating the photorearrangement of 4,4-
dimethyl-2-cyclohexenone (XXXV). The photoreactions of 4,4-dimethyl-2-
cyclohexenone (XXXV) in the presence of 1,1-dimethoxyethylene were selected
for study because they provide a good system for the mechanistic investi-
gation of both photocycloaddition and photorearrangement.

Qualitative Investigation of the Photochemistry of

4,4-Dimethyl-2-cyclohexenone

Photocycloaddition

Irradiation of 4,4-dimethyl-2-cyclohexenone (XXXV) and 1,1-dimethoxy-
ethylene in hexane solution with a Pyrex filter gives three photoproducts
identified as 3,3-dimethoxy-7,7-dimethyl-1-oxaspiro[3.5]non-5-ene (LXXXIV),
cis-5,5-dimethyl-7,7-dimethoxybicyclo[4.2.0]-octan-2-one (LXXXV), and
trans-5,5-dimethyl-7,7-dimethoxybicyclo[4.2.0]-octan-2-one (LXXXVI). These
products are referred to as oxetane, *cis*-cyclobutane, and *trans*-cyclobutane,

XXXV   LXXXIV   LXXXV   LXXXVI
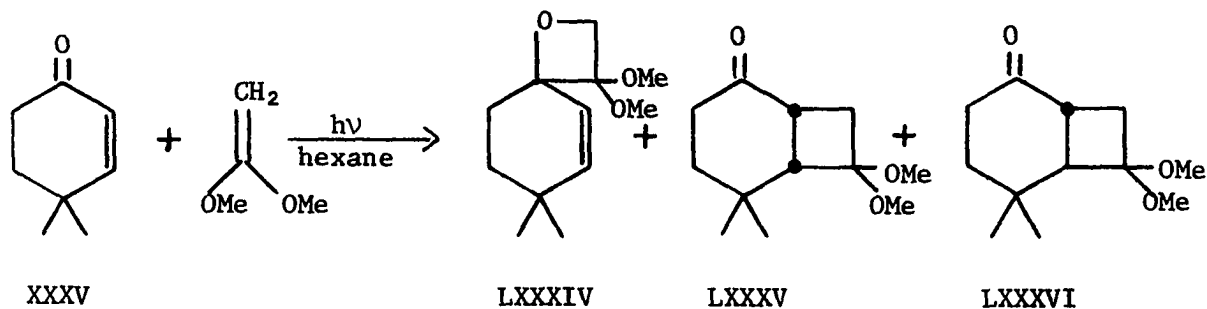
respectively. Formation of oxetane (20%), *cis*-cyclobutane (29%), and

trans-cyclobutane (46%) accounts for 95% of the reaction of 4,4-dimethyl-

2-cyclohexenone by quantitative gas liquid partition chromatography

(g.l.p.c.) A plot of cycloadduct formation and 4,4-dimethyl-2-cyclo-

hexenone destruction as a function of time is presented in Figure 2.

During the last hour of irradiation, products are destroyed faster

than they are formed (see Figure 2). When most of the enone (XXXV) has

reacted, some of the light excites the weak n-π^* transition of the *cis*-

and *trans*-cyclobutanes. The excited *cis*- and *trans*-cyclobutanes probably

undergo Norrish Type I cleavage (α-cleavage). Irradiation (310-410 mμ) of

a mixture of oxetane, *cis*-cyclobutane, and *trans*-cyclobutane in the absence

of enone (XXXV) and 1,1-dimethoxyethylene likewise gives some destruction

of *cis*- and *trans*-cyclobutanes. The missing 5% of reacted 4,4-dimethyl-

2-cyclohexenone may be explained by photoproduct destruction. Hence the

photocycloaddition reactions is almost quantitative.

The oxetane was separated from *cis*- and *trans*-cyclobutanes by spinning

band distillation. Structure LXXXIV was assigned on the basis of the

following evidence. The infrared spectrum (Figure 3) shows no carbonyl

Figure 2. Destruction of 4,4-dimethyl-2-cyclohexenone and formation of
photocycloadducts as a function of time

⬡- Percent destruction of 4,4-dimethyl-2-cyclohexenone

△- Percent formation of *trans*-5,5-dimethyl-7,7-dimethoxy-
bicyclo[4.2.0]octan-2-one

☐- Percent formation of *cis*-5,5-dimethyl-7,7-dimethoxy-
bicyclo[4.2.0]octan-2-one

◯- Percent formation of 3,3-dimethoxy-7,7-dimethyl-1-
oxaspiro[3.5]non-5-ene
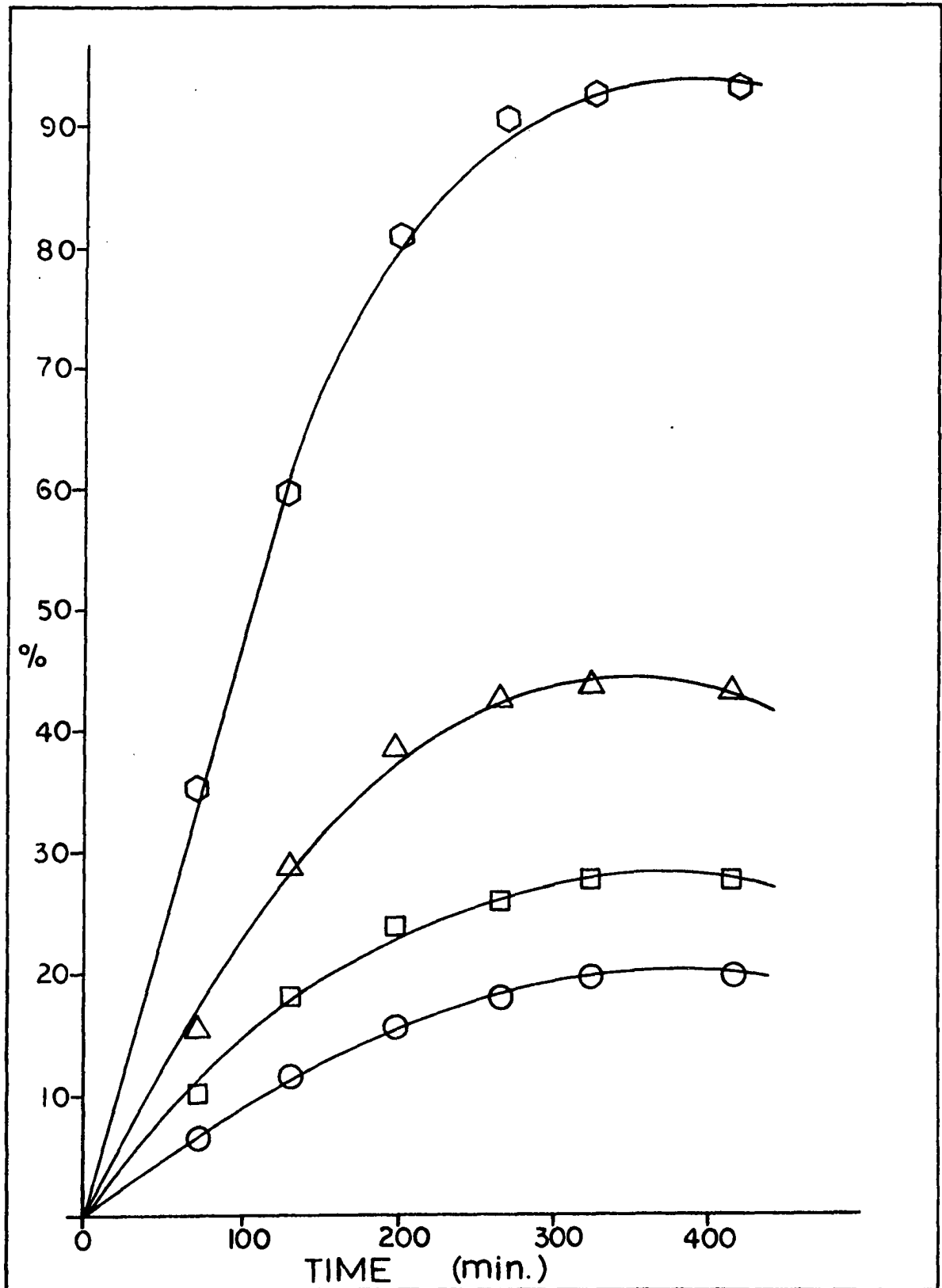
Figure 3. Infrared spectra (neat)

Top - 3,3-dimethoxy-7,7-dimethyl-1-oxaspiro[3.5]non-5-ene

Middle - *cis*-5,5-dimethyl-7,7-dimethoxybicyclo[4.2.0]octan
2-one

Bottom - *trans*-5,5-dimethyl-7,7-dimethoxybicyclo[4.2.0]-
octan-2-one
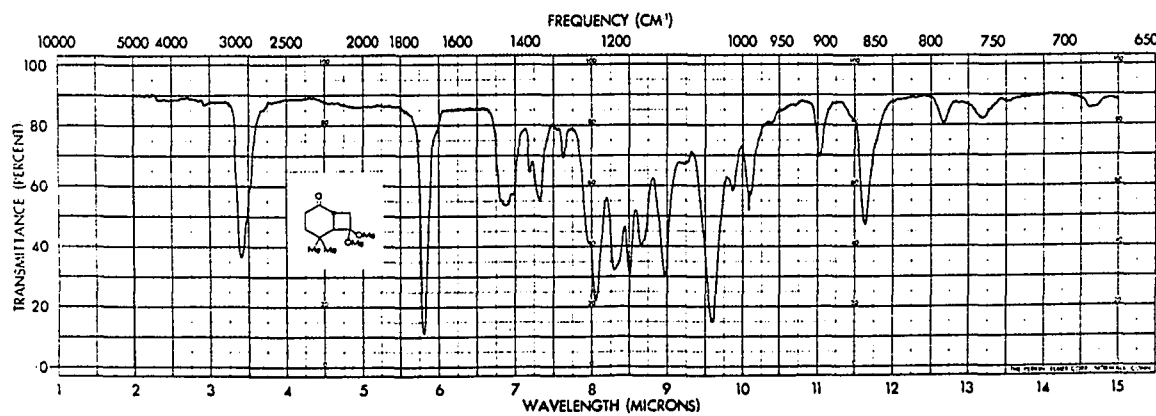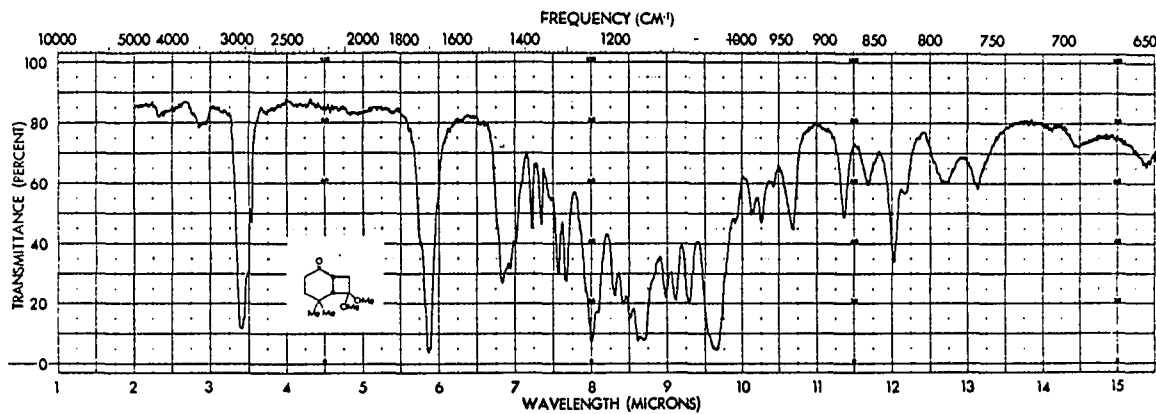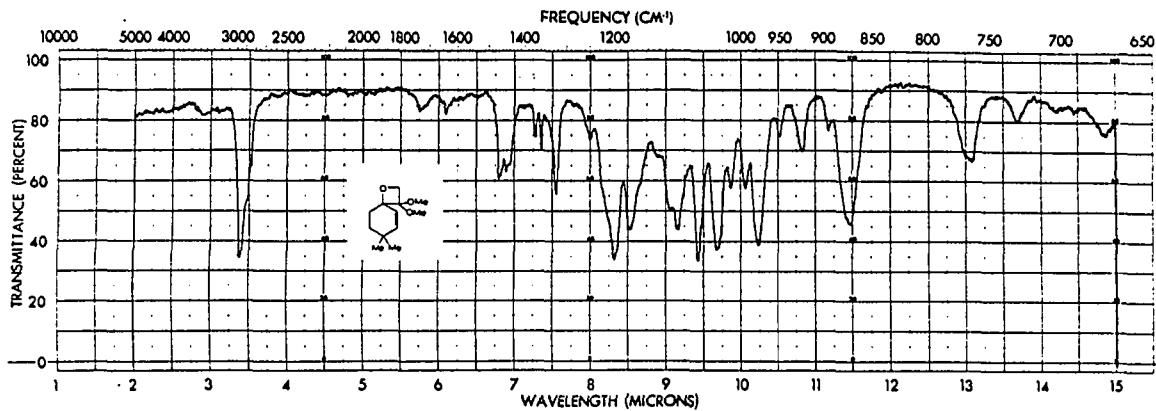
Figure 4. Nucelar magnetic reasonance spectra (CCl$_4$)

Top - 3,3-dimethoxy-7,7-dimethyl-1-oxaspiro[3.5]non-5-ene

Middle - *cis*-5,5-dimethyl-7,7-dimethoxybicyclo[4.2.0]octan 2-one

Bottom - *trans*-5,5-dimethyl-7,7-dimethoxybicyclo[4.2.0]-octan-2-one
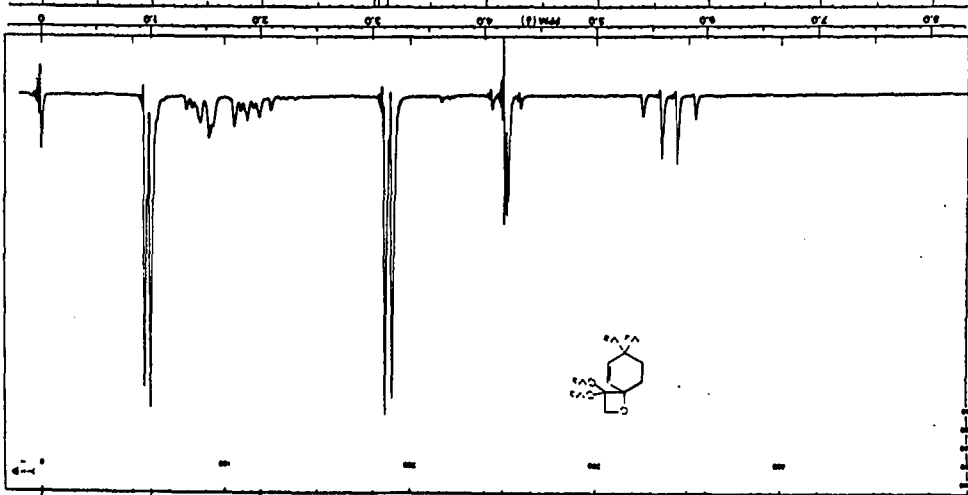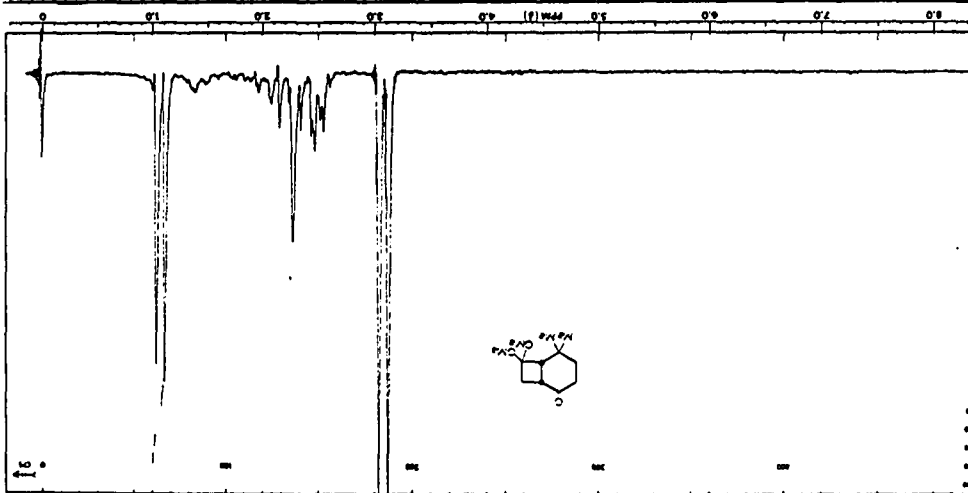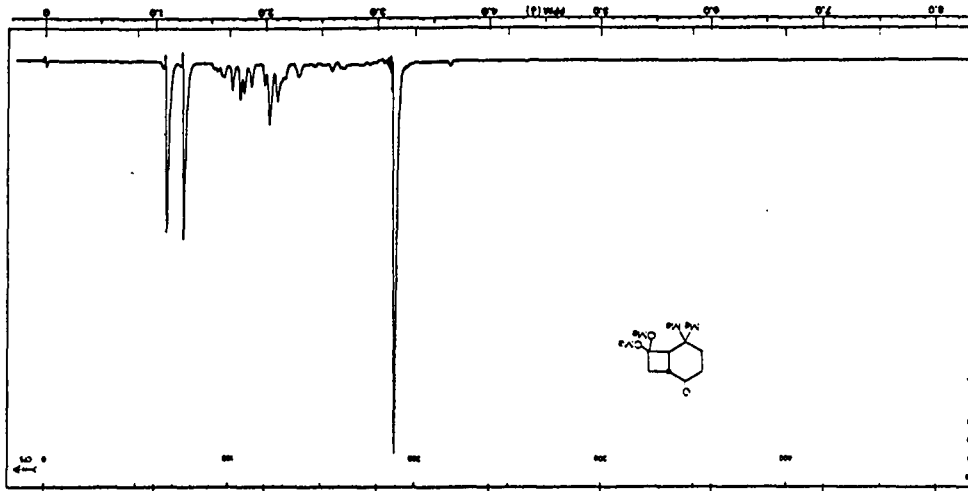
Figure 5. Mass spectra

Top - 3,3-dimethoxy-7,7-dimethyl-1-oxaspiro[3.5]non-5-ene

Middle - *cis*-5,5-dimethyl-7,7-dimethoxybicyclo[4.2.0]octan
octan-2-one

Bottom - *trans*-5,5-dimethyl-7,7-dimethoxybicyclo-[4.2.0]-
octan-2-one
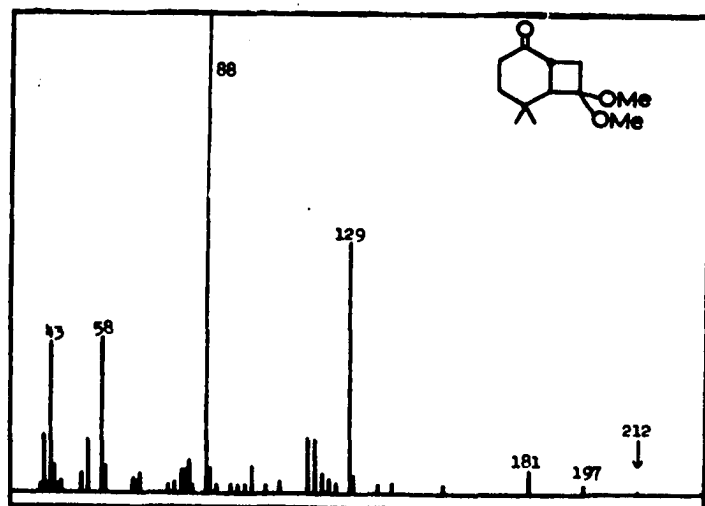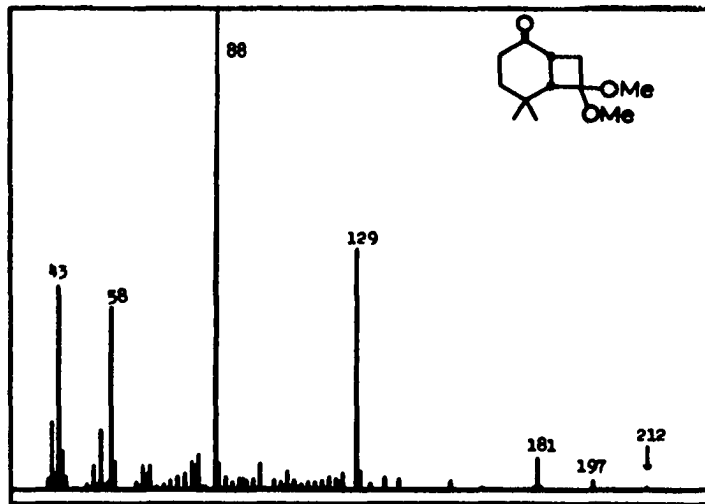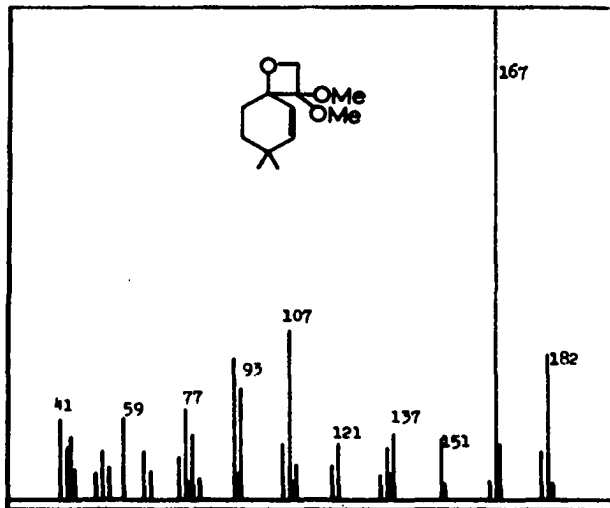
absorption, a weak double bond stretching vibration at 6.10 μ, five
strong bands between 8.5 and 10.0 μ attributed to C–O stretching modes,
and a strong band at 11.45 μ attributed to the *cis*-disubstituted double
bond. The weak absorption at 5.85 μ is probably an overtone of the 11.45
band. The n.m.r. spectrum (Figure 4) is most informative. There are two
methyl singlets at 0.95 and 1.00 δ and two methoxyl singlets at 3.10 and
3.20 δ. The methylene protons of the oxetane ring give an AB pattern at
4.14 and 4.23 δ ($^2J_{AB}$, 7.00 Hz.). The small geminal coupling constant is
a result of the σ electron withdrawing and π electron donating effects of
the adjacent oxygen and the large H–C–H bond angle. The double bond
protons occur as an AB pattern at 5.52 and 5.78 δ ($^3J_{AB}$, 10.1 Hz.). The
two methylene groups of the cyclohexene ring give two multiplets (two
protons each) at 1.25 to 1.65 δ and 1.65 to 2.30 δ. The mass spectrum
(Figure 5) establishes the orientation of the oxetane. There is no parent
ion at m/e 212 even at 10 ev. The first major fragment occurs at m/e 182
(30% of base) and results from loss of formaldehyde. There is a weak
metastable ion at m/e 156 (calculated 156) which relates m/e 182 with the
parent ion. The other possible oxetane structure, 2,2-dimethoxy-7,7-
dimethyl-1-oxaspiro[3.5]non-5-ene (LXXXVII) does not have a favorable path
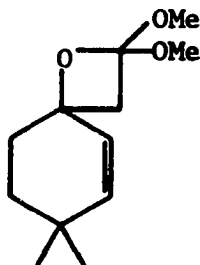
LXXXVII

for loss of formaldehyde from the parent ion. The alternate structure

(LXXXVII) would initially lose dimethyl carbonate or 1,1-dimethoxyethylene.

There are no strong peaks in the mass spectrum to account for either of

these cleavages. The base peak occurs at m/e 167 and represents loss of

methyl from the m/e 182 peak. Peaks at m/e 182 and 167 are related by a

strong metastable ion at m/e 153.5 (calculated m/e 153.3).
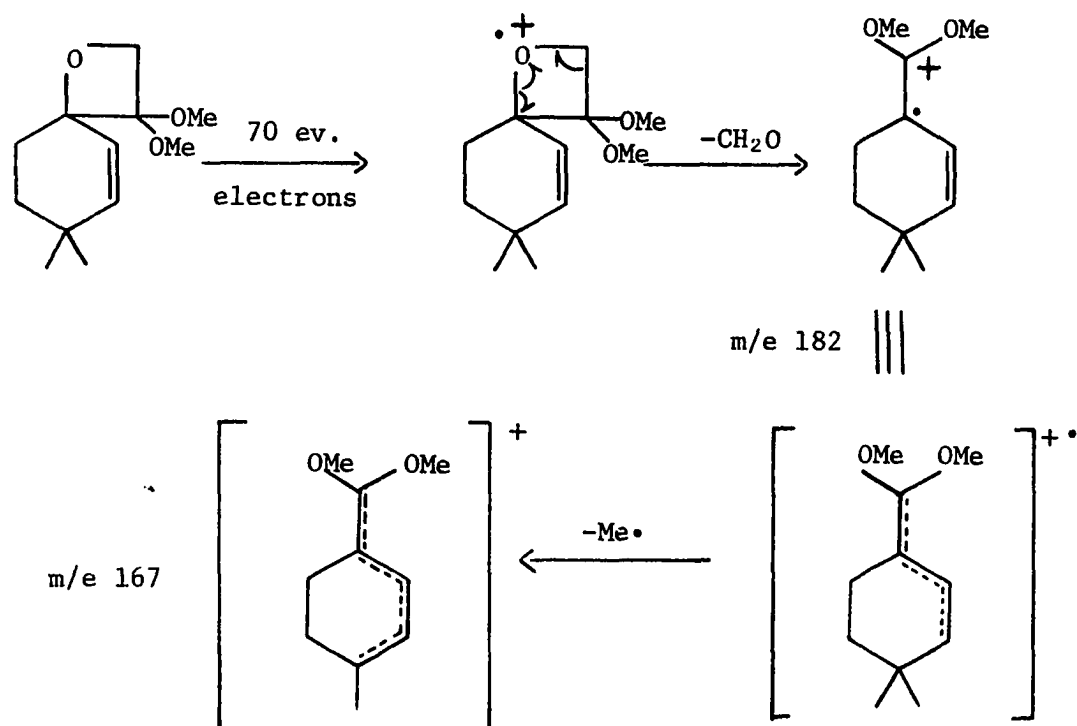
The chemical shift of oxetane methylene absorption in the n.m.r.

spectrum is also consistent with structure LXXXIV. The oxetane methylene

of structure LXXXVII would be significantly upfield from δ 4.14. Arnold

et al. (25) report that on the oxetane ring hydrogens α to oxygen occur at

4.0-5.0 δ while hydrogens β to oxygen occur at 2.6-3.6 δ.

Pyrolysis of oxetane LXXXIV at 320° gives some loss of formaldehyde. The formaldehyde was identified by comparison of its 2,4-dinitrophenyl-hydrazone derivative with an authenic sample. In the pyrolysis reaction, loss of formaldehyde is only one of several reactions. Gas liquid chromatographic analysis of the liquid products indicated that there were eight products. One of the products has the same g.l.p.c. retention time as 4,4-dimethyl-2-cyclohexenone. The other products were not identified. Arnold *et al.* (25) have observed that the *bis-(p*-methoxy)-benzophenone isobutylene oxetane readily loses formaldehyde.

$$p\text{-MeO-}\phi, p\text{-MeO-}\phi \text{ oxetane} \xrightarrow{\Delta} CH_2O + (p\text{-MeO-}\phi)_2C{=}C\begin{smallmatrix}CH_3\\CH_3\end{smallmatrix}$$
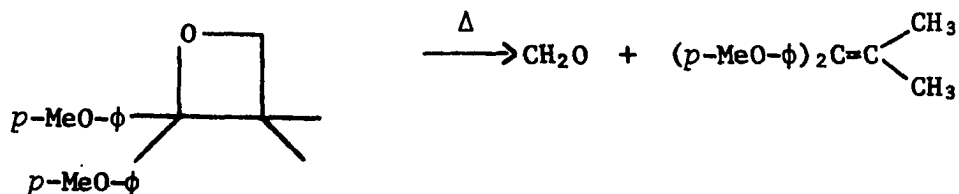
The proposed structure for the oxetane (LXXXIV) agrees with the Büchi rule (23) for orientational specificity. If an intermediate biradical is formed, then the biradical leading to structure LXXXIV would be much more stable than the biradical leading to structure LXXXVII. Even though steric factors favor oxetane LXXXVII, the electronic factors favoring oxetane LXXXIV are more important and result in an orientationally specific addition.

Partial separation of the *cis-* and *trans-*cyclobutanes (LXXXV and LXXXVI) was accomplished by spinning band distillation. Pure samples of *cis-* and *trans-*cyclobutanes were obtained by preparative g.l.p.c. Gram quantities of pure *cis-*cyclobutane were obtained by equilibration of a mixture of *cis-* and *trans-*cyclobutanes on neutral alumina.

The structures for the *cis*- and *trans*-cyclobutanes (LXXXV and LXXXVI) were assigned on the basis of spectroscopic evidence and chemical degradation. The *cis*-cyclobutane (LXXXV) exhibits a strong carbonyl absorption at 5.85 μ in the infrared spectrum (Figure 3). The n.m.r. spectrum (Figure 4) shows two methyl singlets at 1.06 and 1.13 δ and two methoxyl singlets at 3.06 and 3.13 δ. The two methine and six methylene protons occur as a complex multiplet from 1.20 to 2.70 δ. The mass spectrum (Figure 5) has a weak parent ion at m/e 212 (0.3% of base) and a base peak at m/e 88 (loss of 1,1-dimethoxyethylene). The *trans*-cyclobutane has a strong carbonyl at 5.80 μ in the infrared spectrum (Figure 3). The n.m.r. spectrum (Figure 4) exhibits two methyl singlets at 1.10 and 1.26 δ. The methoxyl protons are isochronous and occur as a six proton singlet at 3.15 δ. The two methine and six methylene protons occur as a complex multiplet from 1.50 to 3.00 δ. In the mass spectrum (Figure 5) a weak parent ion occurs at m/e 212 (0.3% of base). Like the *cis*-cyclobutane, the base peak occurs at m/e 88 (loss of 1,1-dimethoxyethylene). The spectroscopic data is consistent with but does not require the proposed *cis*- and *trans*-5,5-dimethyl-7,7-dimethoxybicyclo[4.2.0]octan-2-one structures (LXXXV and LXXXVI). The alternate *cis*- and *trans*-5,5-dimethyl-8,8-dimethoxybicyclo[4.2.0]octan-2-one structures have not been eliminated.
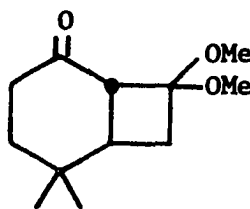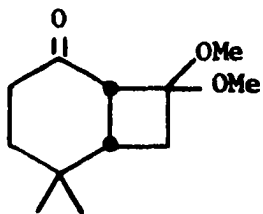
The position of the methoxyl groups was established by chemical degradation. An outline of the structure proof is given in Figure 6.

The cis-cyclobutane is hydrolyzed to cis-5,5-dimethylbicyclo[4.2.0]-octa-2,7-dione (LXXXVIII) with dilute hydrochloric acid. The cis-dione (LXXXVIII) exhibits a four-membered ring carbonyl at 5.62 μ and a six-membered ring carbonyl at 5.90 μ in the infrared spectrum (Figure 7). The n.m.r. spectrum has two methyl singlets at 1.04 and 1.13 δ and three complex multiplets, 1.40 to 2.25 δ (2 protons), 2.25 to 2.65 δ (2 protons), and 2.65 to 3.70 δ (4 protons). The mass spectrum (Figure 8) has a parent ion at m/e 166.

If the dione has structure LXXXVIII shown in Figure 6, then treatment with methanol-OD and hydrogen chloride should result in exchange of six protons. The alternate structure, 5,5-dimethylbicyclo[4.2.0]-octa-2,8-dione should only exchange five protons. Mass spectral analysis of the deuterated dione at 18 ev. indicates that 25% of dione molecules exchanged six protons for deuterons. The deuterium exchange experiment indicated the orientation of the cyclobutane adducts (LXXXV and LXXXVI) and as a result suggested the degradation scheme shown in Figure 6.

Wolff-Kishner reduction of cis-5,5-dimethyl-7,7-dimethoxybicyclo-[4.2.0]octan-2-one (XXXV) gives cis-5,5-dimethyl-7,7-dimethoxybicyclo-[4.2.0]octane (LXXXIX). The ketal (LXXXIX) was not isolated but was hydrolyzed directly to cis-5,5-dimethylbicyclo[4.2.0]octan-7-one (XC). Ketone (XC) exhibits a strong four membered ring carbonyl at 5.61 μ in the infrared spectrum (Figure 7). The n.m.r. spectrum has two methyl singlets at 0.87 and 1.15 δ and three complex multiplets, 0.95-1.80 δ (5 protons), 1.90-2.70 δ (3 protons), and 2.70 to 3.20 δ (2 protons).

Figure 6. Structure proof of *cis*- and *trans*-5,5-dimethyl-7,7-dimethoxy-bicyclo[4.2.0]octan-2-ones
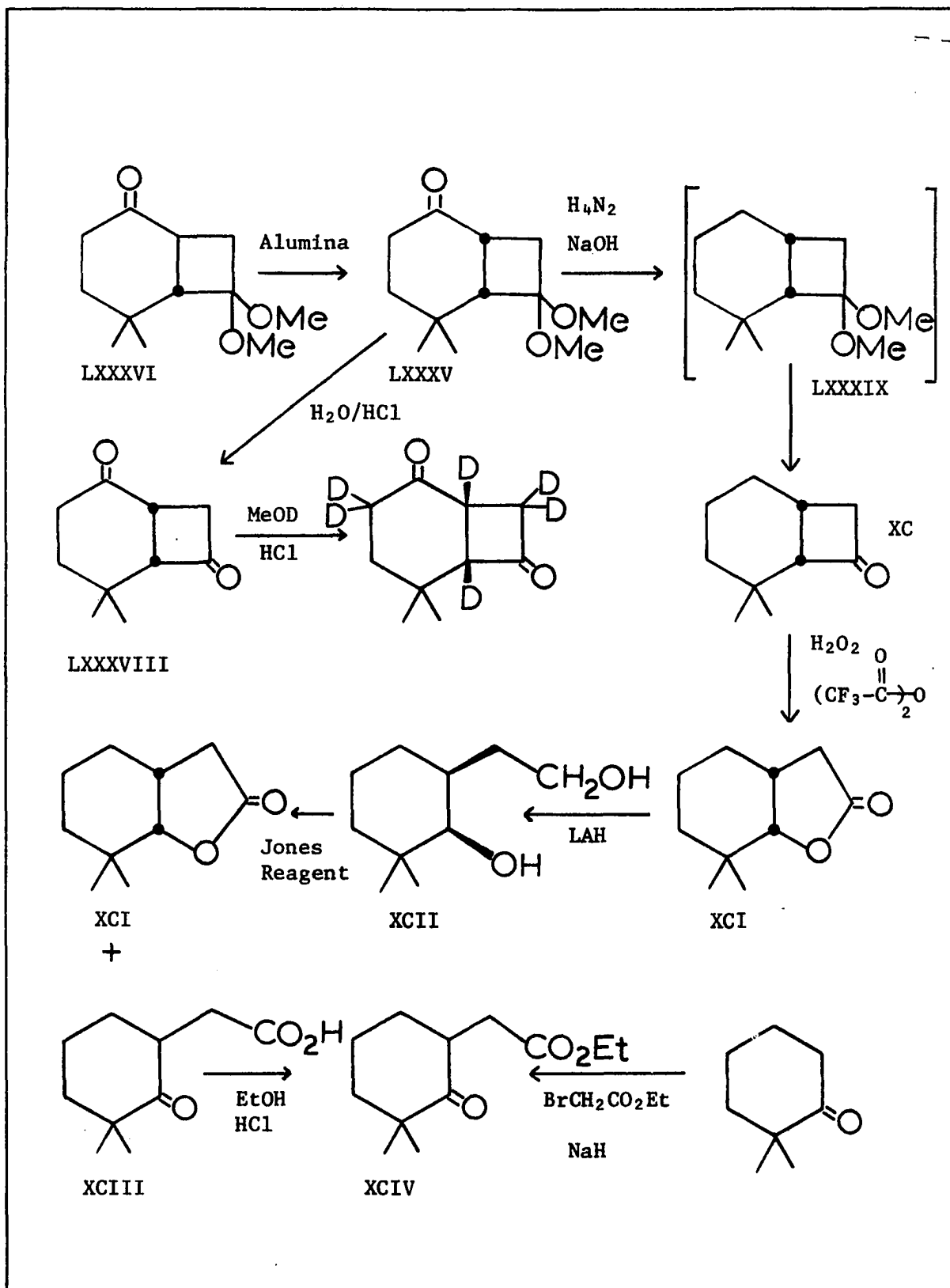
Figure 7. Infrared spectra

Top - *cis*-5,5-dimethylbicyclo[4.2.0]octa-2,7-dione (neat)

Middle - *cis*-5,5-dimethylbicyclo[4.2.0]octan-7-one (CCl₄)

Bottom - *cis*-2,2-dimethyl-9-oxabicyclo[4.3.0]nonan-8-one
          (CCl₄)

FREQUENCY (CM⁻¹)

TRANSMITTANCE (PERCENT)

WAVELENGTH (MICRONS)

FREQUENCY (CM⁻¹)

TRANSMITTANCE (PERCENT)

WAVELENGTH (MICRONS)

FREQUENCY (CM⁻¹)

TRANSMITTANCE (PERCENT)

WAVELENGTH (MICRONS)
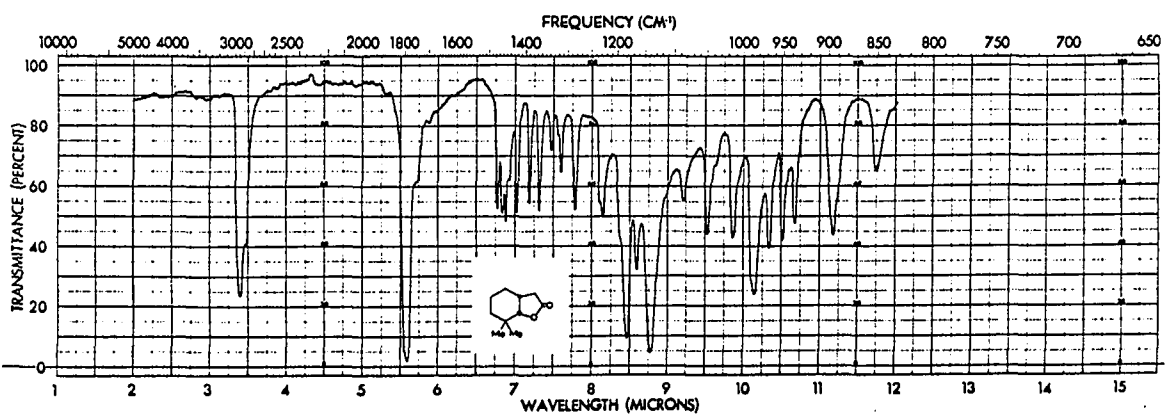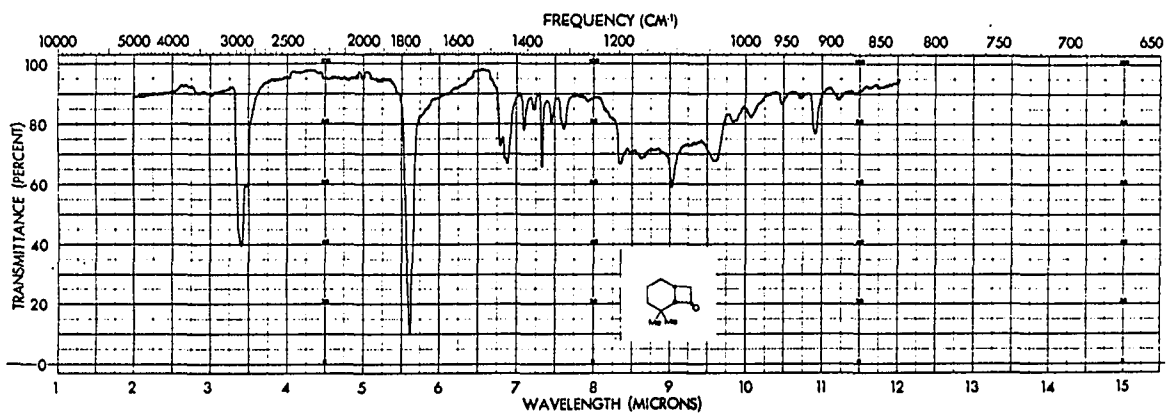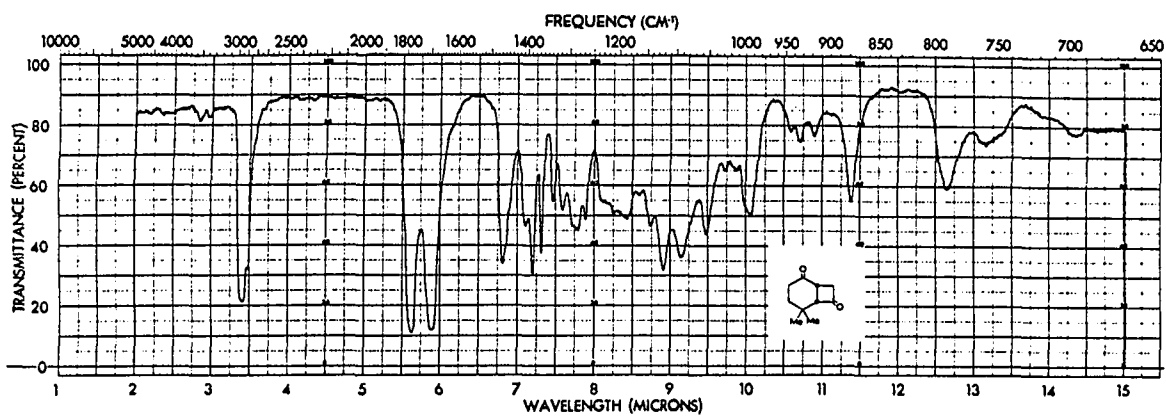
Figure 8. Mass spectra

Top – *cis*-5,5-dimethylbicyclo[4.2.0]octa-2,7-dione

Middle – *cis*-5,5-dimethylbicyclo[4.2.0]octan-7-one
The intensity of the fragment at m/e 43 was divided
by 2.

Bottom – *cis*-2,2-dimethyl-9-oxabicyclo[4.3.0]nonan-8-one
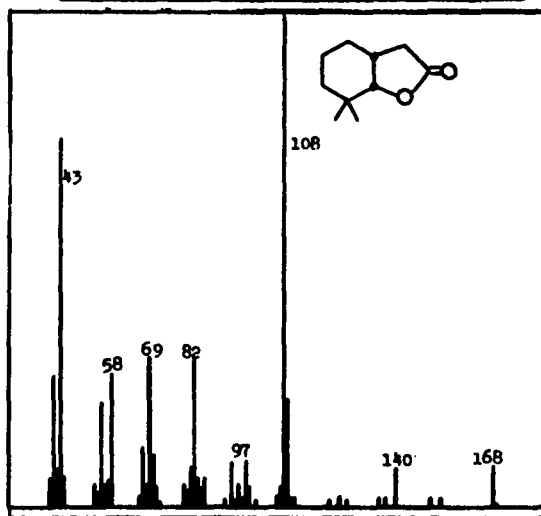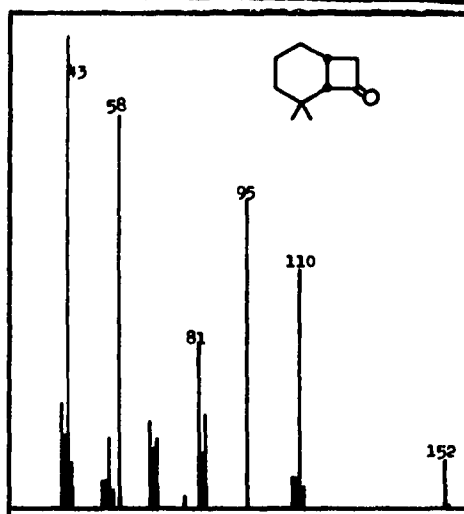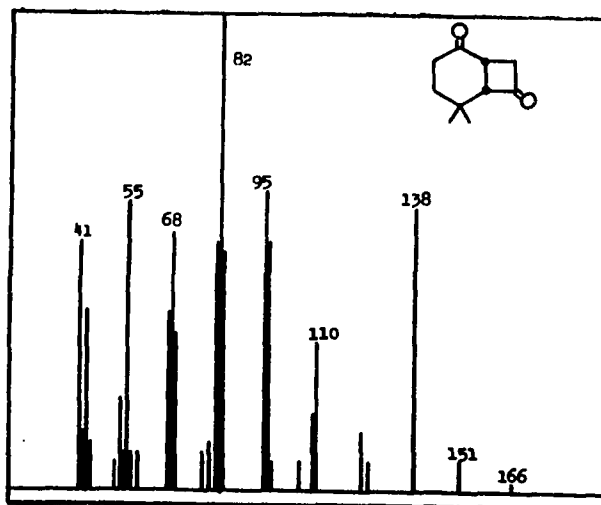
Figure 9. Infrared spectra

Top - *cis*-2,2-dimethyl-6-(β-hydroxyethyl)-cyclohexanol (KBr)

Middle - 2-keto-3,3-dimethylcyclohexyl acetic acid (CHCl$_3$)

Bottom - ethyl (2-keto-3,3-dimethylcyclohexyl)-acetate (CCl$_4$)
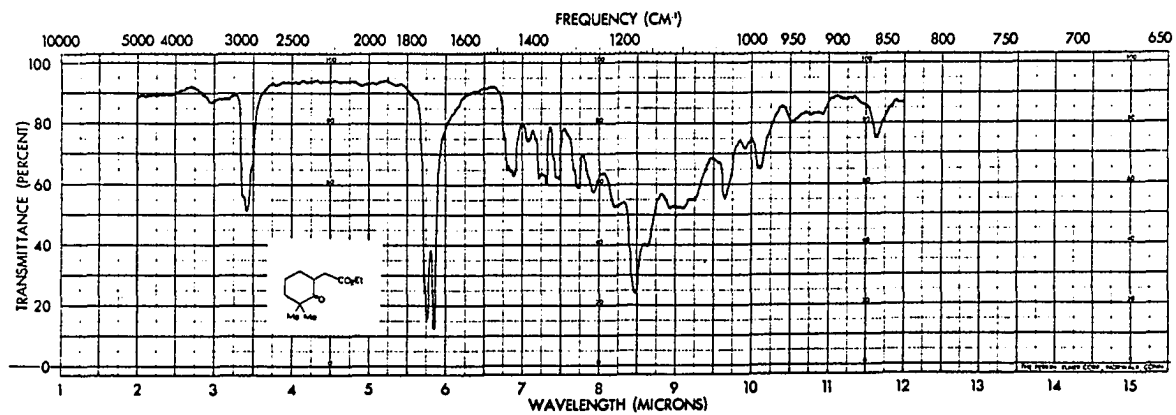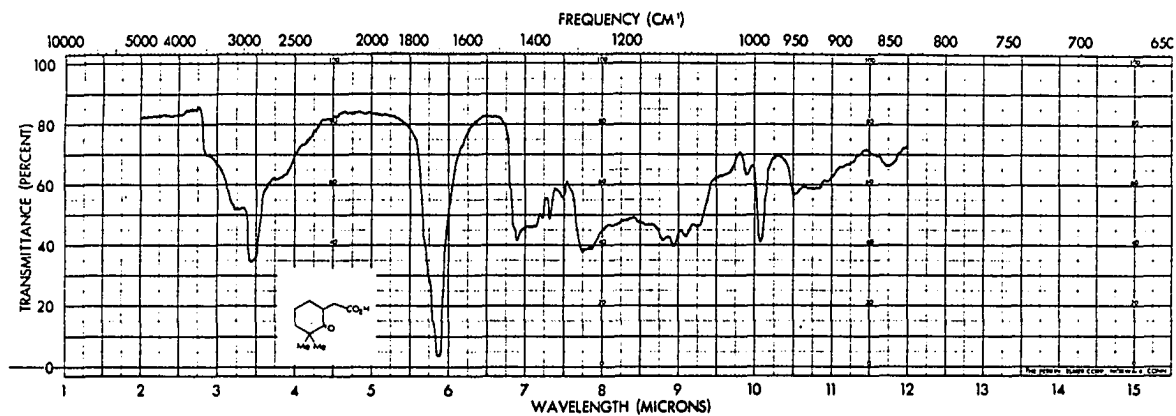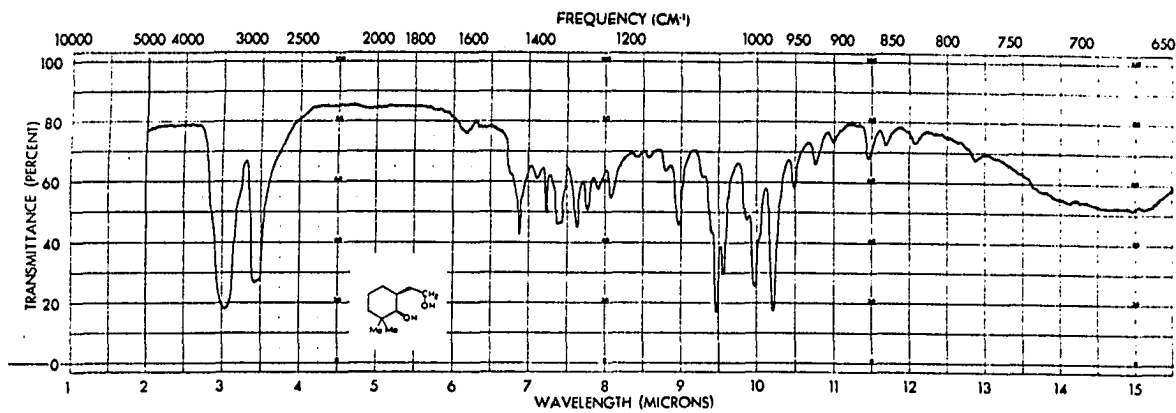
Figure 10. Mass spectra

Top - *cis*-2,2-dimethyl-6-(β-hydroxyethyl)-cyclohexanol

Middle - 2-keto-3,3-dimethylcyclohexyl acetic acid

Bottom - ethyl (2-keto-3,3-dimethylcyclohexyl)-acetate
The intensity of the fragment at m/e 43 was divided
by 2.
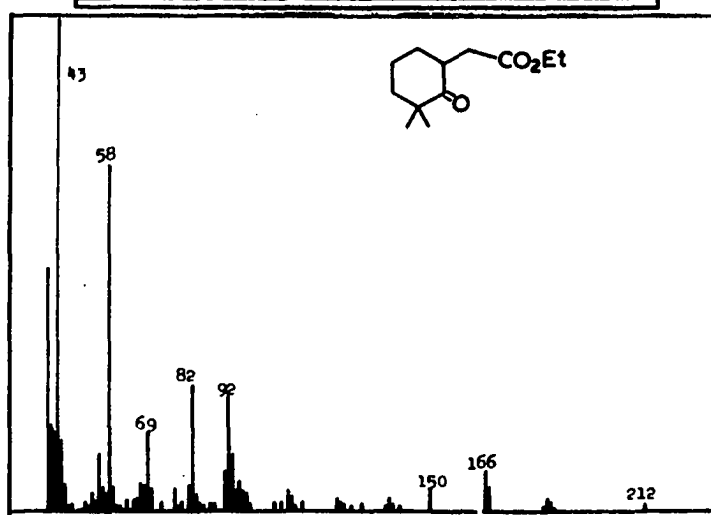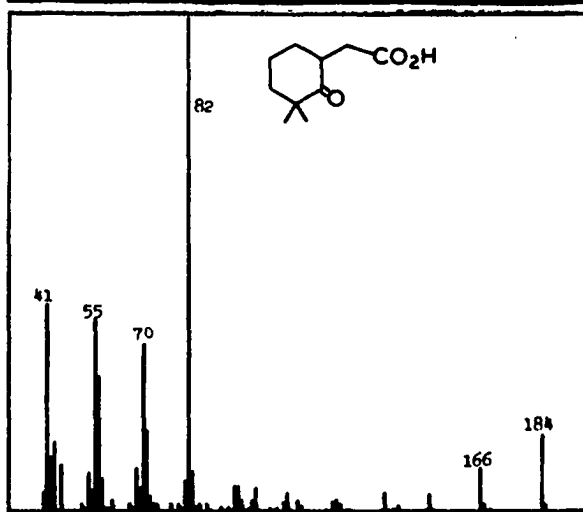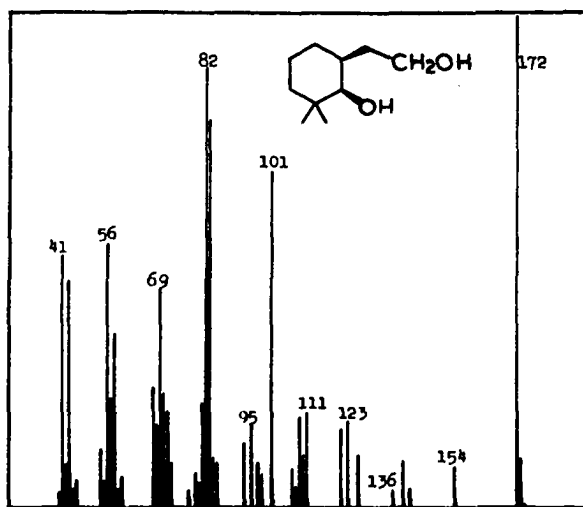
The mass spectrum (Figure 8) shows a parent ion at m/e 152 and an intense peak at m/e 110 (M-42) due to the loss of ketene.

Ketone (XC) is oxidized under Baeyer-Villiger conditions to a γ-lacton, *cis*-2,2-dimethyl-9-oxabicyclo[4.3.0]nonan-8-one (XCI). The i.r. spectrum (Figure 7) of γ-lactone (XCI) exhibits a characteristic 5.60 carbonyl stretching vibration. The n.m.r. spectrum is characteristic and suggestive of the orientation. There are two methyl singlets at 0.95 and 1.07 δ, a six proton multiplet at 0.90 to 1.80 δ, a three proton multiplet at 1.80 to 2.80 δ, and a one proton doublet at 3.87 δ(^{3}J, 3 Hz.). The low field doublet supports structure XCL in Figure 6 for the γ-lactone. The alternate orientation given by structure XCV should not have a low field
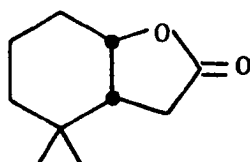
XCV
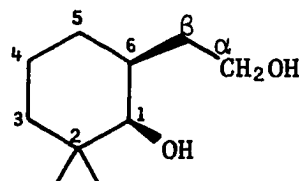
XCII

doublet. The mass spectrum (Figure 8) shows a parent ion at m/e 168.

Reduction of the γ-lacton (XCI) with lithium aluminum hydride gives the *cis* diol, *cis*-2,2-dimethyl-6-(β-hydroxyethyl)cyclohexanol (XCII). The diol shows a strong O-H stretching vibration at 3.05 μ in the infrared spectrum (Figure 9). The n.m.r. spectrum was run in hexadeuteriodimethyl sulfoxide to assign the hydroxyl absorptions (64). The two methyls are isochronous and appear as a six proton singlet at 0.87 δ. Methylene protons at positions 3, 4, 5, and β and methine proton at position 6 occur as a multiplet at 0.90 to 2.0 δ. The methine proton at position 1 appears as a broad doublet at 3.02 δ (^{3}J, 6 Hz.). The 6 Hz. splitting comes from coupling with the hydroxyl proton and the broadening is due to coupling

with methine proton at position 6 and possibly some virtual coupling. The broad doublet collapses to a broad singlet when deuterium oxide is added. A slightly broadened two proton quartet appears at 3.42 δ. This is assigned to the α-methylene group. When deuterium oxide is added the quartet collapses to a triplet (^3J, 6.0 Hz.). The hydroxyl at position 1 occurs as a doublet at 4.05 δ (^3J, 6.0 Hz.). The 4.05 δ doublet disappears upon addition of deuterium oxide. The hydroxyl on the α-position gives rise to a triplet at 4.21 δ (^3J, 5.0 Hz.). The 4.21 δ triplet also disappears upon addition of deuterium oxide. The mass spectrum (Figure 10) exhibits a parent ion at m/e 172 which is also the base peak.

Oxidation of the diol (XCII) under Jones conditions (65) gives a γ-lactone identical to the γ-lactone (XCI) from the Baeyer-Villiger oxidation and a γ-keto-acid, 2-keto-3,3-dimethylcyclohexyl acetic acid (XCIII). The keto-acid is identified by a characteristic broad O-H stretching vibration (2.8-4.5 μ) and a strong carbonyl absorption at 5.86 μ in the i.r. spectrum (Figure 9). The n.m.r. spectrum exhibits two methyl singlet at 1.06 and 1.22 δ, a seven proton multiplet at 1.30 to 2.50 δ, and a two proton multiplet at 2.50 to 3.50 δ. The hydroxyl proton absorption occurs as a broad singlet at 11.32 δ. The mass spectrum (Figure 10) shows a strong parent ion at m/e 184. Esterification with ethanol gives the keto-ester, ethyl (2-keto-3,3-dimethylcyclohexyl)-acetate (XCIV). The i.r. and n.m.r. spectra of the keto-ester (XCIV) are identical to the spectra of synthetic keto-ester.

The keto-ester (XCIV) was synthesized by alkylation of 2,2-dimethyl-cyclohexanone with ethyl bromoacetate. The infrared spectrum (Figure 9) of XCIV exhibits two characteristic carbonyl stretching bands at 5.75 and

and 5.85 μ. The n.m.r. spectrum has two methyl singlets at 1.00 and 1.20

δ and a methyl triplet (^{3}J, 7.0 Hz.) at 1.22 δ. The methylene of the ethyl

group appears as a quartet (^{3}J, 7.0 Hz.) at 4.05 δ. The remaining methylene

and methine protons occur as a seven proton multiplet at 1.40 to 2.40 δ

and two proton multiplet at 2.40 to 3.40 δ. The mass spectrum (Figure 10)

exhibits a weak parent ion at m/e 212.

The identity of the synthetic keto-ester with keto-ester from degra-

dation of *cis*-cyclobutane (LXXXV) rigorously establishes the proposed

orientation of photoaddition of 4,4-dimethyl-2-cyclohexenone to 1,1-

dimethoxyethylene.

Photorearrangement and photoreduction

Chapman *et al.* (32) have shown that 4,4-dimethyl-2-cyclohexenone

(XXXV) photorearranges in *t*-butyl alcohol to 6,6-dimethylbicyclo[3.1.0]-

hexan-2-one (XLII) and 3-isopropyl-2-cyclopentenone (XLIII). In isopropyl

alcohol two new products are observed, 4,4-dimethylcyclohexanone (XCVI)

XXXV   XLII   XLIII
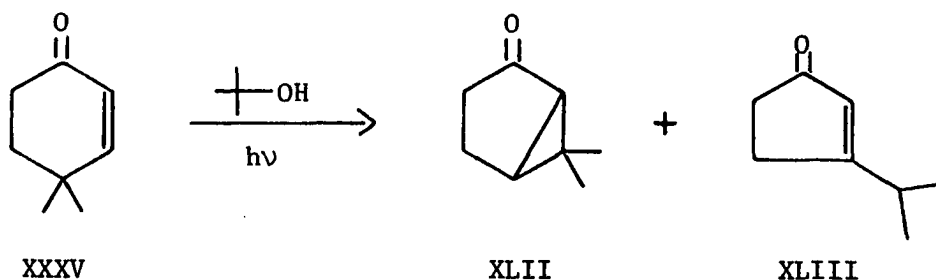
and 3-isopropylcyclopentanone (XCVII). 4,4-Dimethylcyclohexanone (XCVI)

was isolated by preparative g.l.p.c. and identified by comparison of its

i.r. spectrum, n.m.r. spectrum, and melting point 38.5-40.5° [literature

38-41° (66)] with an authentic sample prepared by catalytic hydrogenation of 4,4-dimethyl-2-cyclohexenone.
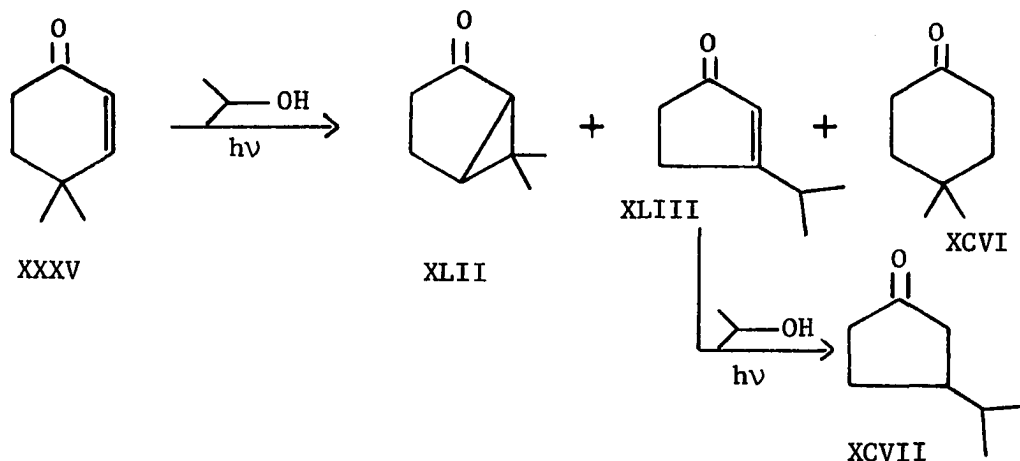
3-Isopropylcyclopentanone (XCVII) is a secondary photoproduct resulting from photoreduction of 3-isopropyl-2-cyclopentenone. Cyclopentanone XCVII was isolated by preparative g.l.p.c. and identified by comparison of its i.r. and n.m.r. spectra with spectra reported by Rettig (21). Rettig obtained XCVII by catalytic hydrogenation of 3-isopropyl-2-cyclopentenone (XLIII).

Quantitative Investigation of the Photochemistry
of 4,4-Dimethyl-2-cyclohexenone

The mechanism of photorearrangement and photocycloaddition of 4,4-dimethyl-2-cyclohexenone was investigated by observing the effect of perturbation of reaction conditions on the efficiency. The efficiency is measured by the quantum yield, defined as the number of molecules that react divided by the number of molecules that absorb light. The perturbations employed include variation of solvent, temperature, and concentration and addition of quenchers and sensitizers.

Both solvent and temperature affect the quantum yield of photo-
rearrangement and photocycloaddition of 4,4-dimethyl-2-cyclohexenone.
Table 5[1] shows the effect of solvent on the relative quantum yield of
rearrangement. t-Butyl alcohol was chosen as a standard and assigned a
relative quantum yield of 1.00. The quantum yields in other solvents are
expressed as ratios of the quantum yield to the quantum yield in t-butyl
alcohol. Photorearrangement occurs most efficiently in polar solvents,
capable of hydrogen bonding. In isopropyl alcohol photoreduction to 4,4-
dimethylcyclohexanone occurs in addition to rearrangement. Some polar
solvent, $e.g.$, acetonitrile and N-methyl-2-pyrrolidone, without hydrogen
bonding capabilities promote rearrangement, but not as efficiently as the
polar hydrogen bonding solvents. In benzene and hexane 4,4-dimethyl-2-
cyclohexenone appears to be photostable ($\phi < 0.0003$). The quantum yields
of formation and destruction are smaller than the corresponding quantum
yields in t-butyl alcohol by a factor of at least fifty. Zimmerman et $al.$
(34) observe that solvent has very little effect on the quantum yield of
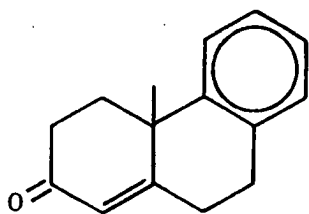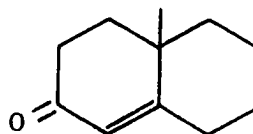
XLVI   XLVII

[1]Tables occur in the thesis in numerical order. Tables 1 and 2 are
in the Results and Discussion Section. The remaining tables are in the
Experimental Section. Page numbers for the tables are given in the List
of Tables at the beginning of the thesis.

rearrangement of phenanthrone XLVI and octalone XLVII (*vide supra*).

The effect of solvent on photocycloaddition is expressed in Table 1.

Oxetane exhibits the most dramatic change. In hexane oxetane is the major

product; in benzene oxetane is a minor product and in *t*-butyl alcohol

oxetane is not an observable product. As a result it has not been possible

to study rearrangement and oxetane formation concurrently. The ratio of

cis-cyclobutane to *trans*-cyclobutane changes from 0.88 in hexane to 0.59

in *t*-butyl alcohol. Like rearrangement, the overall quantum yield of

photocycloaddition is higher in polar solvents than in non-polar solvents.

Table 1. Effect of solvent on the quantum yield of photocycloaddition[a]

Solvent	$\phi_{oxetane}$	ϕ_{cis}	ϕ_{trans}	ϕ_{total}
t-butyl alcohol[b]	0.000	0.022	0.037	0.060
benzene	0.0014	0.0036	0.0053	0.010
hexane	0.0046	0.0029	0.0033	0.011

[a]For 0.10 M 1,1-dimethoxyethylene, 0.20 M 4,4-dimethyl-2-cyclo-
hexenone, temperature 43°.

[b]The quantum yield of rearrangement was 0.011.

The effect of solvent on photocycloaddition is well documented. As

mentioned previously, solvent significantly influences product ratios in

photodimerization of cyclopentenone, cyclohexenone, and isophorone (see

Review of Literature Section). In the photoaddition of isophorone to 1,1-

dimethoxyethylene, the *cis*-cyclobutane to *trans*-cyclobutane product ratio

decreases in going from non-polar to polar solvents.[1]

The effect of temperature on photocycloaddition and photorearrangement is presented in Tables 14 and 15, respectively. Higher temperatures favor formation of oxetane in both hexane and benzene solution, although the effect is not dramatic. Lower temperatures favor photorearrangement in *t*-butyl alcohol. The change in quantum yield of rearrangement as a function of temperature is expressed by a linear plot in Figure 11. At liquid nitrogen temperature no detectable photorearrangement occurs. As a result the quantum yield of rearrangement must reach a maximum someplace between 28° and -190°.

The temperature effects may be explained in terms of rates. In the photocycloaddition reaction the activation energy (vibrational energy in the excited state) for oxetane formation may be a little higher than the activation energy for cyclobutane formation for steric reasons. Consequently the rate of oxetane formation may show more temperature dependence than predicted by a mere change in the rate of collision. In the photorearrangement reaction the rate of decay of the excited state may increase with temperature faster than the rate of rearrangement. This is reasonable since decay can result in part from bimolecular processes which naturally increase in rate with temperature.

The solvent and temperature effects are important when photorearrangement and photocycloaddition are employed in synthesis. This is exemplified by the preparative photocycloaddition reaction described earlier (Page 41).

---

[1]O. L. Chapman and P. J. Nelson, Department of Chemistry, Iowa State University of Science and Technology, Ames, Iowa. Private communication. 1968.

Figure 11.   The effect of temperature on the quantum yield of photo-
          rearrangement; slope $-(0.148 \pm 0.024) \times 10^{-3}$ deg.$^{-1}$
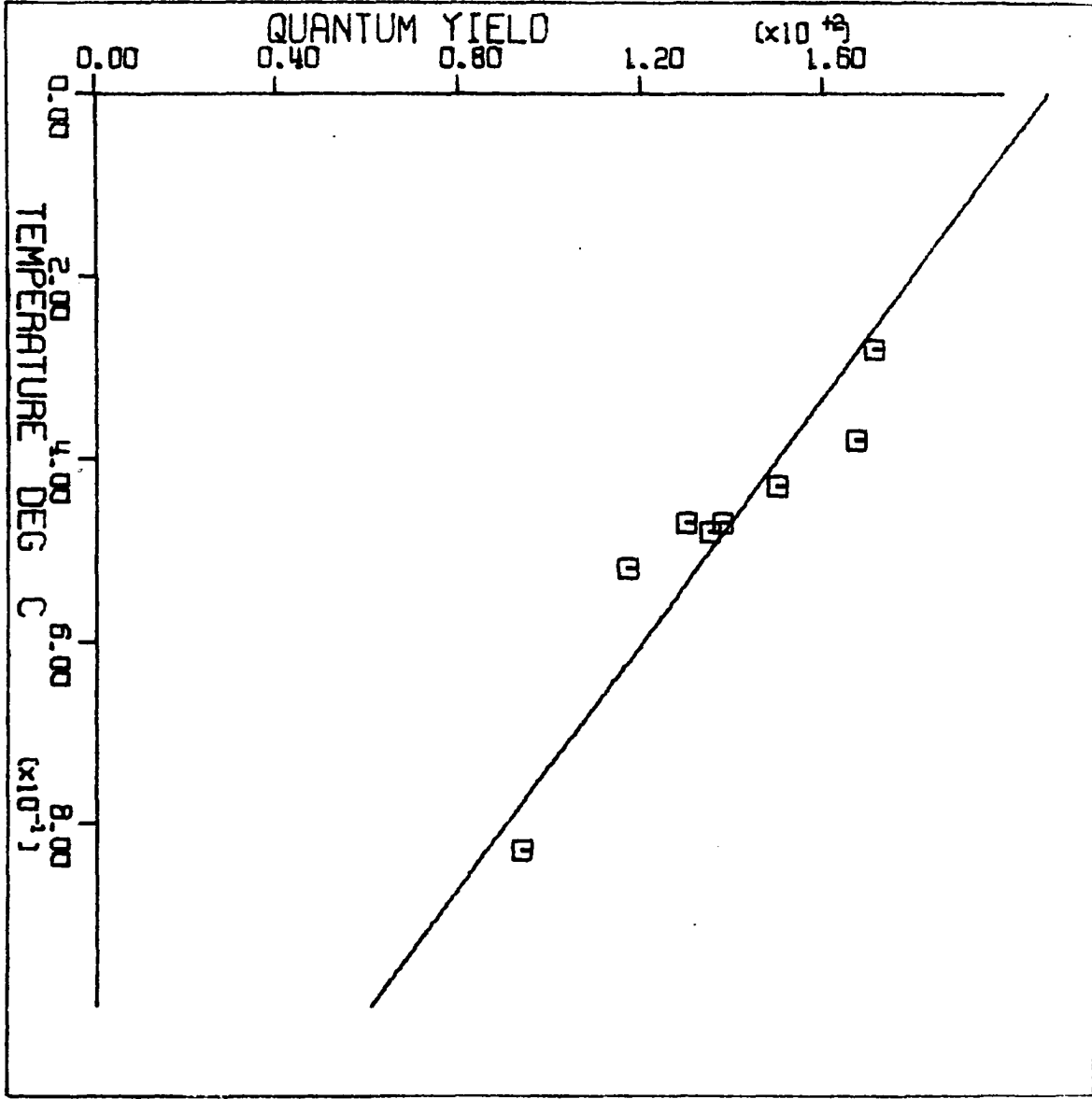
A high concentration of 1,1-dimethoxyethylene and 4,4-dimethyl-2-cyclo-hexenone in hexane solution was irradiated at room temperature. The high polarity of the effective solvent as a result of high concentrations of reactants coupled with the low temperature gave only a 20% yield of oxetane. With the conditions described in Table 1 (43°, 0.10 M olefin, 0.20 M enone), a 42% yield of oxetane was obtained in hexane solution. Corey *et al.* (14) report no oxetane product from the irradiation of 2-cyclohexenone and 1,1-dimethoxyethylene in pentane solution; however, the irradiation was done at high concentrations of reactants and Dry Ice-ethanol temperature. The yield of *trans*-cyclobutane can be maximized by using *t*-butyl alcohol as a solvent. The best conditions for rearrangement are low temperature and aqueous ethanol (20% water) solvent.

The reciprocal of quantum yield of photocycloaddition shows a linear dependence on the reciprocal of olefin concentration in both hexane and benzene solution. This linearity is displayed by plots of $1/\phi$ versus $1/[O]$ for total cycloadduct formation in hexane and benzene in Figures 12 and 14, respectively. Figures 13 and 15 show the same data plotted for individual product formation. The slopes and intercepts reported with standard deviations were obtained by least squares analysis. The negative intercepts do not have physical reality and may reflect a slight solvent effect caused by changing 1,1-dimethoxyethylene concentration. In other words a linear plot may not be the best representation of the data. There is no indication, however, that the product ratios are a function of olefin concentration over the range studied in these plots. The preparative photocycloaddition reaction does indicate that the product ratios are different at 0.5 M olefin. Hammond and co-workers (9) observed signifi-

Figure 12. Plot of reciprocal of total quantum yield of photocycloaddition versus reciprocal of olefin concentration in hexane; slope 8.55 ± 0.20 moles/ℓ, intercept 1.81 ± 1.81
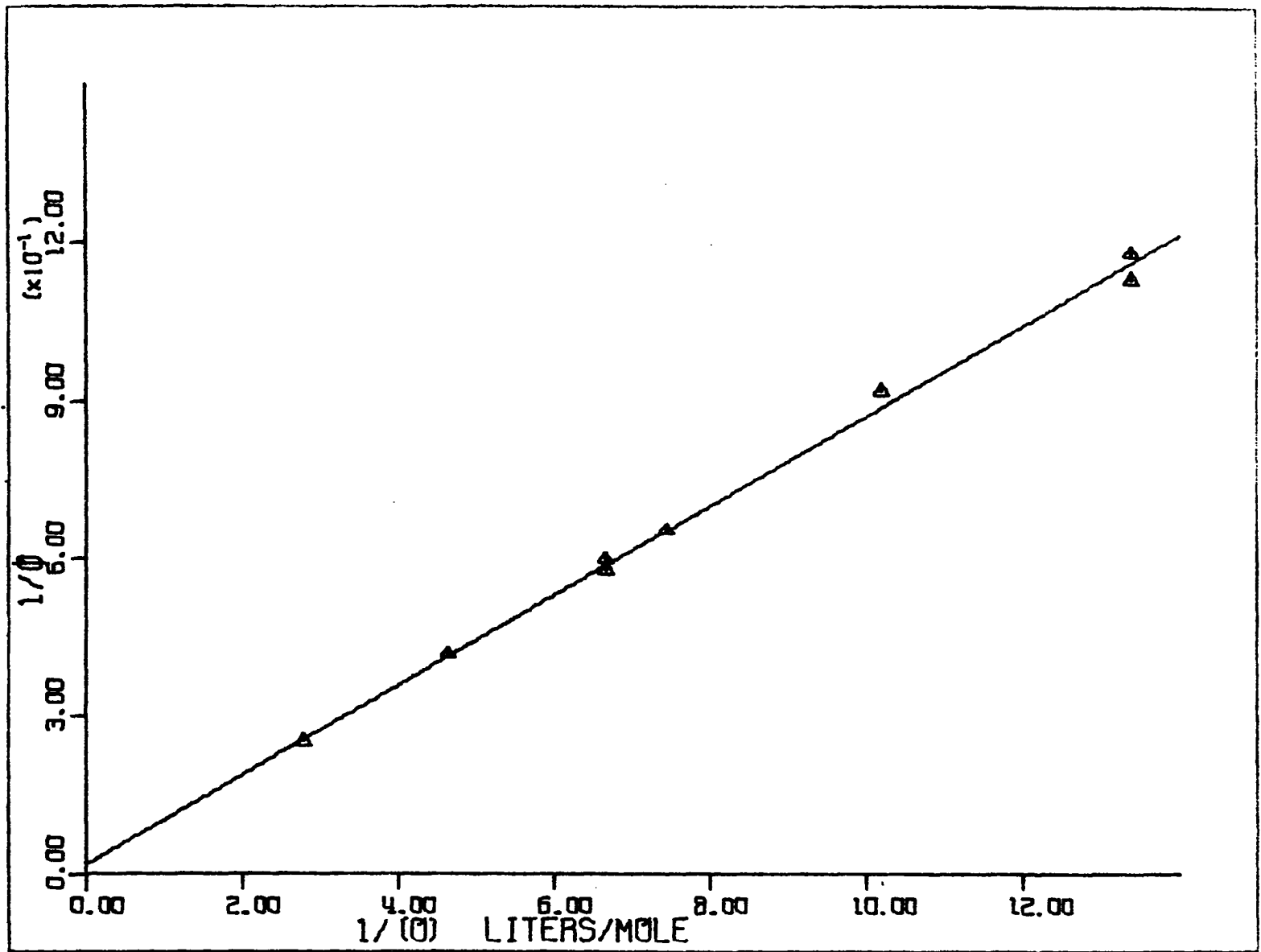
Figure 13. Plots of reciprocal of quantum yield of formation of photocycloadducts versus reciprocal of olefin concentration in hexane

* - oxetane; slope 18.6 ± 0.9 moles/ℓ, intercept 11.6 ± 8.0

□ - *cis*-cyclobutane; slope 35.4 ± 1.3 moles/ℓ, intercept -3.91 ± 11.3

△ - *trans*-cyclobutane; slope 28.9 ± 0.5 moles/ℓ, intercept -2.72 ± 4.24
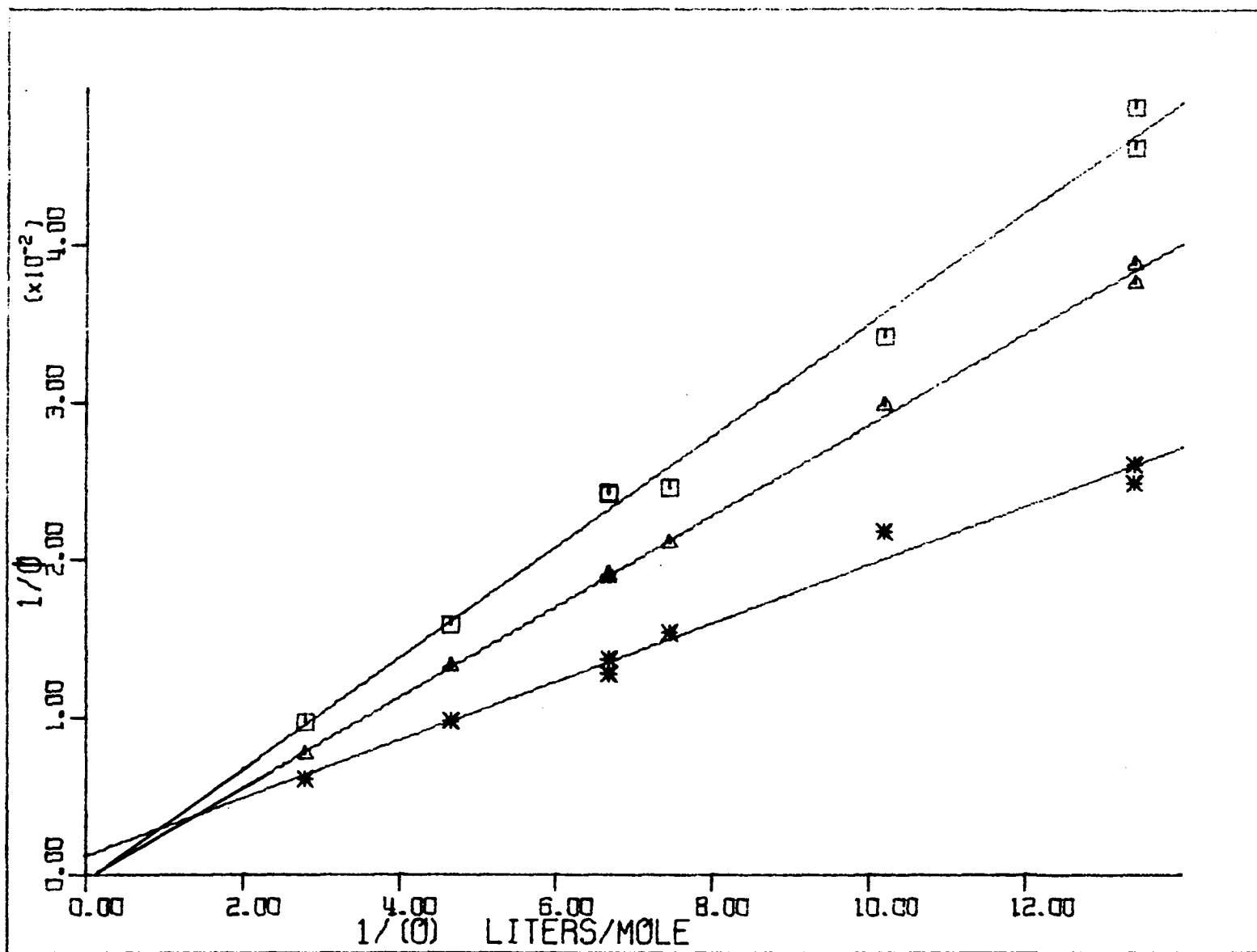
Figure 14. Plot of reciprocal of total quantum yield of photocycloaddition versus reciprocal of olefin concentration in benzene; slope 10.1 ± 0.2 moles/ℓ, intercept -2.3 ± 2.0
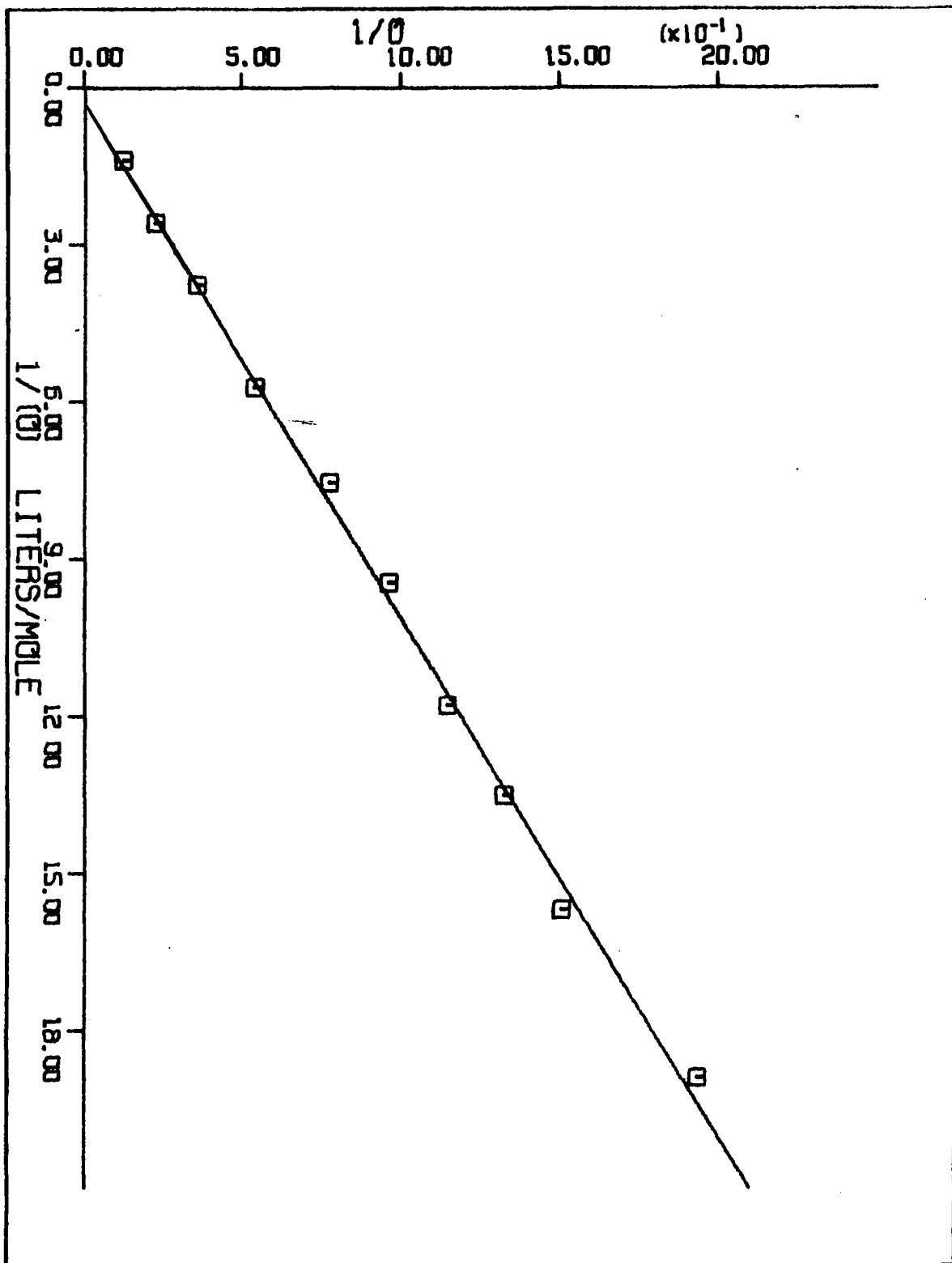
Figure 15. Plots of reciprocal of quantum yield of formation of photocycloadducts versus reciprocal of olefin concentration in benzene

☐- oxetane; slope 82.8 ± 5.2 moles/ℓ, intercept -34.8 ± 55.1

* - *cis*-cyclobutane; slope 29.1 ± 0.4 moles/ℓ, intercept -8.3 ± 4.4

△- *trans*-cyclobutane; slope 19.1 ± 0.3 moles/ℓ, intercept -2.5 ± 3.5
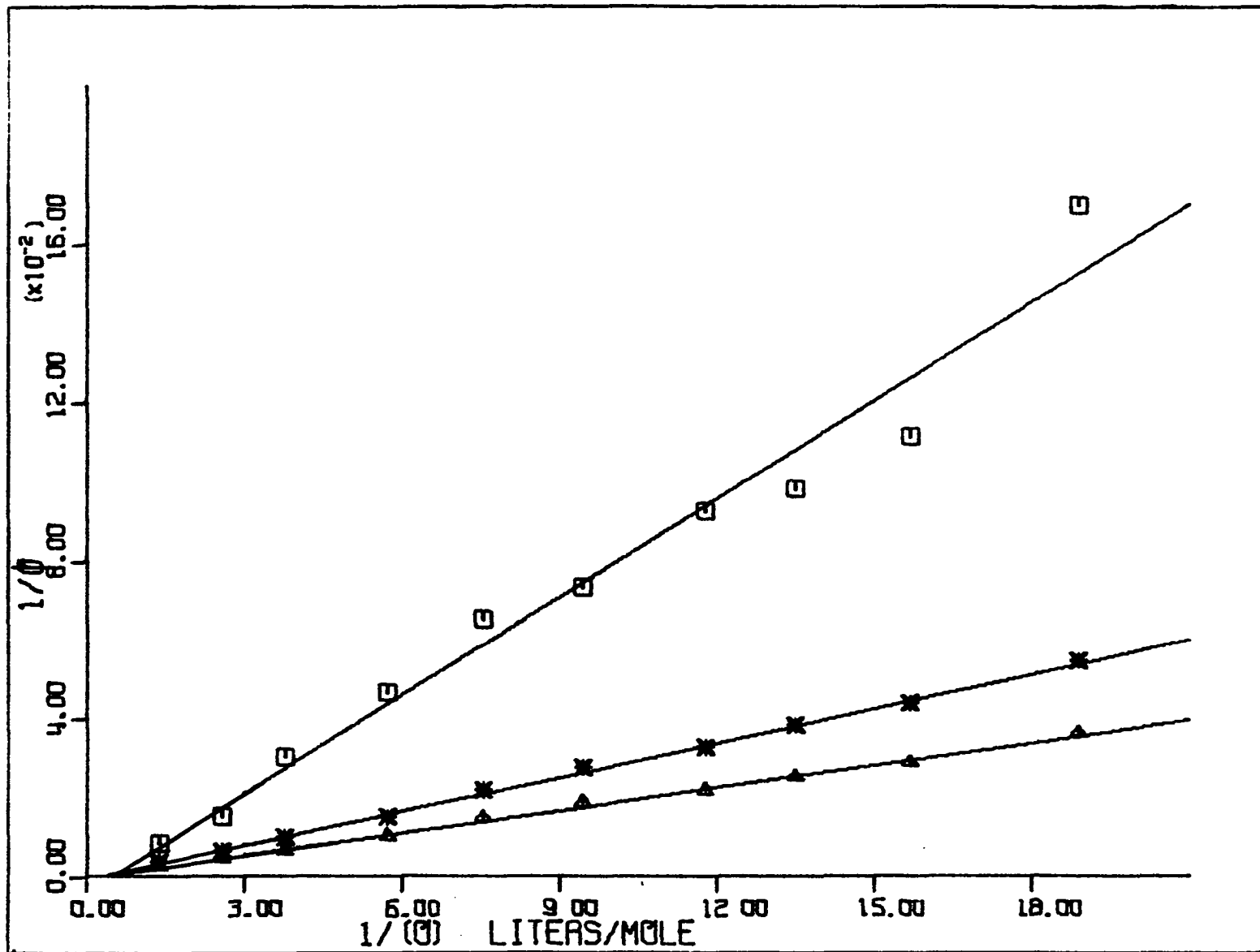
cant bending of a plot of reciprocal of quantum yield versus reciprocal of olefin concentration for photodimerization of 2-cyclohexenone. Irrespective of a slight solvent effect, the plots (Figures 12, 13, 14, and 15) are in harmony with a simple bimolecular mechanism in which excited enone reacts with ground state olefin.

Sensitization data (Table 13) indicate that photocycloaddition results from a triplet state of 4,4-dimethyl-2-cyclohexenone. In the presence of either triphenylamine (E_T 71)[1] or triphenylene (E_T 66), absorbing most of the incident light, the photocycloaddition reaction proceeds identically (within 5% experimental error) to the same reaction in the absence of the sensitizers. In other words the quantum yield and product ratios are the same whether the enone triplet is populated by intersystem crossing or triplet energy transfer. The sensitization experiment, described here for establishing a triplet state for the photocycloaddition reaction, has been called the fingerprint technique by Zimmerman (68). Zimmerman argues that product ratios represent a fingerprint of a photochemical reaction. If sensitization of a reaction gives the same product ratio, or fingerprint, as the unsensitized reaction, then the sensitized and unsensitized reactions must be resulting from the same triplet state.

Since the singlet energies of both triphenylene and triphenylamine are probably higher than the n-π^* singlet energy of 4,4-dimethyl-2-cyclohexenone, the probability of singlet energy transfer should be considered. In the sensitization experiments the concentration of 4,4-dimethyl-2-cyclo-

---

[1]Triplet energies of sensitizers and quenchers were taken from Reference 67, unless otherwise specified.

hexenone in benzene was 0.10 M. The rate of diffusion of 4,4-dimethyl-2-cyclohexenone and sensitizers in benzene is estimated to be 10^{10} ℓ/mole/ sec. at 45° by the Debye equation (69) assuming equal collisional diameters. Hence, the pseudounimolecular rate of collision of sensitizer molecules with enone molecules is 10^9 sec.$^{-1}$ Using 0.88 for the intersystem crossing efficiency of triphenylamine and 0.5 for the oscillator strength ($f_{S_0-S_1}$) of the $S_0 \rightarrow S_1$ transition, Hammond and co-workers (70) calculated a relative rate of intersystem crossing for triphenylamine equal to 3.7. The relative rate of intersystem crossing of acetophenone was estimated to be greater than or equal to unity. The absolute rate of intersystem crossing of triphenylamine at room temperature has not been determined. Wilkinson and Dubois (71) estimate the singlet lifetime of acetophenone to be $\leq 10^{-10}$ sec. at room temperature. Since the intersystem crossing efficiency of aceto-phenone is unity (70), the rate of intersystem crossing of acetophenone must be $\geq 10^{10}$ sec.$^{-1}$ The relative rates of intersystem crossing for acetophenone and triphenylamine are of the same order of magnitude as indicated by Hammond's calculation (70). Therefore, the absolute rate of intersystem crossing of triphenylamine is approximately 10^{10} sec.$^{-1}$ If triphenylamine transfers singlet energy by collision, then the rate of intersystem crossing is ten times the rate of singlet energy transfer. Hence, 90% of the observed sensitization of photocycloaddition by tri-phenylamine is triplet sensitization. Bartlett and Engel (72) have shown that triphenylene efficiently transfers singlet energy to azo-2-methyl-2-propane. The slope of a Stern-Volmer plot for quenching of triplenylene fluorescence by azo-2-methyl-2-propane indicates that the singlet life-time of triphenylene is 2×10^{-8} sec. Hence the possibility of singlet

sensitization of photocycloaddition by triphenylene cannot be eliminated.

Thioxanthone (E_T 65), phenanthrene (E_T 62), and Michler's ketone (E_T 61) give only marginal sensitization of photocycloaddition (Table 13). The Michler's ketone data must be considered separately, since Michler's ketone is destroyed during irradiation and pinacols of 4,4-dimethyl-2-cyclohexenone are major products.

Porter and Wilkinson (73) have observed that when the triplet state energy of the sensitizer is less than 5 kcal. above the triplet state energy of the acceptor, the probability of energy transfer is low. Consequently, the triplet energy of 4,4-dimethyl-2-cyclohexenone is estimated at 61 kcal./mole above the ground state, 5 kcal. below the triplet state energy of triphenylene. Hammond and co-workers (9) have shown by three Saltiel plots that the triplet state energy of 2-cyclohexenone is 61 kcal./mole.

The photorearrangement of 4,4-dimethyl-2-cyclohexenone is also a triplet reaction. Rettig (21) has shown that benzophenone (E_T 69) sensitizes rearrangement of 0.05 M 4,4-dimethyl-2-cyclohexenone giving approximately the same fingerprint as the unsensitized reaction. Di-t-butyl nitroxide quenches rearrangement. The quenching is illustrated by a linear Stern-Volmer plot (slope 30.1 ± 1.4 ℓ/mole) in Figure 16.

A Stern-Volmer plot is a plot of the ratio of the quantum yield in the absence of quencher to the quantum yield in the presence of quencher versus the quencher concentration. The appearance of the Stern-Volmer plot is indicative of the photochemical state or states involved in the reaction. If the products come from only one state, the plot will be linear. If two or more states of different lifetimes yield the same

Figure 16. Stern–Volmer plot for quenching photorearrangement by di-*t*-butyl nitroxide in *t*-butyl alcohol; slope 30.1 ± 1.4 ℓ/mole
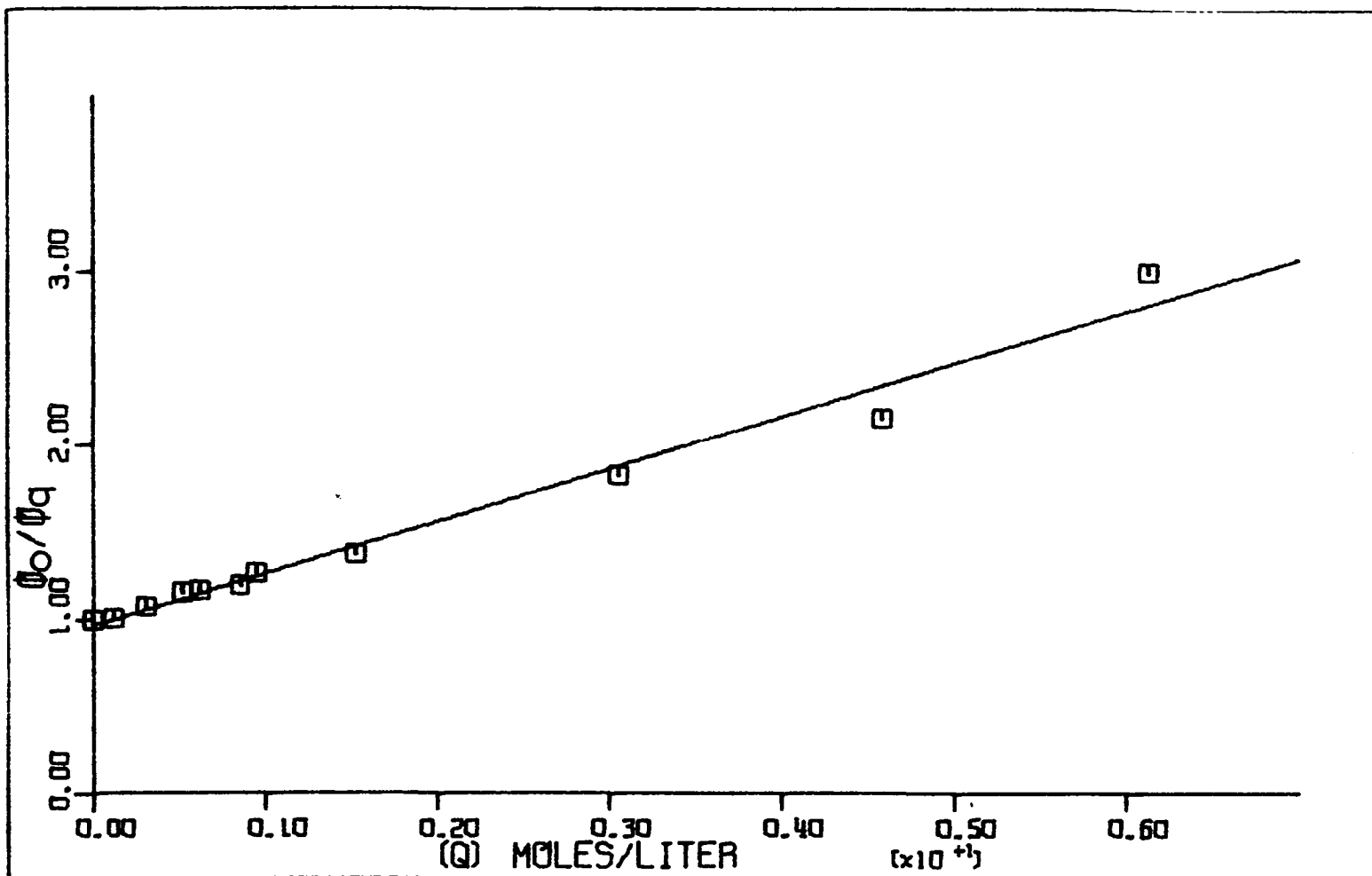
products and if both states are quenched, the plot will be non-linear, bending toward the abscissa. Yang (29) has reported an example of a non-linear Stern-Volmer plot. The slope of the Stern-Volmer plot is equal to the lifetime of the reactive species times the quenching rate constant. If the quenching rate constant is known, then the average reactive lifetime can be calculated. For the calculation of the lifetime, the quenching rate constant is generally assumed equal to the rate of diffusion calculated by the Debye equation (69).

Reactive lifetimes of singlet states ($\leq 10^{-8}$ sec.) are in general shorter than reactive lifetimes of tiplet states ($\geq 10^{-8}$ sec.). The fact that a reactive lifetime is short, however, does not demand that the reaction is occurring from the singlet state. The reactive lifetimes of 2-cyclopentenone (5) and 2-cyclohexenone (9) calculated from linear Stern-Volmer plots are 5×10^{-10} sec. and 7×10^{-10} sec., respectively. In both reactions the reactive states were assigned to the triplet manifold. The reactive lifetime of 4,4-dimethyl-2-cyclohexenone is also short. Using 1.55 centipoises (74) for the viscosity of t-butyl alcohol at 45°, the diffusion rate constant calculated by the Debye equation is 4.5×10^{9} ℓ/mole/sec. From the slope of the Stern-Volmer plot (Figure 16) and the diffusion rate constant the reactive lifetime of 4,4-dimethyl-2-cyclohexenone triplet state is 7×10^{-9} sec.

A simple kinetic scheme for photocycloaddition and photorearrangement consistent with the data presented is shown in Figure 17. In the mechanism both rearrangement and photocycloaddition result from the same triplet state, $^{3}K^{*}$. From the kinetic scheme, relationships between the quantum yields of product formation and olefin concentration and quencher con-

Figure 17. A one triplet mechanism for photocycloaddition and
            photorearrangement

$$K + h\nu \longrightarrow {}^1K^*$$

$${}^1K^* \xrightarrow{k_d} K$$

$${}^1K^* \xrightarrow{k_{ic}} {}^3K^*$$

$${}^3K^* \xrightarrow{k_r} \text{Rearrangement products}$$

$${}^3K^* + O \xrightarrow{k_o} \text{Oxetane}$$

$${}^3K^* + O \xrightarrow{k_c} \textit{cis-}\text{Cyclobutane}$$

$${}^3K^* + O \xrightarrow{k_t} \textit{trans-}\text{Cyclobutane}$$

$${}^3K^* \xrightarrow{k'_d} K$$

$${}^3K^* + Q \xrightarrow{k_q} K + Q^*$$

$${}^3S^* + K \longrightarrow {}^3K^* + S$$
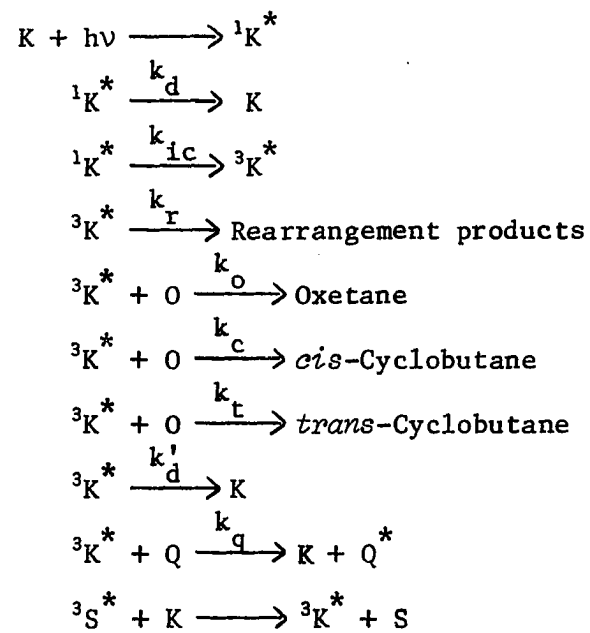
K ≡ 4,4-dimethyl-2-cyclohexenone

O ≡ 1,1-dimethoxyethylene

Q ≡ quencher

S ≡ sensitizer

Figure 18. Quantum yield relationships for the one triplet mechanism
            in Figure 17

18.1   Intersystem crossing efficiency $= \phi_{ic} = \dfrac{k_{ic}}{k_d + k_{ic}}$

Stern-Volmer equation

18.2 $\phi_o/\phi_q = 1 + \dfrac{k_q[0]}{k_r + k_d' + (k_o + k_c + k_t)[0]}$

18.3   when $[0] = 0 \quad \phi_o/\phi_q = 1 + \dfrac{k_q[Q]}{k_r + k_d'}$

18.4 $\phi_{rearrangement} = \dfrac{\phi_{ic} \, k_r}{k_r + k_d'}$

Dependence on olefin concentration

18.5 $1/\phi_{oxetane} = 1/\phi_{ic} \left[1 + \dfrac{k_c + k_t}{k_o} + \dfrac{k_d'}{k_o[0]} \right]$

18.6 $1/\phi_{cis} = 1/\phi_{ic} \left[1 + \dfrac{k_o + k_t}{k_c} + \dfrac{k_r + k_d'}{k_c[0]} \right]$

18.7 $1/\phi_{trans} = 1/\phi_{ic} \left[1 + \dfrac{k_o + k_c}{k_t} + \dfrac{k_r + k_d'}{k_t[0]} \right]$

18.8 $1/\phi_{total} = 1/\phi_{ic} \left[1 + \dfrac{k_r + k_d'}{(k_o + k_c + k_t)[0]} \right]$

centration (Figure 18) were derived with the assumption that the singlet ($^1K^*$) and triplet ($^3K^*$) species exist in a steady state. Since photochemical reactions are extremely fast the steady state approximation is valid.

The relationships in Figure 18 are consistent with the Stern–Volmer plot for rearrangement (Figure 16) and plots of reciprocal of quantum yield versus reciprocal of olefin concentration, Figures 12, 13, 14 and 15.

For bimolecular photocycloaddition reactions from triplet states, the intercept of a plot of reciprocal of quantum yield versus reciprocal of olefin concentration should approximate the reciprocal of the intersystem crossing efficiency (ϕ_{ic}). This is evident from equation 18.8 (Figure 18). Because of the solvent effects described above, the intercept is not a good measure of the intersystem crossing efficiency of 4,4-dimethyl-2-cyclohexenone.

Since the ratio of the quantum yield of the sensitized to the quantum yield of the unsensitized photocycloaddition reaction is essentially unity for sensitizers triphenylamine and triphenylene (Table 13), the intersystem crossing efficiency of 4,4-dimethyl-2-cyclohexenone is close to unity in benzene solution. DeMayo *et al.* (16) find that the intersystem crossing efficiency of 2-cyclopentenone is close to unity. The intercept of a plot of the reciprocal of quantum of dimerization versus reciprocal of 2-cyclohexenone concentration (9) indicates that the intersystem crossing efficiency of 2-cyclohexenone is 0.70.

With the assumption that the intersystem crossing efficiency of 4,4-dimethyl-2-cyclohexenone is unity in *t*-butyl alcohol, rate constants k_r and k'_d for rearrangement (Figure 17) can be calculated from the slope of

the Stern-Volmer plot (Figure 16) and the quantum yield. Since the rate constants k_r and k_d' and the quantum yield for rearrangement are temperature dependent, the quantum yield at the temperature at which the Stern-Volmer data was obtained must be used (45°). The quantum yield of rearrangement (from Figure 11) at 45° is 0.014. Assuming k_q is 4.5×10^9 ℓ/mole/sec. (rate of diffusion) k_r and k_d' were calculated to be 2.1×10^6 sec.$^{-1}$ and 1.5×10^8 sec.$^{-1}$, respectively, from equations 18.3 and 18.4 (Figure 18). See the Appendix for details of the calculation.

Zimmerman *et al.* (33, 34) report rate constants k_r and k_d' equal to 3×10^5 and 4×10^7 sec.$^{-1}$, respectively, for photorearrangement of phenanthrone XLVI at 25°.
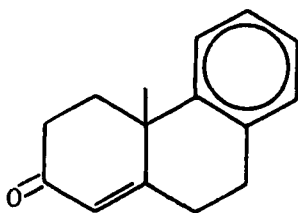
XLVI

Rettig (21) has reported some evidence that 4,4-dimethyl-2-cyclohexenone rearranges in part by way of the singlet state. The Stern-Volmer quenching plot (Figure 16) indicates that at least 70% of the rearrangement reaction is triplet derived. Hence the possibility that part of the reaction results from rearrangement of the singlet state still exists.

The kinetic scheme in Figure 17 predicts that the photocycloadducts, oxetane, *cis*-cyclobutane, and *trans*-cyclobutane, will be quenched equally.

In other words the three Stern-Volmer quenching plots for formation of each of the cycloadducts will have the same slope. The Stern-Volmer quenching plots for photocycloaddition are presented in Figures 19 and 20. Figure 19 shows a linear plot for quenching of total cycloadduct formation by di-t-butyl nitroxide (slope 98.0 ± 1.7). Figure 20 portrays the same data for individual product formation. Contrary to the prediciton of the kinetic scheme in Figure 17, the three Stern-Volmer quenching plots for formation of each of the cycloadducts have different slopes, 81.0 ± 2.1 (oxetane), 90.2 ± 2.0 ($trans$-cyclobutane), and 157 ± 2.4 ℓ/mole (cis-cyclobutane). The slopes of the quenching plots for formation of oxetane and $trans$-cyclobutane may be within experimental error, but the slope of the quenching plot for formation of cis-cyclobutane is distinctly different. The data in Figure 20 necessitate a change in the simple kinetic scheme presented in Figure 17.

Oxygen also preferentially quenches cis-cyclobutane adduct formation. The oxygen quenching ratios (ϕ_o/ϕ_q) are 3.16, 3.65, and 5.37 for oxetane, $trans$-cyclobutane, and cis-cyclobutane, respectively. These quenching ratios reflect the corresponding ratios obtained with 0.0285 M di-t-butyl nitroxide, 3.19, 3.40, and 5.37 for oxetane $trans$-cyclobutane, and cis-cyclobutane, respectively.

A number of other quenchers were investigated. Table 2 lists ϕ_o/ϕ_q ratios for quenching by 0.05 M naphthalene, 0.03 M 1-methylnaphthalene, 0.03 M p-terphenyl, 0.03 M biacetyl, and 0.03 M 1,3-cyclohexadiene as 1.37, 1.14, 1.00, 1.27, 1.04, respectively. None of these quenchers is very effective when compared with oxygen and di-t-butyl nitroxide. Furthermore, there was no evidence of differential quenching.

Figure 19.   Stern-Volmer plot for quenching photocycloaddition by di-*t*-butyl nitroxide in hexane, slope 98.0 ± 1.7 ℓ/mole
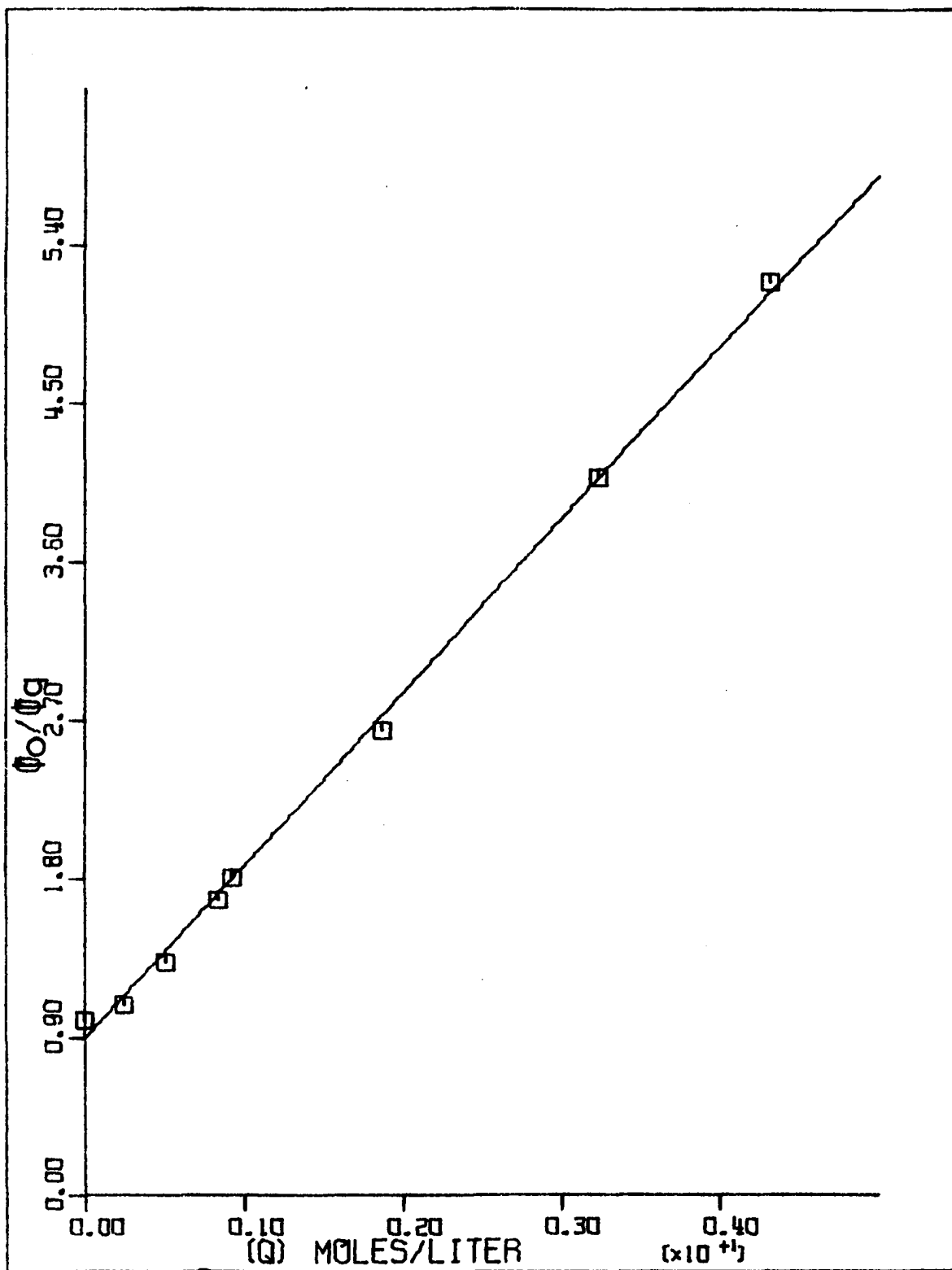
Figure 20. Stern-Volmer plots for quenching formation of photocyclo-
adducts by di-*t*-butyl nitroxide in hexane

☐ - oxetane; slope 81.0 ± 2.1 ℓ/mole

* - *cis*-cyclobutane; slope 157 ± 2.4 ℓ/mole

△ - *trans*-cyclobutane; slope 90.2 ± 2.0 ℓ/mole
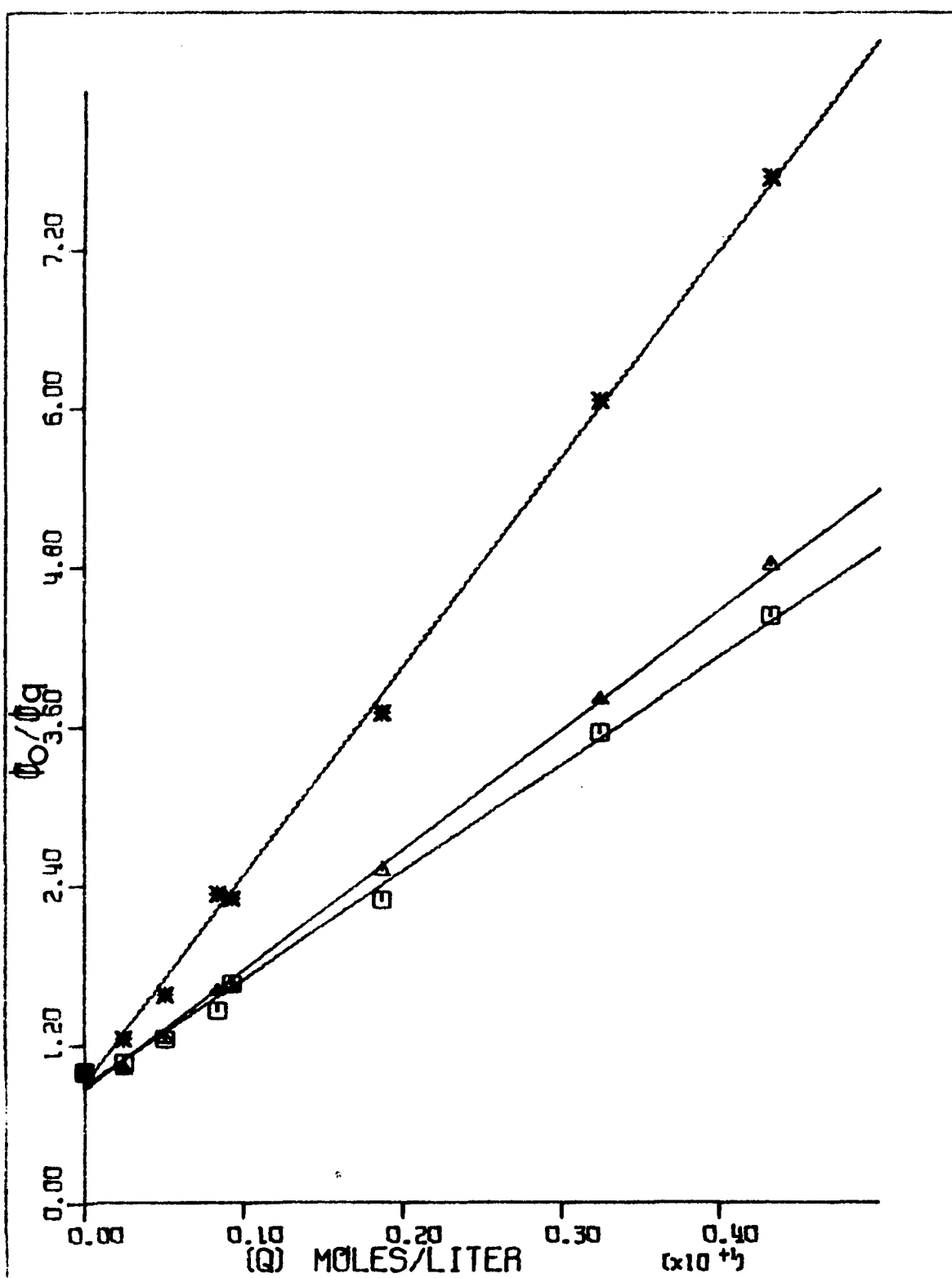
Table 2. Quenching of photocycloaddition

Quencher	[Q]	E^a (kcal./mole)	(Reference)	(ϕ_o/ϕ_q) total
di-t-butylnitroxide	0.032	53	(75)	4.20^b
oxygen	~0.01	37.7	(62)	3.74^b
napthalene	0.050	61	(67)	1.37
1-methylnaphthalene	0.030	61	(67)	1.14
p-terphenyl	0.030	58	(76)	1.00
biacetyl	0.030	54	(67)	1.27
1,3-cyclohexadiene	0.032	53.5	(58)	1.04

[a]Excitation energy or triplet energy.

[b]Differential quenching of cycloadducts observed.

In order to relate photorearrangement to photocycloaddition the two reactions were studied together in t-butyl alcohol. Irradiation of 4,4-dimethyl-2-cyclohexenone in the presence of low concentrations of 1,1-dimethoxyethylene (0.07 M) in t-butyl alcohol at 40° gives comparable yields of photorearrangement and photocycloaddition.

XXXV   XLII   XLIII   LXXXV   LXXXVI
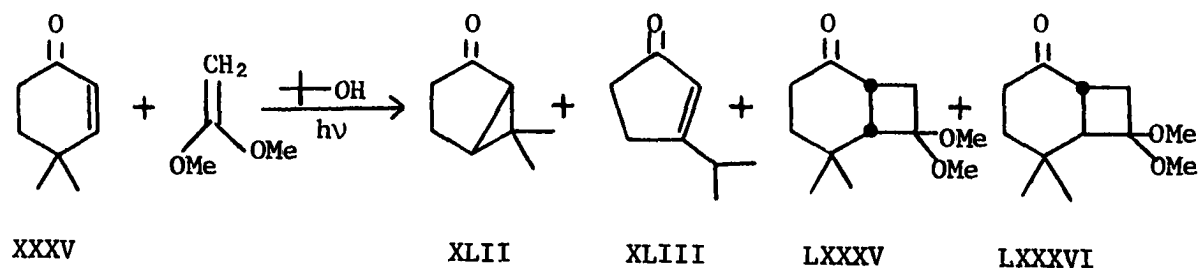
Figure 21 represents the Stern-Volmer plot for quenching photo-rearrangement and photocycloaddition by di-t-butyl nitroxide. Again the slopes of the three plots are different, 17.5 ± 2.0, 34.9 ± 4.2, and 75.6 ± 6.0 ℓ/mole for rearrangement, $trans$-cyclobutane, and cis-cyclobutane, respectively. As observed previously in Figure 21 formation of cis-cyclobutane is quenched more than formation of the other products.

The effect of olefin concentration on the quantum yield of photo-rearrangement and photocycloaddition is shown in Figures 22 and 23. Figure 22 shows a linear plot (slope 294 ± 30) of the reciprocal of quantum yield of rearrangement versus the olefin concentration. The presence of 1,1-dimethoxyethylene lowers the quantum yield of rearrangement, but not dramatically. In Figure 23, the plots of reciprocal of quantum yield of cis- and $trans$-cyclobutane formation versus reciprocal of olefin concentration deviate severely from linearity. This is in contrast to the linear plots in hexane and benzene solution, Figures 12 and 14.

A kinetic scheme which will explain the additional data must be complex. An example of such a scheme is presented in Figure 24. The major difference between the scheme in Figure 17 and the scheme in Figure 24 is the formation of daughter triplets ^3K and $^3K'$. Daughter triplet ^3K gives cis-cyclobutane and daughter $^3K'$ gives $trans$-cyclobutane and either re-arrangement or oxetane depending on conditions. The triplet $^3K^*$ is pre-sumed to be the spectroscopic triplet initially formed by intersystem crossing or energy transfer from sensitizers.

Quantum yield relationships based on the kinetic scheme in Figure 24 are listed in Figure 25. Stern-Volmer equations 25.2, 25.3, 25.4, and 25.5 predict that oxetane and $trans$-cyclobutane, and rearrangement and $trans$-

Figure 21. Stern-Volmer plots for quenching formation of photocycloadducts and photorearrangement products by di-*t*-butyl nitroxide in *t*-butyl alcohol

    * - photorearrangement products; slope 17.5 ± 2.0 ℓ/mole

    △ - *trans*-cyclobutane; slope 34.9 ± 4.2 ℓ/mole

    ⊡ - *cis*-cyclobutane; slope 75.6 ± 6.0 ℓ/mole
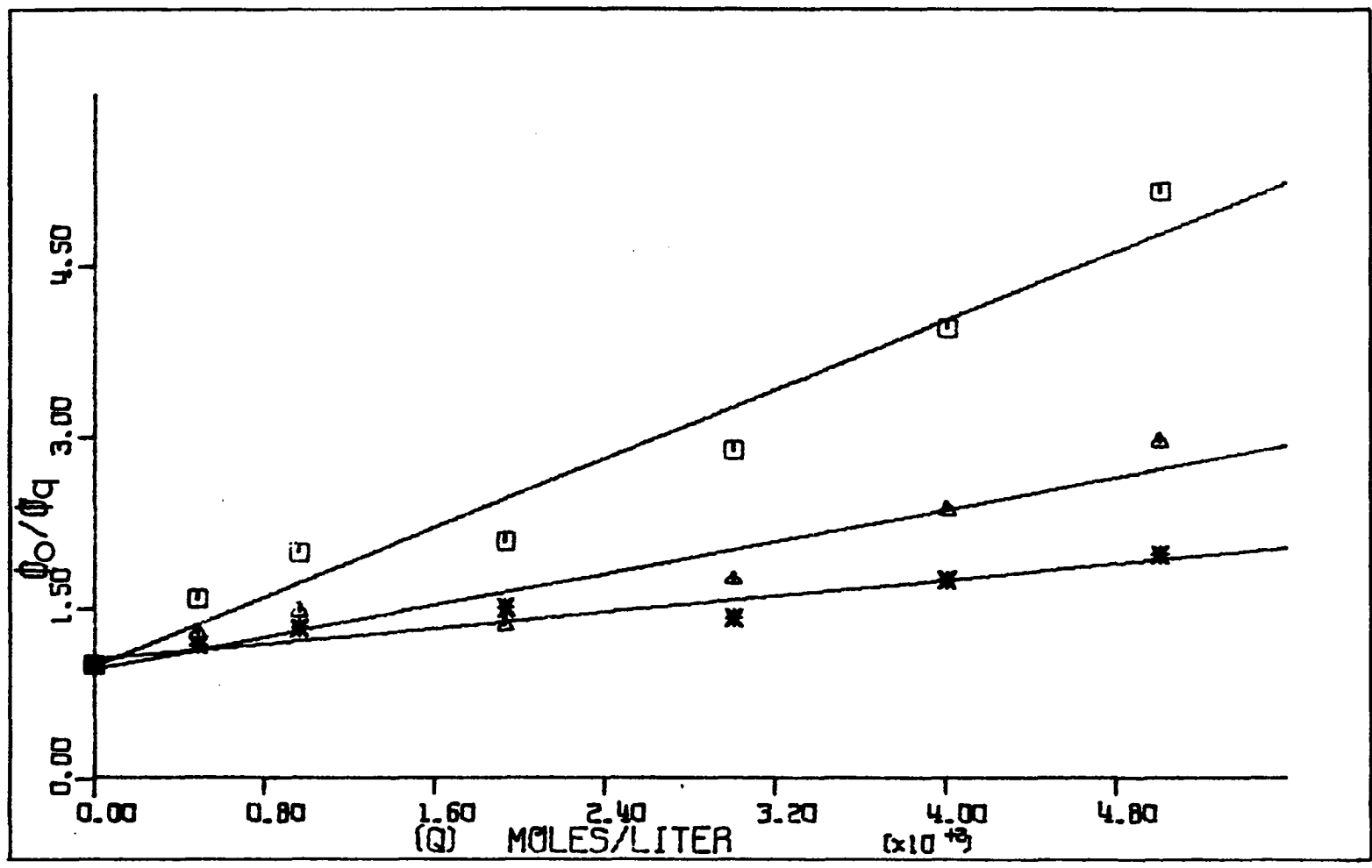
Figure 22. Plot of reciprocal of the quantum yield of photorearrangement versus olefin concentration in *t*-butyl alcohol; slope 294 ± 30 ℓ/mole, intercept 59.8 ± 3.2
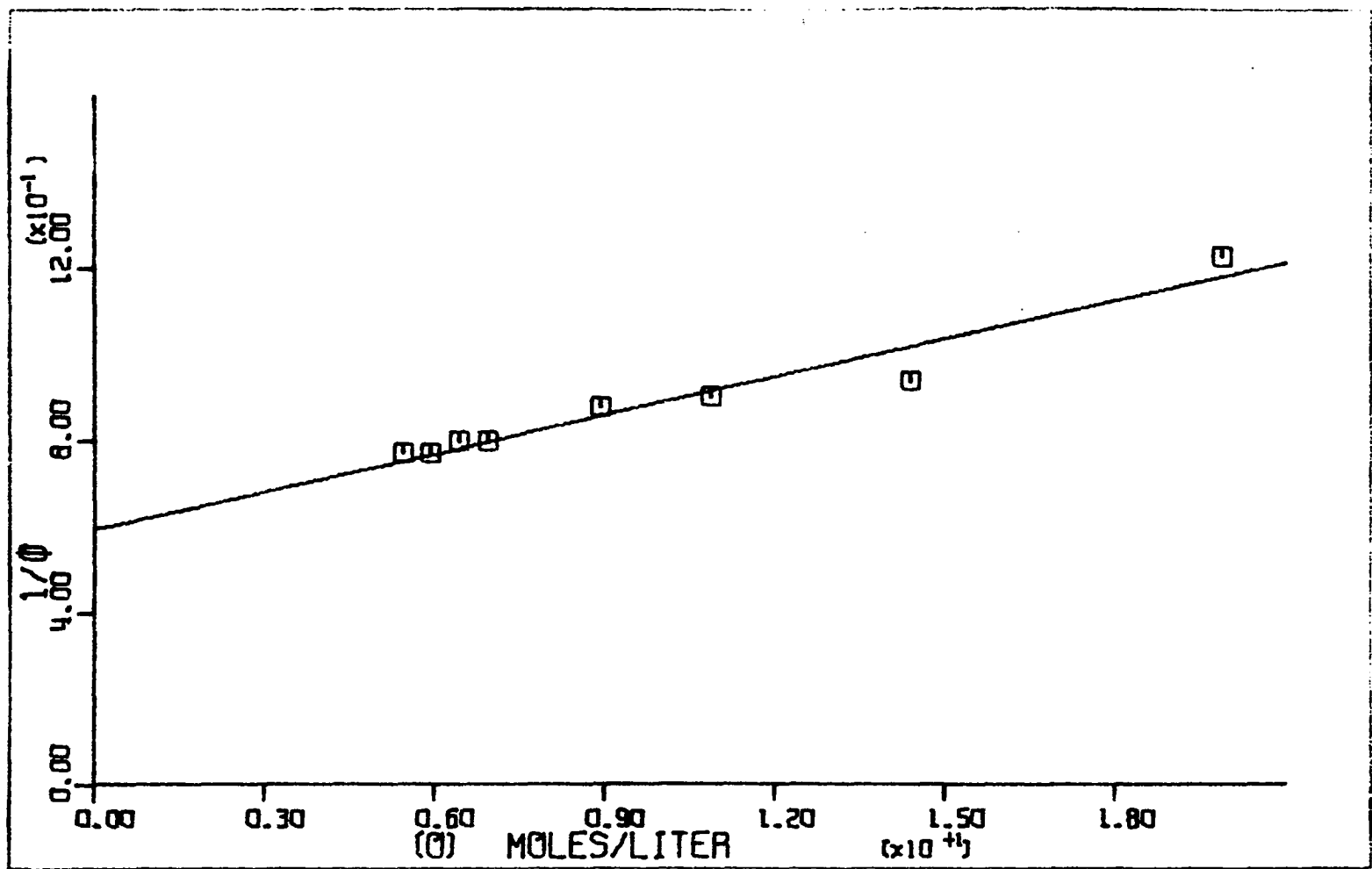
Figure 23. Plots of reciprocal of quantum yield of formation of photocycloadducts versus reciprocal of olefin concentration in t-butyl alcohol

◯ - *cis*-cyclobutane

☐ - *trans*-cyclobutane
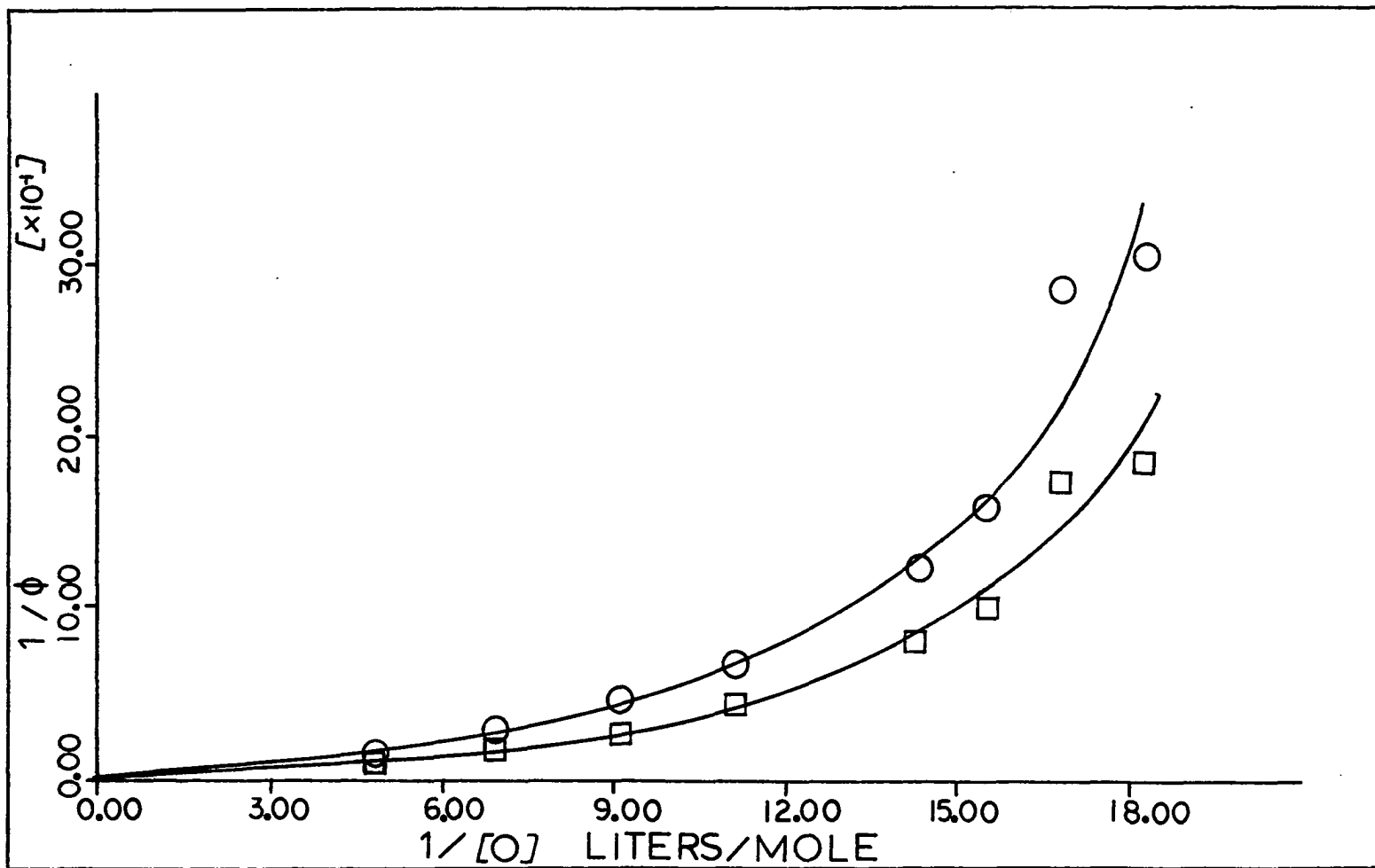
Figure 24.   A three triplet mechanism for photocycloaddition and
             photorearrangement

$$K + h\nu \longrightarrow {}^1K^*$$

$${}^1K^* \xrightarrow{k_d} K$$

$${}^1K^* \xrightarrow{k_{ic}} {}^3K^*$$

$${}^3K^* \xrightarrow{k_d'} K$$

$${}^3K^* \begin{cases} \xrightarrow{k_{it}} {}^3K \\ \xrightarrow{k_{it}'} {}^3K' \end{cases}$$

$${}^3K + O \xrightarrow{k_c} cis\text{-Cyclobutane}$$

$${}^3K \xrightarrow{k_d''} K$$

$${}^3K + Q \xrightarrow{k_q} K + Q^*$$

$${}^3K' + O \xrightarrow{k_o} \text{Oxetane}$$

$${}^3K' + O \xrightarrow{k_t} trans\text{-Cyclobutane}$$

$${}^3K' \xrightarrow{k_r} \text{Rearrangement products}$$

$${}^3K' \xrightarrow{k_d'''} K$$

$${}^3K' + Q \xrightarrow{k_q} K + Q^*$$

$${}^3S^* + K \longrightarrow {}^3K^* + S$$
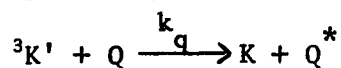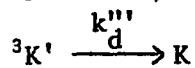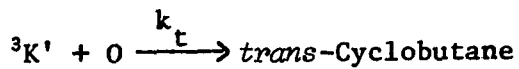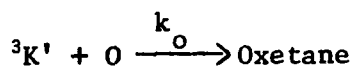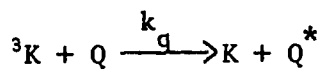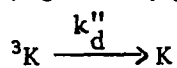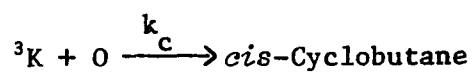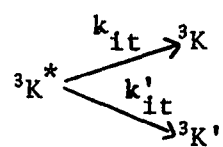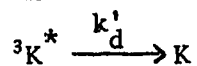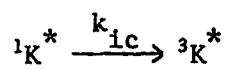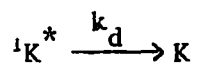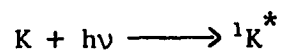
Figure 25.   Quantum yield relationships for the three triplet mechanism
             in Figure 24

$$25.1 \quad \phi_{ic} = \frac{k_{ic}}{k_{ic} + k_d} \quad , \quad \phi_{ic} = \frac{\phi_{ic} \; k_{it}}{k_{it} + k_d' + k_{it}'} \quad , \quad \phi_{ic}'' = \frac{\phi_{ic} \; k_{it}'}{k_{it} + k_d' + k_{it}'}$$

Stern–Volmer relationships

$$25.2 \quad (\phi_o/\phi_q)_{cis} = 1 + \frac{k_q \, [0]}{k_d + k_c[0]} = 1 + \tau k_q[Q]$$

$$25.3 \quad (\phi_o/\phi_q)_{oxetane} = 1 + \frac{k_q \, [Q]}{k_d''' + (k_o + k_t)[0]} = 1 + \tau' k_q[Q]$$

$$25.4 \quad (\phi_o/\phi_q)_{trans} = 1 + \frac{k_q \, [Q]}{k_d''' + k_r + (k_o + k_t)[0]} = 1 + \tau' k_q[Q]$$

$$25.5 \quad (\phi_o/\phi_q)_{rearrangement} = 1 + \frac{k_q \, [Q]}{k_d''' + k_r + k_t[0]} = 1 + \tau' k_q[Q]$$

Dependence on olefin concentration

$$25.6 \quad 1/\phi_{rearrangement} = 1/\phi_{ic}'' \left[1 + \frac{k_d'''}{k_r} + \frac{k_t[0]}{k_r} \right]$$

$$25.7 \quad 1/\phi_{trans} = 1/\phi_{ic}'' \left[1 + \frac{k_o}{k_t} + \frac{k_d + k_r}{k_t[0]} \right]$$

$$25.8 \quad 1/\phi_{oxetane} = 1/\phi_{ic}'' \left[1 + \frac{k_t}{k_o} + \frac{k_d'''}{k_o[0]} \right]$$

$$25.9 \quad 1/\phi_{cis} = 1/\phi_{ic}' \left[1 + \frac{k_d''}{k_c[0]} \right]$$

$$25.10 \quad \phi_{cis} = \frac{k_c[0]\phi_{ic}'}{k_d'' + k_c[0]}$$

$$25.11 \quad \phi_{oxetane} = \frac{k_o[0]\phi_{ic}''}{k_d''' + k_o[0] + k_t[0]}$$

$$25.12 \quad \phi_{trans} = \frac{k_t[0] \, _{ic}''}{k_d''' + k_o[0] + k_t[0]}$$

cyclobutane should have the same Stern-Volmer plots. Figure 20 indicates that oxetane and *trans*-cyclobutane have very similar Stern-Volmer plots; however, in Figure 21 the slope of the Stern-Volmer plot for *trans*-cyclobutane is twice the slope of the Stern-Volmer plot for rearrangement. The data for the Stern-Volmer plot in Figure 21 was obtained at 83°. Because the quantum yield of rearrangement is quite low at high temperatures, the analysis of the amount of rearrangement was difficult. As a result, the slope of the rearrangement Stern-Volmer plot in Figure 21 may be erroneous.

Equations 25.6, 25.7, 25.8, and 25.9 are reasonably consistent with the data. Plots of reciprocal of quantum yield versus reciprocal of olefin concentration are linear for oxetane, *cis*-cyclobutane, and *trans*-cyclobutane formation in hexane and benzene (Figures 13 and 15). A plot of the reciprocal of quantum yield of rearrangement versus olefin concentration (Figure 22) is also linear as predicted by equation 25.6. However, the non-linear plots of reciprocal of quantum yield of *cis*- and *trans*-cyclobutane formation versus reciprocal of olefin concentration in *t*-butyl alcohol (Figure 23) are not consistent with the kinetic scheme in Figure 24. If the mechanism is correct, then some or all of rate constants k_t, k_c, k_d'', and k_d''' must be a function of olefin concentration in *t*-butyl alcohol. Small changes in the olefin concentration, especially at low olefin concentration, may cause large changes in the effective viscosity of the solvent. *t*-Butyl alcohol probably solvates 4,4-dimethyl-2-cyclo-hexenone strongly. Hydrogen bonds to the carbonyl may be the reason oxetane is not a product in *t*-butyl alcohol solution. If the addition of small quantities of 1,1-dimethoxyethylene weakens the solvation of 4,4-dimethyl-2-cyclohexenone by alcohol molecules, then the rate constants

k_t and k_c should be a function of olefin concentration. Wagner (77, 78) has reported that viscous solvents such as t-butyl alcohol often cause non-linearity of Stern-Volmer plots.

If $trans$-cyclobutane and rearrangement are related by the same daughter triplet ($^3K'$) and if a plot of the reciprocal of quantum yield of $trans$-cyclobutane versus reciprocal of olefin concentration is non-linear, then the plot of the reciprocal of quantum yield of rearrangement versus olefin concentration ought to reflect this non-linearity. The plot of reciprocal of quantum yield of rearrangement versus olefin concentration is shown in Figure 22 as linear. There is not sufficient data to indicate that the plot does not bend in the high olefin concentration region ([O] > .14 M). The intercept (59.8 ± 3.2) of the plot in Figure 22 gives a value of 0.016 for the quantum yield of rearrangment at 40° at zero olefin concentration. The plot of quantum yield of rearrangement versus temperature (Figure 11) indicates that the quantum yield should be 0.014. If Figure 22 were redrawn to give the correct value for the intercept, then the plot would deviate from linearity at the high olefin concentration region as predicted. The absence of a dramatic change in the plot of reciprocal of quantum yield of rearrangement versus olefin concentration may simply reflect the inefficiency of the rearrangement reaction.

To explain the data observed some restrictions have to be placed on the triplet excited states $^3K^*$, ^3K, and $^3K'$. The lifetime of $^3K^*$ must be too short for effective quenching by low concentrations of di-t-butyl nitroxide. If all three triplets were quenched by di-t-butyl nitroxide, the Stern-Volmer plots in Figures 16, 19, 20, and 21 would be non-linear. An order of magnitude can be assigned to the lifetime of $^3K^*$. If the rate

of quenching by di-t-butyl nitroxide is diffusion controlled (k_q =
2.5 × 10^{10} ℓ/mole/sec.), then the maximum pseudounimolecular rate of
quenching observed is 0.043 moles/ℓ × 2.5 × 10^{10} ℓ/mole/sec. or 1.1 ×
10^9 sec.$^{-1}$ The rate of decay of $^3K^*$ is given by $k_{it} + k'_{it} + k'_d$ and must
be at least 10 × 1.1 × 10^9 sec.$^{-1}$ (ten times the pseudounimolecular rate
of quenching). Hence the lifetime of $^3K^*$ is $\leqslant$ 9 × 10^{-10} sec. The nature
of ^3K and $^3K'$ must be such that they are not produced directly by energy
transfer. Sensitization by triphenylamine, triphenylene, thioxanthone,
and phenanthrene does not lead to product ratios which differ from product
ratios obtained in the absence of sensitizers. Hence $^3K^*$ must be the 61
kcal./mole triplet and the only triplet populated by energy transfer and
intersystem crossing. Internal conversion of $^3K^*$ to ^3K and $^3K'$ may involve
a geometric or structural change. Then direct sensitization of ^3K and $^3K'$
would violate the Franck–Condon Principle.

The mechanism by which di-t-butyl nitroxide and oxygen are quenching
the photocycloaddition reaction must be considered. Buchachenko et al.
(75) have demonstrated that tertiary nitroxides structurally similar to
di-t-butyl nitroxide quench excited singlet states by exothermic energy
transfer. They estimate the 0-0 transition of the first absorption band
to be 53 kcal./mole above ground state. The fluorescence of rubrene (0-0
band 53 kcal./mole) is not quenched by tertiary nitroxides, but the fluo-
rescence of rodamine 6G (0-0 band 54 kcal./mole) is quenched by tertiary
nitroxides.

The possibility that di-t-butyl nitroxide is quenching 4,4-dimethyl-
2-cyclohexenone singlets by energy transfer can be eliminated. The maxi-
mum in the n-π^* absorption spectrum of 4,4-dimethyl-2-cyclohexenone indi-

cates that the singlet energy is approximately 84 kcal./mole above the ground state. If the singlet lifetime of 4,4-dimethyl-2-cyclohexenone is long enough, di-t-butyl nitroxide should quench 4,4-dimethyl-2-cyclohexenone singlets. If di-t-butyl nitroxide is quenching singlets, then biacetyl should also quench 4,4-dimethyl-2-cyclohexenone singlest. Biacetyl, a popular singlet quencher, has a low energy transition at 422 mμ (68 kcal./mole) and should quench 4,4-dimethyl-2-cyclohexene singlets by exothermic energy transfer. Table 2 indicates that biacetyl does not quench the photocycloaddition reaction efficiently. Hence the singlet lifetime of 4,4-dimethyl-2-cyclohexenone must be too short for quenching by collisional energy transfer. Di-t-butyl nitroxide must be quenching 4,4-dimethyl-2-cyclohexenone triplets. The mechanisms by which tertiary nitroxides quench triplet states is not known. The rate of triplet quenching by di-t-butyl nitroxide appears to be same as the rate of quenching by non-paramagnetic species. Zimmerman et al. (33, 34) have shown that di-t-butyl nitroxide quenches phenanthrone (XLVI) rearrangement as effectively as naphthalene. Yang et al. (29) have observed that di-t-butyl nitroxide is as effective as piperylene for quenching the photocycloaddition of benzaldehyde to trimethylethylene. The mechanism by which di-t-butyl nitroxide quenches the photocycloaddition of 4,4-dimethyl-2-cyclohexenone to 1,1-dimethoxyethylene must be more complicated than just collisional energy transfer. Di-t-butyl nitroxide and 1,3-cyclohexadiene have approximately the same quenching energies (53 kcal./mole). Yet di-t-butyl nitroxide quenches photocycloaddition very efficiently and 1,3-cyclohexadiene quenches very little (see Table 2). The quenching data may be explained in terms of the daughter triplet mechanism (Figure 24). If the

daughter triplets are structurally different from the spectroscopic triplet $^3K^*$, then quenching of the daughter triplets by vertical energy transfer would not give the ground vibrational level of the S_0 state of 4,4-dimethyl-2-cyclohexenone. Quenching by energy transfer may populate a high vibrational level of the S_0 state of 4,4-dimethyl-2-cyclohexeone or the ground state of high energy species structurally different from 4,4-dimethyl-2-cyclohexenone. In any event, for exothermic energy transfer to occur by a vertical process, the triplet energy of the quencher would have to be quite low (< 53 kcal./mole). Di-t-butyl nitroxide may be quenching the daughter triplets by a spin inversion process followed by thermal relaxation of vibrationally excited 4,4-dimethyl-2-cyclohexenone. Oxygen may be quenching by either exothermic energy transfer or spin inversion. The small quenching by naphthalene, 1-methylnaphthalene, biacetyl, and 1,3-cyclohexadiene (Table 2) that is observed is probably quenching of the spectroscopic triplet, $^3K^*$, by exothermic energy transfer.

Since the quenching of the daughter triplets by di-t-butyl nitroxide (^3K and $^3K'$) does not occur by simple exothermic energy transfer, the triplet energy of the daughter triplets cannot be established. The internal conversion of $^3K^*$ to ^3K and $^3K'$ is probably an exothermic process because of the large estimated rate constant for decay of $^3K^*$. Hence the triplet energies of the daughter triplets are somewhat less than 61 kcal./mole above the ground state of 4,4-dimethyl-2-cyclohexenone.

The three triplets $^3K^*$, $^3K'$, and ^3K are shown on an energy level diagram in Figure 26. The parent triplet $^3K^*$ is assigned to the spectroscopic T_1 state. Daughter triplets ^3K and $^3K'$ are produced by some undefined internal conversion process. Daughter triplets are shown in

Figure 26. An energy level diagram of 4,4-dimethyl-2-cyclohexenone
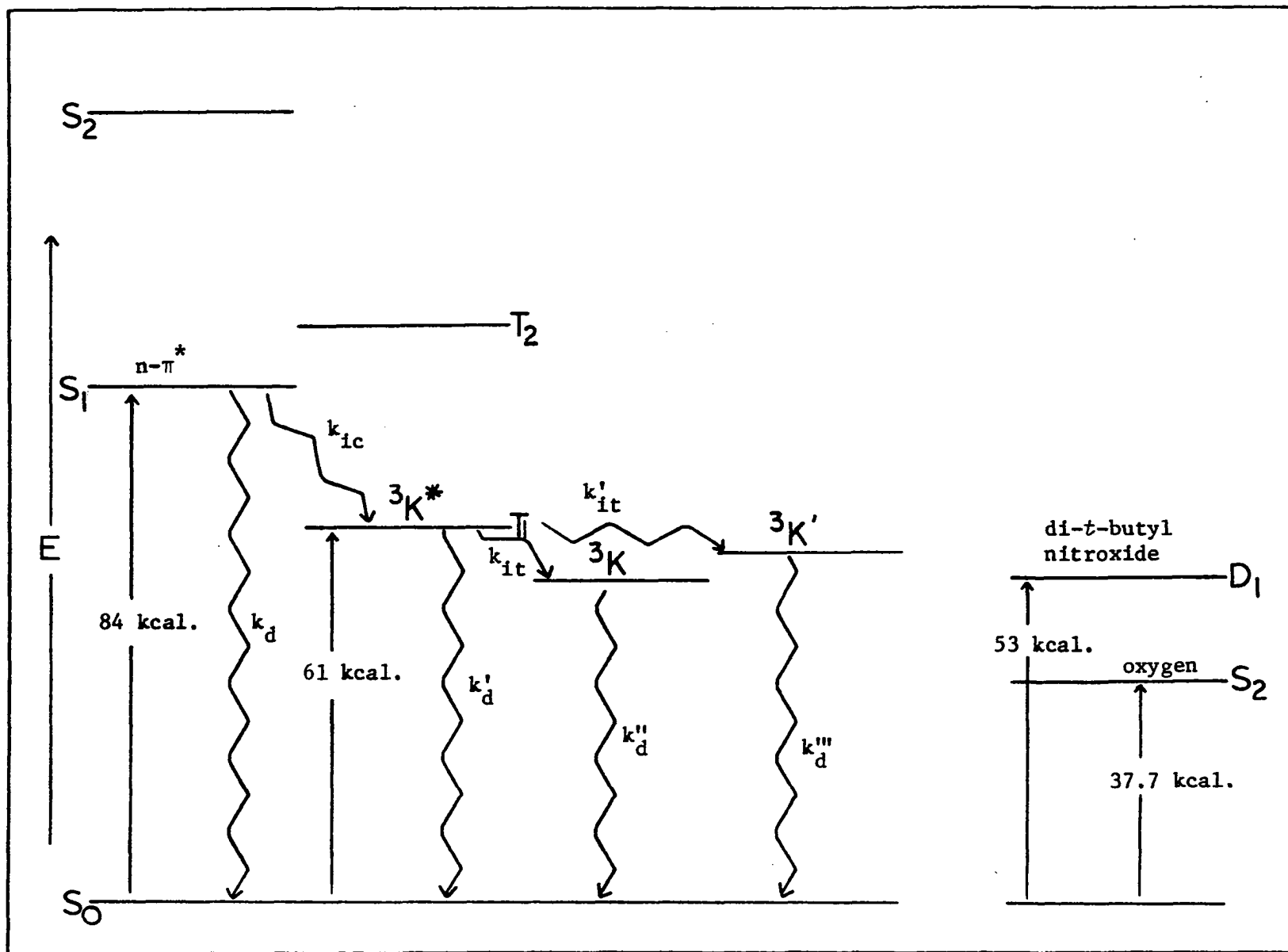
different triplet manifolds from each other and from the parent triplet.

If the daughter triplets were in the same manifold as $^3K^*$, then low energy

sensitizers would sensitize daughter triplets directly. The daughter

triplets are each shown in different manifolds because they must not be

interconvertible. Any mechanism involving interconversion of daughter

triplets does not lead to linear quantum yield expressions (Figure 25).

Likewise formation of ^3K and $^3K'$ from $^3K^*$ must be an irreversible process.

The data does not indicate the structural or electronic nature of

any of the triplets proposed. Even the electronic nature ($n-\pi^*$ or $\pi-\pi^*$)

of the spectroscopic triplet $^3K^*$ is unknown. Zimmerman (34) feels that

the lowest spectroscopic triplet of 2-cyclohexenone is $n-\pi^*$, and Hammond

(9) has stated that it is probably $\pi-\pi^*$. Even less is known about the

daughter triplets. They may differ from the parent triplet $^3K^*$ and each

other in structure and electronic configuration. The quenching and

sensitization data are consistent with a structural change. Some possible

structural changes include bond rotation, bond formation, and bond cleavage.
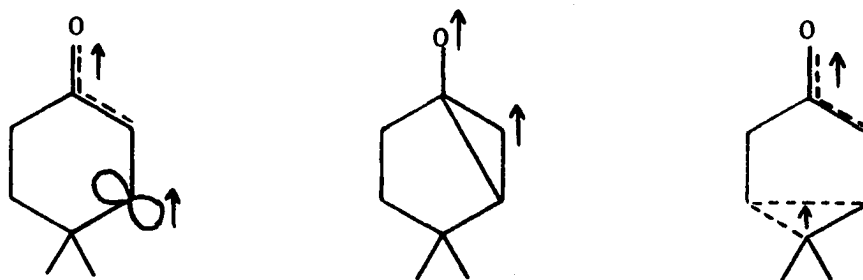
The average lifetimes of daughter triplets ^3K and $^3K'$ can be estimated

from slopes of the Stern-Volmer plots in Figures 21 and 22. If quenching

by di-t-butyl nitroxide occurs at a diffusion controlled rate (2.5×10^{10}

ℓ/mole/sec.), then the average lifetimes of ^3K and $^3K'$ are 6×10^{-9} sec. and 3×10^{-9} sec. in hexane and 1×10^{-8} and 4×10^{-9} sec. in t-butyl alcohol respectively. The longer lifetimes in t-butyl alcohol parallel the higher quantum yields of photocycloaddition in t-butyl alcohol (Table 1).

From the plots in Figure 13 and 20 and the quantum yield relationships in Figure 25, rate constants k_d'', k_d''', k_o, k_t, and k_c and intersystem crossing efficiencies ϕ_{ic}' and ϕ_{ic}'' can be calculated for photocycloaddition in hexane with the assumption that quenching by di-t-butyl nitroxide occurs at a diffusion controlled rate. For the calculation of k_d''', k_c and ϕ_{ic}' equations 25.2, 25.9, and 25.10 give three equations in three unknowns. For the calculation of k_d''', k_o, k_t, and ϕ_{ic}'', equations 25.3, 25.4, 25.7, 25.8, 25.11, and 25.12 give five equations in four unknowns. The calculated rate constants and intersystem crossing efficiences are as follows.

$$\phi_{ic}' = .17 \qquad k_d'' = 1.6 \times 10^8 \text{ sec.}^{-1}$$

$$\phi_{ic}'' = .22 \qquad k_d''' = 2.8 \times 10^8 \text{ sec.}^{-1}$$

$$k_c = 2.6 \times 10^7 \text{ } \ell/\text{mole/sec.}$$

$$k_t = 4.4 \times 10^7 \text{ } \ell/\text{mole/sec.}$$

$$k_o = 6.8 \times 10^7 \text{ } \ell/\text{mole/sec.}$$

See the Appendix for details of the calculations. Singer and Davis (79, 80) calculated the rate constants for the photoaycloaddition of fluorenone and benzophenone to dimethyl-N-(cyclohexyl)-ketenimine to be 3×10^8 and 4×10^8 ℓ/mole/sec., respectively. Singer's rate constants are approximately a factor of seven larger than the rate constants for photocycloaddition

of 4,4-dimethyl-2-cyclohexenone to 1,1-dimethoxyethylene.

The rate constants k_r and k_d''' for photorearrangement can be recalculated for the mechanism in Figure 24, if the intersystem crossing efficiency ϕ_{ic}'' is assumed to be the same in hexane and t-butyl alcohol. Using 0.22 for the intersystem crossing efficiency, rate constants k_r and k_d''' were calculated to be 9.5×10^6 sec.$^{-1}$ and 1.4×10^8 sec.$^{-1}$, respectively.

The steady state analysis of the kinetic mechanism in Figure 24 does not give an expression which predicts a linear Stern-Volmer plot for quenching of total product formation and a linear plot for reciprocal of total quantum yield versus reciprocal of olefin concentration. Experimentally, as shown in Figure 19, the Stern-Volmer plot in question is quite linear, and in Figures 12 and 14 the plots of reciprocal of total quantum yield versus reciprocal of olefin concentration are linear in both hexane and benzene. As shown in the Appendix the Stern-Volmer plot in Figure 19 can be approximated from quantum yield expressions 25.2, 25.3, and 25.4, the calculated lifetimes τ and τ' of daughter triplet states ^3K and $^3K'$, and the quantum yields of oxetane, cis-cyclobutane, and $trans$-cyclobutane in the presence of quencher. The slope of the calculated Stern-Volmer plot deviates from the slope of the experimental Stern-Volmer plot by 2.5%. An expression for the reciprocal of total quantum yield of photocycloaddition is given in the Appendix. Since rate constants k_d'', k_d''', k_o, k_c, and k_t and intersystem crossing efficiencies ϕ_{ic}' and ϕ_{ic}'' are known the quantum yield expression can be greatly simplified by judiciously neglecting those quantitites which are small. The simplified quantum yield expression is linear in reciprocal of olefin concentration and has a slope which deviates

from the experimental slope (Figure 19) by 1%. Even though the mechanism in Figure 24 does not predict the linear plots in Figure 12, 14, and 19, the plots are consistent with the mechanism.

The mechanims in Figure 24 successfully explains the inconsistency in Hammonds (9) measurement of the intersystem crossing efficiency of 2-cyclohexenone described in the Review of Literature Section. The intersystem crossing efficiency of 2-cyclohexenone was 0.33 from the triplet counting experiments and 0.7 from the intercept of a plot of reciprocal of quantum yield versus reciprocal of olefin concentration. The mechanism in Figure 24 predicts that the error lies with the triplet counting experiment. Using 0.05 M 1,2-diphenylpropene as the acceptor, Hammond showed that the measured intersystem crossing efficiency was relatively independent of 2-cyclohexenone concentration. However, he didn't show that the measured intersystem crossing efficiency was independent of 1,2-diphenylpropene concentration. If 1,2-diphenylpropene is quenching a short lived state $^3K^*$ which internally converts to daughter triplets ^3K and $^3K'$ not quenched by 1,2-diphenylpropene, the measured intersystem crossing efficiency will be directly dependent on 1,2-diphenylpropene concentration. Consequently, at higher 1,2-diphenylpropene concentration (*e.g.* 0.10 M) the measured intersystem crossing efficiency should approach 0.7.

An alternate mechanism (Figure 27) involving reaction from triplet complexes will satisfy most of the experimental data. The triplet complexes take the place of the daughter triplets ^3K and $^3K'$ described above. Since the mechanism involves four different triplet complexes, the slopes of the Stern-Volmer plots (Figure 20 and 21) do not have to be the same. Furthermore, this mechanism predicts linear plots of $1/\phi$ versus $1/[O]$ for

Figure 27. A mechanism for photocycloaddition and photorearrangement
           from excimers

$$K + h\nu \longrightarrow {}^1K^*$$

$${}^1K^* \xrightarrow{k_d} K$$

$${}^1K^* \xrightarrow{k_{ic}} {}^3K^*$$

$${}^3K^* \xrightarrow{k_d'} K$$

$${}^3K^* + K \xrightarrow{k_r^c} [{}^3K^* \cdots K]$$

$$[{}^3K^* \cdots K] \xrightarrow{k_r^d} K + K$$

$$[{}^3K^* \cdots K] \xrightarrow{k_r} \text{Rearrangement products} + K$$

$$[{}^3K^* \cdots K] + Q \xrightarrow{k_q} K + K + Q^*$$

$${}^3K^* + 0 \xrightarrow{k_o^c} [{}^3K^* \cdots 0]_o$$

$$[{}^3K^* \cdots 0]_o \xrightarrow{k_o^d} K + 0$$

$$[{}^3K^* \cdots 0]_o \xrightarrow{k_o} \text{Oxetane}$$

$$[{}^3K^* \cdots 0]_o + Q \xrightarrow{k_q} K + 0 + Q^*$$

$${}^3K^* + 0 \xrightarrow{k_c^c} [{}^3K^* \cdots 0]_c$$

$$[{}^3K^* \cdots 0]_c \xrightarrow{k_c^d} K + 0$$

$$[{}^3K^* \cdots 0]_c \xrightarrow{k_c} \textit{cis}\text{-Cyclobutane}$$

$$[{}^3K^* \cdots 0]_c + Q \xrightarrow{k_q} K + 0 + Q^*$$

$${}^3K^* + 0 \xrightarrow{k_t^c} [{}^3K^* \cdots 0]_t$$

$$[{}^3K^* \cdots 0]_t \xrightarrow{k_t^d} K + 0$$

$$[{}^3K^* \cdots 0]_t \xrightarrow{k_t} \textit{trans}\text{-Cyclobutane}$$

$$[{}^3K^* \cdots 0]_t + Q \xrightarrow{k_q} K + 0 + Q^*$$
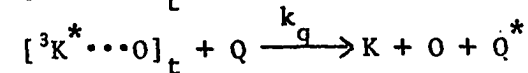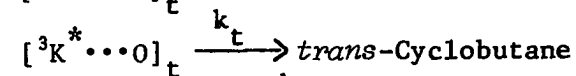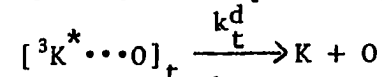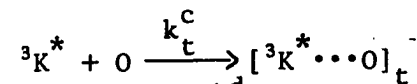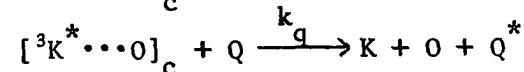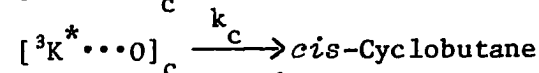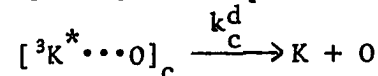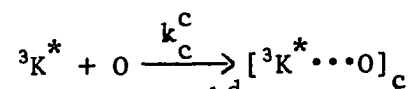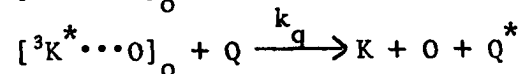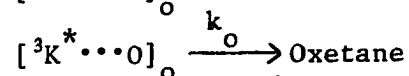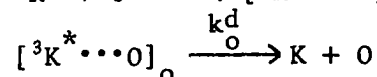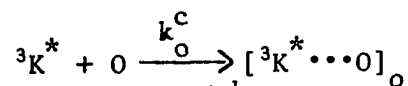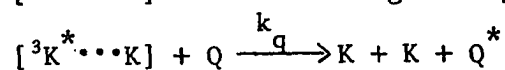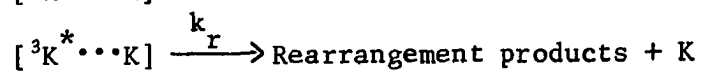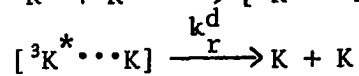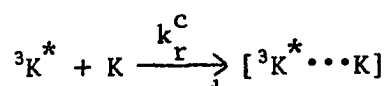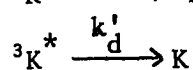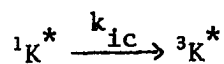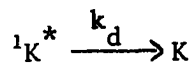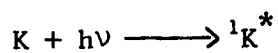
oxetane, cis-cyclobutane, trans-cyclobutane, and total cycloadduct

formation. The plot in Figure 22 of reciprocal of rearrangement quantum

yield versus olefin concentration is also predicted linear. The only

restriction placed on the complexes is that they do not revert back to

excited state species plus ground state species. The mechanism does not

predict non-linear plots of reciprocal of quantum of cis- and trans-cyclo-

butane formation in t-butyl alcohol (Figure 23). Ground state complexes

were not invoked in the mechanism in Figure 27 because ground state com-

plexing was not observed in the u.v. spectrum. The presence of 1,1-

dimethoxyethylene had no effect on the shape or extinction coefficient of

the $n-\pi^*$ absorption of 4,4-dimethyl-2-cyclohexenone.

A number of other investigations have indicated that excited state

complex formation may be important in the photocycloaddition reaction.

deMayo et al. (16) have presented evidence that complexes are important in

the photocycloaddition of 2-cyclopentenone to olefins. A mechanism for

this reaction is given in the Review of Literature Section. The mechanism

for the photocycloaddition of 2-cyclohexenone to olefins suggested by Corey

et al. (14) invokes initial complex formation. Singer and Davis (80)

believe that excimer formation occurs in the photoaddition of benzophenone

to dimethyl-N-(cyclohexyl)-ketenimine. Singer and Davis invoke initial

excimer formation to explain the large reaction rate constant $(4 \times 10^8$ $\ell/$

mole/sec.) observed.

There is one serious problem with the mechanism involing excimer

formation. Since the Stern-Volmer plots (Figure 19 and 20) are linear, the

lifetime of $^3K^*$ must be so short that $^3K^*$ is not quenched by di-t-butyl

nitroxide. The maximum rate at which $^3K^*$ could complex with olefin is a

diffusion controlled rate (2.5×10^{10} ℓ/mole/sec. in hexane at 43°). The olefin concentration in the Stern-Volmer experiment was 0.10 M. Hence the maximum pseudounimolecular rate of complex formation is 2.5×10^{9} sec.$^{-1}$ If quenching occurs at a diffusion controlled rate, then the pseudounimolecular rate of quenching at 0.043 M di-t-butyl nitroxide is 1.1×10^{9} sec.$^{-1}$ Hence quenching of $^{3}K^{*}$ ought to be competitive with complex formation. Consequently, the Stern-Volmer plots (Figures 19 and 20) ought to deviate from linearlity at the higher concentrations of di-t-butyl nitroxide, bending away from the abscissa. This is contrary to fact.

Di-t-butyl nitroxide differentially quenches product formation in several other systems. In the cycloaddition of 1,1-dimethoxyethylene to 2-cyclohexenone and isophorone (15), di-t-butyl nitroxide preferentially quenches formation of cis-cyclobutane adducts XVI and XXIX. Furthermore,
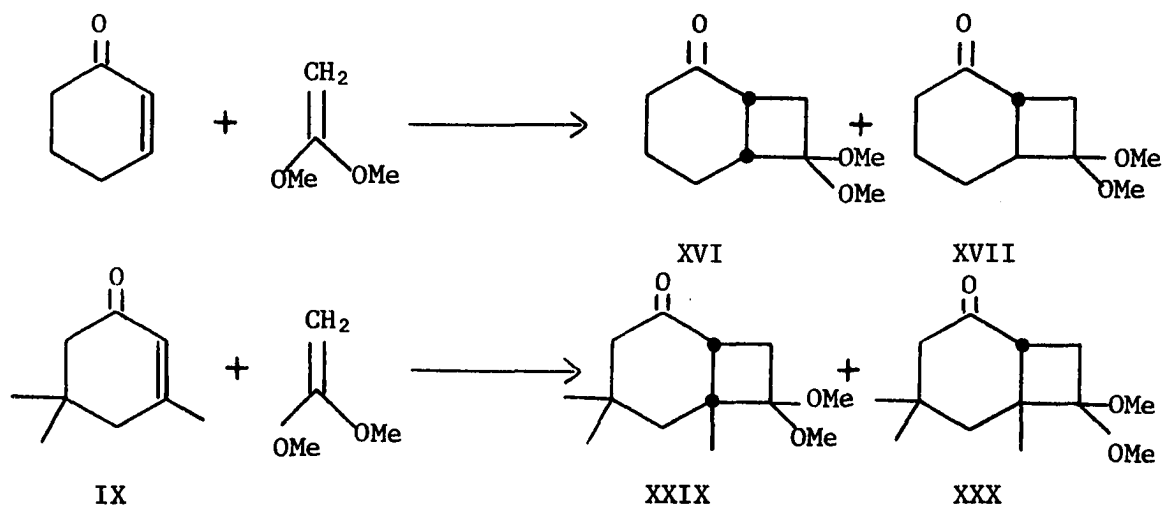
di-t-butyl nitroxide preferentially quenches the formation of the head-to-head dimer (VII) of 2-cyclohexenone and the head-to-tail dimers (XI and

XII) of isophorone (IX)[1].

VII   VIII

IX   X   XI   XII
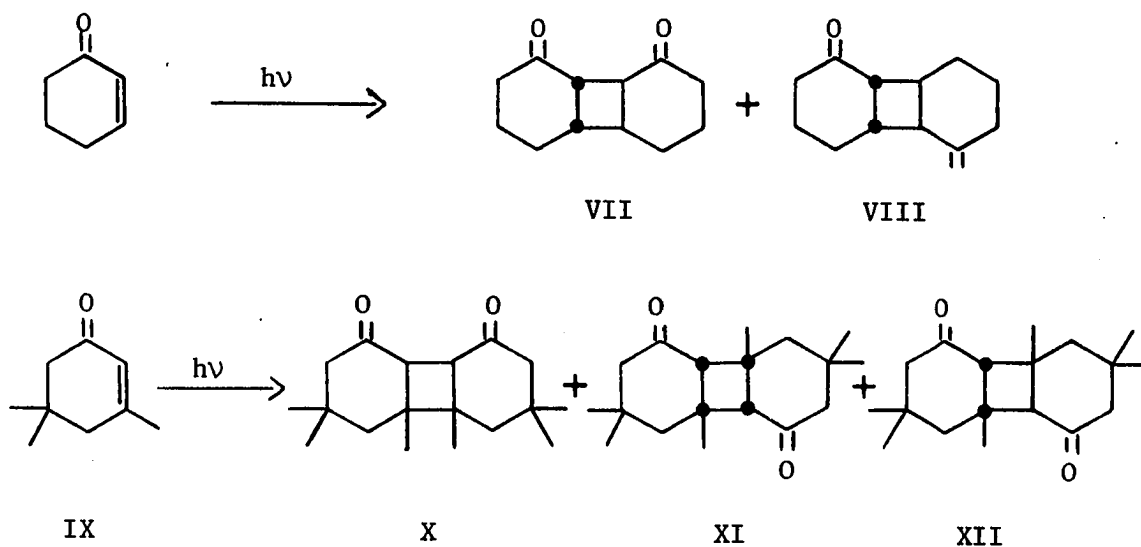
It is intereating to note that Hammond's (9) study of photo-

dimerization of 2-cyclohexenone includes evidence which negates an excimer

mechanism for dimerization. In the triplet counting experiment, the

intersystem crossing efficiency was measured at different concentrations

of 2-cyclohexenone. If energy transfer were competing against excimer

formation, the measured intersystem crossing efficiency would be a direct

function of 2-cyclohexenone concentration. Experimentally, the 2-cyclo-

hexenone concentration does not affect significantly the measured inter-

system crossing efficiency. Hence in photodimerization the daughter

triplet mechanism looks promising.

---

[1]O. L. Chapman and M. D. Druelinger, Department of Chemistry, Iowa
State University of Science and Technology, Ames, Iowa. Photodimerization
of 2-cyclohexenone and isophorone. Private communication. 1968.

Even though a picture of the nature of the daughter triplets is somewhat vague, their existence does explain the stereochemistry of the photocycloaddition reaction. In contrast to Corey's (14) suggestion that *trans*-cyclobutanes result from ring closure of a highly energetic biradical, the investigation described here indicates that *trans*-cyclobutanes are formed from a unique daughter triplet state. In other words the stereochemistry of addition is controlled by the structure of the daughter triplet states, one giving *cis*-cyclobutane and one, *trans*-cyclobutane.

The factors governing the orientation of the photocycloaddition are not entirely clear. Both electronic and steric effects are important. In the absence of a 3-methyl substituent on the cyclohexenone ring the orientation of addition appears to be goverened by dipole-dipole interactions (14). This is illustrated by the photocycloaddition of 2-cyclohexenone to 1,1-dimethyoxyethylene and allene. The actual charge distribution in excited 2-cyclohexenone is not known. For the sake of argument the charge distribution was assigned for 2-cyclohexenone in an n-π^* state. The orientation of addition of 3-methyl-2-cyclohexenones to olefins is

XVI   XVII

XXIII
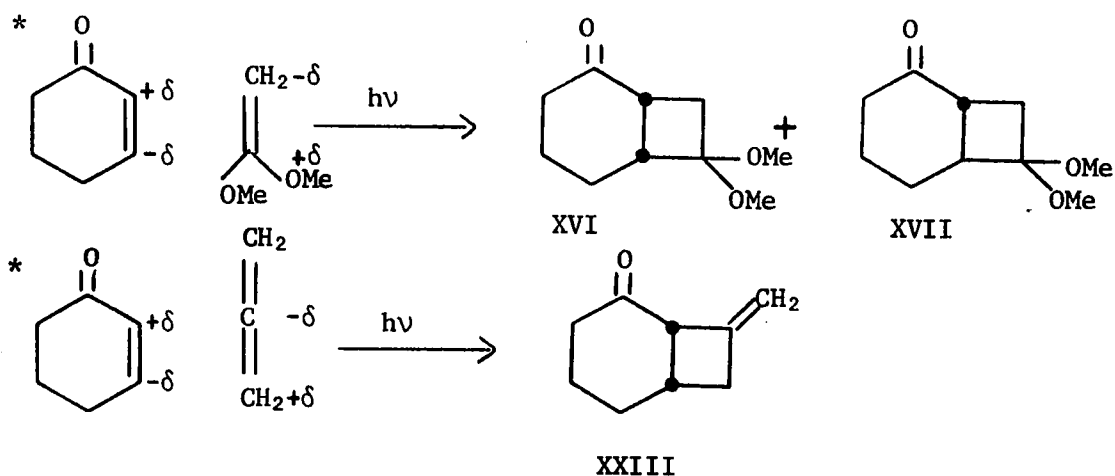
influenced by both dipole-dipole interactions and steric interference.
3-Methyl-2-cyclohexenone adds to isobutylene to give one *cis*-cyclobutane
adduct (XXVIII) with the 8,8-orientation. 2-Cyclohexenone adds to iso-
butylene to give predominantly *cis*- and *trans*-cyclobutanes with the 7,7-
orientation (XVIII and XIX). Isobutylene does not have a large dipole
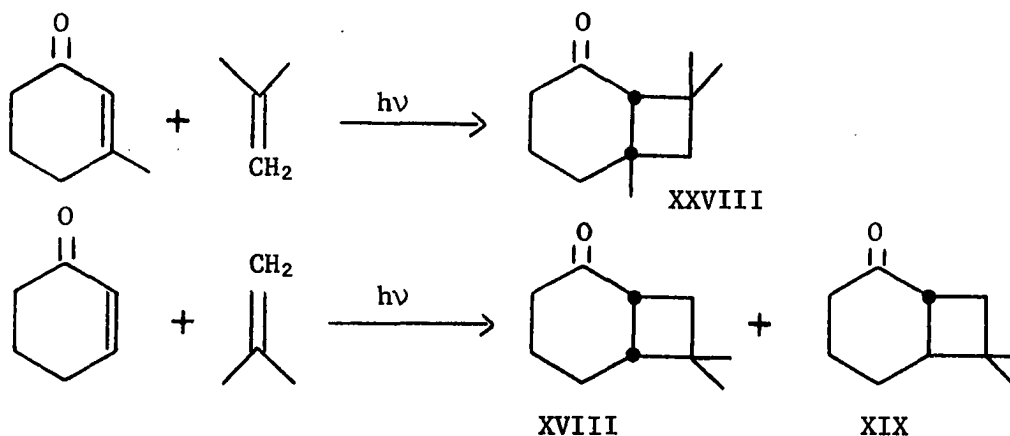
moment. The orientation of addition then is influenced considerably by
steric interference. The 3-methyl group of 3-methyl-2-cyclohexenone
provides enough steric interference to reverse the orientation of addition
from that observed for 2-cyclohexenone. Isophorone (IX) adds to 1,1-
dimethoxyethylene to give *cis*- and *trans*-cyclobutanes with the 7,7-
orientation (XXIX and XXX). The strong dipole-dipole interaction between
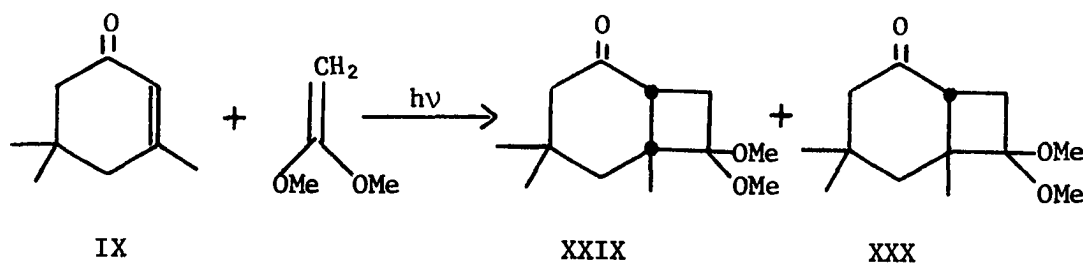
excited isophorone and 1,1-dimethoxyethylene controls the orientation of addition irrespective of the steric interference of the 3-methyl substituent.

Formation of daughter triplets ^3K and $^3K'$ may be important in the reactions of cyclohexenones with solvent. Examples of solvent additions to five, six, and seven membered ring α,β-unsaturated ketones are presented in the Review of Literature Section. There are two kinds of solvent additions, free radical additions and polar additions. Free radical additions include double bond reduction, pinacol formation, and addition of solvent radicals. Polar additions result in ether formation. Cyclopentenones react with solvent in a free radical manner. Cyclohexenones undergo both free radical and polar reactions with solvent. Cycloheptenones react only in a polar fashion. The two types of solvent additions in cyclohexenone photochemistry may be explained in terms of daughter triplets, one daughter triplet giving free radical reactions and the other, polar reactions. It is interesting to note that cyclopentenones react with solvent only in free radical fashion and likewise give only one stereochemistry of photocycloaddition, cis-stereochemistry.

In the last part of the Review of Literature Section, a summary of some multiple state mechanisms is given. The mechanisms proposed by Yang (29, 30), Liu (53, 54, 55), and Kearns (62, 63) invoke reactions from spectroscopic states and thus are only casually related to the mechanism proposed here. DeMayo (16, 50) has reported that 2-cyclopentenone photoadds to olefins from its second excited triplet state. In some respects this reaction may resemble the photoaddition of 2-cyclohexenone to olefins. The T_2 state of 2-cyclopentenone may be internally converting

to a daughter triplet which then reacts with olefins to give photoadducts.
A mechanism of this type is consistent with the data presented by deMayo.
If a daughter triplet is formed, quenching of photoaddition of 2-cyclo-
pentenone to olefins by di-*t*-butyl nitroxide ought to be substantial. The
only multiple state mechanism reported in the literature which bares a
resemblance to the daughter triplet mechanism is that proposed by Chapman
(10) for the photodimerization of isophorone (IX).

SUMMARY

4,4-Dimethyl-2-cyclohexenone undergoes four basic photochemical

reactions, reduction by solvent, rearrangement, oxetane formation, and

addition of olefins to the double bond. Solvent often dramatically
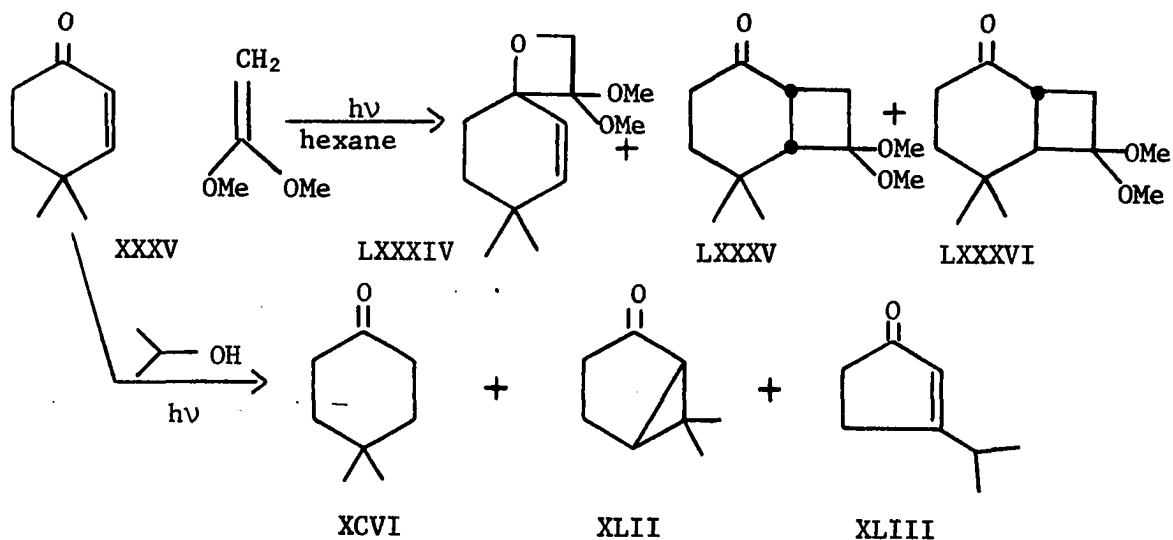
controls product formation. The reactions are sensitized by triplet

sensitizers and quenched by some triplet quenchers. Di-t-butyl nitroxide

and oxygen selectively quench formation of cis-cyclobutane photoadduct.

A mechanism consistent with the experimental results involves formation

of daughter triplets from an n-π^* or π-π^* triplet (61 kcal./mole). One

daughter triplet (^{3}K) gives cis-cyclobutane (LXXXV) and the other daughter

triplet (^{3}K') gives rearrangement (XLII and XLIII), oxetane (LXXXIV), and

$trans$-cyclobutane (LXXXVI). The origin of photoreduction by solvent is

not known. There is no data to indicate the electronic or geometric

structures of the daughter triplets. The daughter triplets, ^{3}K and ^{3}K',

are populated with efficiencies 0.17 and 0.22 and have reactive triplet

lifetimes of 6×10^{-9} and 3×10^{-9} sec., respectively, in hexane for 0.10 M 1,1-dimethoxyethylene. Rate constants for formation of rearrangement products, oxetane, *cis*-cyclobutane, and *trans*-cyclobutane are 9.5×10^{6} sec.$^{-1}$, 6.8×10^{7} l/mole/sec., 2.6×10^{7} l/mole/sec., and 4.4×10^{7} l/mole/sec., respectively. The unimolecular rates of decay of daughter triplets ^{3}K and $^{3}K'$ are 1.6×10^{8} sec.$^{-1}$ and 2.8×10^{8} sec.$^{-1}$, respectively.

EXPERIMENTAL

Instruments and Methods for Qualitative Study

Melting points and boiling points are uncorrected and reported in degrees centrigrade. Melting points were determined with a Kofler microscope hot stage equipped with a polarizer. Infrared spectra were recorded with a Perkin-Elmer Model 21 spectrophotometer; n.m.r. spectra, with a Varian Associates A-60 spectrometer; and u.v. spectra, with a Cary Model 14 spectrophotometer. An Aerograph Model 1520 gas chromatograph was used for analytical and preparative gas liquid chromatography. Peak areas were measured by disc integration. Microanalyses were performed by Spang Microanalytical Laboratories, Ann Arbor, Michigan.

Purification of Reagents

4,4-Dimethyl-2-cyclohexenone was distilled through an 18 in. Nester-Faust spinning band column at 77°, 23 mm. [literature b.p. 76°, 21 mm.(21)]. 1,1-Dimethoxyethylene was distilled through a 30 in. Nester-Faust spinning band column at 88.5-89° [literature b.p. 88-91° (14)] and stored in polyethylene bottles in the freezer. Di-t-butyl nitroxide was distilled through an 18 in. Nester-Faust spinning band column at 55-56°, 10 mm. [literature b.p. 60°, 11 mm. (81)]. Biacetyl (Eastman white label) was distilled at 88-89° [literature b.p. 87.5-88.5°, 740 mm. (82)] prior to use. Reagent grade naphthalene (Baker) was vacuum sublimed at room temperature, m.p. 81-81.5° [literature m.p. 79.5-80.0° (83)]. p-Terphenyl (Eastman white label) was recrystallized from benzene and sublimed twice at 150°, 0.025 mm. [m.p. 211-213°; literature m.p. 204-206° (84)].

Michler's ketone [4,4'-bis-(dimethylamino)-benzophenone] was recrystallized twice from ethanol-water, m.p. 170-171° [literature m.p. 172° (85)]. Triphenylamine (Eastman white label) was recrystallized from 95% ethanol, m.p. 126-127° [literature m.p. 126-127° (86)]. Phenanthrene (Aldrich) was recrystallized from ethanol-water, m.p. 98-99.5° [literature m.p. 96-98° (87)]. Triphenylene (Aldrich) was sublimed at 125°, 0.04 mm. [m.p. 195-195.5°; literature m.p. 197-198° (88)]. Thioxanthone (Baker Sensitizer Kit) was used without further purification, m.p. 211-212° [literature m.p. 215-217° (89)]. Fisher spectrograde hexane was used for quantum yield measurements without purification. Reagent grade benzene was stirred with concentrated sulfuric acid for several days followed by extraction with water and saturated sodium bicarbonate solution. The benzene was dried over sodium hydroxide and distilled from phosphorous pentoxide prior to use. Baker reagent grade tertiary-butyl alcohol and isopropyl alcohol were distilled from calcium hydride prior to use. Fluorobenzene (Aldrich) and reagent grade acetonitrile were distilled from phosphorous pentoxide. Reagent grade methanol was distilled from magnesium methoxide. Reagent grade ethyl acetate was dried over phosphorous pentoxide and distilled from magnesium sulfate. Monoglyme (Ansal) was distilled from sodium under an atmosphere of prepurified nitrogen. N-methyl-2-pyrrolidone (General Aniline and Film Corporation) was distilled from calcium hydride, b.p. 102-3° at 32 mm. [literature b.p. 78°, 10 mm. (90)].

Preparative Photocycloaddition and Photorearrangement

Initial irradiation of 1,1-dimethoxyethylene and 4,4-dimethyl-2-cyclo-
hexenone in hexane solution

A solution containing 8.66 g. (0.07 moles) of 4,4-dimethyl-2-cyclo-
hexenone (referred to as enone), 30.67 g. (0.35 moles) of 1,1-dimethoxy-
ethylene, 330 ml. of reagent grade hexane, and 7.20 g. of cis-decalin
(internal g.l.p.c. standard) was degassed with nitrogen (purified with
Fieser's solution) for 1.5 hrs. The reaction mixture was irradiated for
6.2 hrs. (86% destruction of enone) with a 550-watt Hanovia medium
pressure lamp. Analysis by g.l.p.c. through 7.5 ft. by 0.25 in. of 5%
FS-1265 on 80/100 mesh Diatoport S at 137° (He, 75 cc/min.) indicated
that three major products were formed (ratios of retention times to
retention time of cis-decalin: 3.3, 7.4, 9.9). After rotary evaporation
of the solvent and excess 1,1-dimethoxyethylene, the reaction mixture was
vacuum distilled through a Nester-Faust annular spinning band column. The
cis-decalin, unreacted 4,4-dimethyl-2-cyclohexenone, and low boiling
products were collected without separation in the first five fractions.
The last three fractions contained the first major photoproduct (retention
ratio 3.3), b.p. 92-112° (0.04 mm.[1]). The other two photoproducts remained
in the distillation pot. The pot residue was distilled through a micro
distillation column packed with glass helices, b.p. 68-69°, 0.06 mm. The
distillate contained a mixture of the second and third photoproducts

---

[1]The pressure indicated is the pressure at the pump and not an
accurate indication of the distillation pressure. The annular spinning
band column has a pressure differential of approximately 3 mm.

(retention ratios 7.4 and 9.9, respectively).

The 3.3 retention ratio photoproduct was identified as 3,3-dimethoxy-7,7-dimethyl-1-oxaspiro[3.5]non-5-ene (known hereafter as oxetane) by its n.m.r. spectrum (Figure 4), i.r. spectrum (Figure 3), and mass spectrum (Figure 5). An analytical sample (b.p. 100°, 6.4 mm.) was obtained by redistillation of the oxetane fractions through a Nester-Faust 18 in. semi-micro spinning band column.

Anal. Calcd. for $C_{12}H_{20}O_3$: C, 67.89; H, 9.50. Found: C, 68.03, H, 9.49.

The oxetane is not stable to solid-liquid chromatography on silica gel and flash vaporization in the gas chromatograph. As a result analysis of cycloadducts was done by g.l.p.c. using on column injection.

The 7.4 and 9.9 retention ratio photoproducts were separated by preparative gas-liquid chromatography through 12 ft. by 3/8 in. column of 10% FS-1265 on 80/100 mesh Diatoport S (column A) at 168° (He 100 cc/min., injection port 238°). The 7.4 retention ratio photoproduct was tentatively identified as *cis*-5,5-dimethyl-7,7-dimethoxybicyclo[4.2.0]-octan-2-one (known hereafter as *cis* or *cis*-cyclobutane) by its n.m.r. spectrum (Figure 4), i.r. spectrum (Figure 3), and mass spectrum (Figure 5). An analytical sample was prepared by preparative gas-liquid chroma-tography through column A (*vide supra*).

Anal. Calcd. for $C_{12}H_{20}O_3$: C, 67.89, H, 9.50. Found: C, 68.08; H, 9.62.

The 9.9 retention ratio photoproduct was tentatively identified as *trans*-5,5-dimethyl-7,7-dimethoxybicyclo[4.2.0]octan-2-one referred to as *trans* or *trans*-cyclobutane) by its n.m.r. spectrum (Figure 4), i.r.

spectrum (Figure 3), and mass spectrum (Figure 5) and by its isomerization to *cis*-cyclobutane on neutral alumina (*vide infra*). An analytical sample was prepared by preparative g.l.p.c. through column A (*vide supra*).

Anal. Calcd. for $C_{12}H_{20}O_3$: C, 67.89; H, 9.50. Found: C, 67.98; H, 9.50.

Preparative irradiation of 4,4-dimethyl-2-cyclohexenone and 1,1-dimethoxy-ethylene in hexane

A Pyrex immersion well was charged with 15 g. (0.121 moles) of 4,4-dimethyl-2-cyclohexenone, 50 g. (0.568 moles) of 1,1-dimethoxyethylene, and 225 ml. of Baker reagent grade hexane. After degassing for 30 min. with argon, the stirred solution was irradiated with a 550-watt Hanovia medium pressure lamp for 7 hrs. A constant flow of argon was bubbled through the solution during the irradiation. Six 1.0 ml. samples were periodically removed for g.l.p.c. analysis of product formation and 4,4-dimethyl-2-cyclohexenone destruction. The g.l.p.c. analysis with column B 7% FS-1265, 0.5% Polyterg J-200, 92.5% 60/80 mesh Diatoport S at 145° using piperonal as an external standard gave the data presented in Table 3 and plotted in Figure 2. The g.l.p.c. data were corrected for differences in thermal conductivity. The hexane and excess 1,1-dimethoxyethyene were removed by rotary evaporation. The crude irradiation mixture was fractionally distilled through an 18 in. Nester-Faust semi-micro spinning band column (Table 4) and the fractions were analyzed by g.l.p.c. using column B. The first three distillation fractions contained some unidentified materials. The isolated yield of products as determined by quantitative g.l.p.c. was 3.28 g. (14%) oxetane, 7.27 g. (30%) *cis*-cyclobutane,

and 9.82 g. (41%) *trans*-cyclobutane. The total isolated yield of cyclo-adducts was 85%, corrected for 4% recovery of starting 4,4-dimethyl-2-cyclohexenone.

Table 3. Preparative photocycloaddition as a function of time

Time (min.)	% destruction 4,4-dimethyl-2-cyclohexenone	% formation		
		oxetane	*cis*-cyclobutane	*trans*-cyclobutane
72	34.7	6.5	10.2	16.2
135	59.5	11.5	18.0	28.4
203	81.0	16.4	24.4	37.8
270	91.3	17.9	25.8	42.5
330	92.6	19.4	27.7	43.4
420	93.0	18.9	26.9	42.8

Table 4. Distillation of photocycloadducts

boiling point	pressure (mm.)	yield (g.)	% composition	
60-77°	2.1	0.66	31% enone	18% oxetane
77-81°	2.1	1.46	22% enone	40% oxetane
81-83°	2.1	2.93	3% enone	88% oxetane
83-85°	1.9 ± 0.2	2.89	86% *cis*	14% *trans*
64-65°	0.04	2.19	86% *cis*	14% *trans*
65-66°	0.03	2.68	59% *cis*	41% *trans*
67-74°	0.04	3.30	29% *cis*	71% *trans*
74-75°	0.04	3.78	9% *cis*	91% *trans*
75°	0.04	2.28	2% *cis*	98% *trans*

Preparative rearrangement and photoreduction in isopropyl alcohol

A small Pyrex immersion well was charged with 12.4 g. (0.10 moles) of 4,4-dimethyl-2-cyclohexenone in 175 ml. of reagent grade isopropyl alcohol. After degassing with argon for 40 min., the solution was irradiated for 28 hrs. with a 550-watt Hanovia medium pressure lamp. The isopropyl alcohol was removed by rotary evaporation, and the resulting oil was steam distilled. The steam distillate was saturated with sodium chloride and extracted with ether. After drying over magnesium sulfate, the ether was rotary evaporated to yield 2.31 g. of steam volatile products. The steam non-volatile products amounted to 10.65 g. and were not investigated. Gas liquid chromatographic analysis through 5% Ucon Water Soluble on 60/80 mesh Chromasorb W at 100° (injection port, 128°; He, 78 cc/min.) indicated that three major products were formed and that 4,4-dimethyl-2-cyclohexenone was completely destroyed. The products were separated by preparative g.l.p.c. through an 11 ft. by 3/8 in. column of Ucon Water Soluble (F & M Corp.) on 60/80 mesh Chromasorb W at 127° (Injection port, 235°; He, 86 cc/min.). The products were identified as 3-isopropylcyclopentanone, 4,4-dimethylcyclohexanone [m.p. 38.5-40.5°, literature 38-41° (66)], and 6,6-dimethylbicyclo[3.1.1]hexan-2-one. The i.r. and n.m.r. spectra of 3-isopropylcyclopentanone and 6,6-dimethylbicyclo[3.1.0]hexan-2-one were identical to the spectra reported by T. A. Rettig (21). The i.r. and n.m.r. spectra of 4,4-dimethylcyclohexanone were identical to the spectra of 4,4-dimethylcyclohexanone obtained by catalytic hydrogenation of 4,4-dimethyl-2-cyclohexenone (*vide infra*).

The steam volatile product mixture was analyzed by quantitative

g.l.p.c. using the analytical Ucon Water Soluble column and conditions described. Acetophenone was used as an external standard, and the thermal conductivities of the products were assumed to be identical. The composition of the steam volatile product mixture was 10% 3-isopropylcyclopentanone, 16% 4,4-dimethylcyclohexanone, and 45% 6,6-dimethylbicyclo[3.1.1]-hexan-2-one; 29% of the steam volatile product mixture was not identified.

Structure Proof of Photoproducts

Catalytic hydrogenation of 4,4-dimethyl-2-cyclohexenone

Palladium (10%) on charcoal (0.10 g.) suspended in 15 ml. of 95% ethyl alcohol was prehydrogenated for 0.5 hr. in a low pressure hydrogenation apparatus. 4,4-Dimethyl-2-cyclohexenone (1.00 g., 0.0081 moles) in 10 ml. of 95% ethyl alcohol was added, and the stirred reaction mixture absorbed 193 ml. of hydrogen in 45 min. (atmospheric pressure 737 mm., temperature 25.5°). The volume of hydrogen absorbed corrected to 1 atm., 0° was 203 ml. (95% of theoretical volume). The catalyst was removed by filtration, and the ethyl alcohol was removed by rotary evaporation to yield 0.76 g. of semi-solid 4,4-dimethylcyclohexanone (75% yield). Preparative g.l.p.c. through a 10 ft. by 3/8 in. column of 10% Ucon Water Soluble on 60/80 mesh Chromasorb W at 168° (injection port, 260°; He, 71 cc/min.) yielded an analytical sample: m.p. 41-42.5°, $\lambda_{max}^{CCl_4}$ 5.84 µ; n.m.r. spectrum (CCl$_4$), δ 1.09 (singlet, 3H), 1.45-1.95 (multiplet, 2H), and 2.05-2.45 (multiplet, 2H).

Anal. Calcd. for C$_8$H$_{14}$O: C, 76.14; H, 11.18. Found: C, 76.16; H, 11.13.

Pyrolysis of oxetane

Oxetane (0.20 g., 0.94 mmoles) in 7.5 ml. of reagent grade hexane
was passed with a stream of prepurified nitrogen through a 10 in.
pyrolysis column packed with glass helices at 320°. Liquid products
(0.071 g.) were collected at 0° and gaseous products were bubbled through
25 ml. of 2,4-dinitrophenylhydrazine solution. The column was washed
with hexane after the pyrolysis column had cooled yielding 0.067 g. of a
yellow oil. Gas liquid chromatographic analysis of the liquid products
through 7% FS-1265 on 60/80 Diatoport S (Column B) at 130° indicated eight
significant products. One of the products was identified as 4,4-dimethyl-
2-cyclohexenone by g.l.p.c. retention time. No attempt was made to ident-
ify the other products. Recrystallization from methanol-water followed by
benzene-hexane yielded 0.0079 g., m.p. 162-163°, and 0.0104 g., m.p. 158-
162° (total yield 9%). The 2,4-dinitrophenylhydrazone of formaldehyde
was prepared and recrystallized from methanol water, m.p. 163.5-164.5°
[Literature melting point 155° (91)]. The i.r. spectra of the 2,4-dinitro-
phenylhydrazone synthesized from the gaseous pyrolysis product and the 2,4-
dinitrophenylhydrazone of formaldehyde were identical.

Hydrolysis of cis-5,5-dimethyl-7,7-dimethoxybicyclo[4.2.0]octan-2-one

Cis-5,5-dimethyl-7,7-dimethoxybicyclo[4.2.0]octan 7-one (0.672 g.) in
50 ml. of ether was refluxed under nitrogen with 0.5 ml. of water and 2
drops of concentrated hydrochloric acid for 20 hrs. The reaction mixture
was then extracted with 10 ml. of 5% sodium bicarbonate and 10 ml. of
saturated salt solution. After drying over magnesium sulfate, the ether
was removed by rotary evaporation to yield 0.430 g. (72%) of a light yellow

oil. Low temperature recrystallization from ether-pentane (1:1) yielded

0.308 g. (52%) of semi-solid *cis*-5,5-dimethylbicyclo[4.2.0]octa-2,7-dione

Five additional low temperature recrystallizations of a small sample of

dione gave white crystalline material, m.p. 44-46°. An analytical sample

was prepared by preparative gas liquid chromatography on 3/8 in. by 12 ft.

column of 10% FS-1265 on 80/100 mesh Diatoport S (column A) at 188°: λ_{max}^{neat},

5.62 and 5.90 μ (Figure 7); n.m.r. spectrum CCl₄, δ 1.04 (singlet, 3H),

1.13 (singlet, 3H), 1.40-2.25 (multiplet, 2H), 2.25-2.65 (multiplet, 2H),

and 2.65-3.70 (multiplet, 4H); mass spectrum (Figure 8) m/e 166 (M^+, 2.1%

of base).

Anal. Calcd. for $C_{10}H_{14}O_2$: C, 72.26; H, 8.49. Found: C, 72.14;

H, 8.40.

Deuteration of 5,5-dimethylbicyclo[4.2.0]octa-2,7-dione

Cis-5,5-dimethylbicyclo[4.2.0]octa-2,7-dione (0.308 g.) was dis-

solved in 10 ml. of methanol-OD (98% OD). Three drops of concentrated

hydrochloric acid were added and the reaction mixture was heated to 72 ±

2° for 18 hrs. under an atmosphere of purified nitrogen. The reaction

mixture was diluted with ether distilled from sodium. The methanol and

ether were removed by rotary evaporation, leaving deuterated product,

deuterium oxide, and deuterium chloride. The deuterated product was

extracted with dry ether-pentane (1:1). The solution was dried over

magnesium sulfate,and ether and pentane were removed by rotary evapora-

tion to yield 0.288 g. of crude deuterated dione. The deuterated material

was crystallized from ether-pentane (1:1) at Dry Ice temperature by seed-

ing with undeuterated dione. Two recrystallizations from ether-pentane

(1:1) yielded 0.164 g. (51%) of deuterated *cis*-5,5-dimethylbicyclo[4.2.0]-octa-2,7-dione   m.p. 46.5-47.5°: n.m.r. (CCl₄), δ 1.02 (singlet, 3H), 1.12 (singlet, 3H), 1.3-2.2 (multiplet, 2H), and 2.2-3.7 (multiplet, 1H); mass spectrum (18 ev.), 25.4% M + 6, 33.8% M + 5, 18.7% M + 4, 6.3% M + 3, 5.8% M + 2, 5.3% M + 1, and 3.6% M.

Isomerization of *trans*-5,5-dimethyl-7,7-dimethoxybicyclo[4.2.0]octan-2-one to *cis*-5,5-dimethyl-7,7-dimethoxybicyclo[4.2.0]octan-2-one

A photoadduct mixture (6.01 g.) consisting of 25% *cis*-5,5-dimethyl-7,7-dimethoxybicyclo[4.2.0]octan-2-one and 75% *trans*-5,5-dimethyl-7,7-dimethoxybicyclo[4.2.0]octan-2-one was dissolved in a 10 ml. of reagent grade dry ether. The solution was added to a 45 × 100 mm. neutral alumina column (Woelm activity grade I) packed in ether. The photoadducts were allowed to stand on the column for 30 min. prior to elution with ether. The ether was removed with a rotary evaporator and the *cis* photoadduct was distilled through a semi-micro vigreux column at 81-81.5° at 1 mm. pressure to yield 4.45 g. (74%). Gas liquid chromatography through 5% FS-1265 on 80/100 mesh Diatoport S indicated that the product was at least 99% *cis*-5,5-dimethyl-7,7-dimethoxybicyclo[4.2.0]octan-2-one. The i.r. and n.m.r. spectra of the isomerization product were identical with those of the *cis*-cyclobutane photoadduct obtained by preparative gas liquid chromatography (Figure 3 and 4).

Wolff-Kishner reduction of *cis*-5,5-dimethyl-7,7-dimethoxybicyclo[4.2.0]-octan-2-one

The procedure used was essentially the Huang-Minlon modified Wolff-

Kishner reduction (92). A 100 ml. three-neck flask was charged with 4.20 g. (19.7 mmoles) of *cis*-5,5-dimethyl-7,7-dimethoxybicyclo[4.2.0]octan-2-one, 2.66 g. (84.3 mmoles) of Eastman 95% hydrazine, 2.72 g. (68 mmoles) of sodium hydroxide, and 40 ml. of diethylene glycol. The reaction mixture was heated to 200° under an atmosphere of prepurified nitrogen for 1 hr. Water and excess hydrazine were then removed by distillation through a micro-distillation head at 200-210° for 40 min. The reaction mixture was heated at 200 ± 5° for an additional 2 hrs. After cooling to room temperature the reaction mixture was acidified with 5% hydrochloric acid, saturated with salt, and extracted five times with ether. The combined ether extracts were refluxed with 15 ml. of 5% hydrochloric acid solution for 30 min. The ether was separated from the acidic aqueous phase and extracted with 15 ml. of 5% sodium bicarbonate solution followed by saturated salt solution. After drying over magnesium sulfate, the ether was removed by distillation at atmospheric pressure. The crude product was distilled through a semi-micro column at 114-115° at 5 mm. to yield 1.83 g. (61%) of *cis*-5,5-dimethylbicyclo[4.2.0]octan-7-one. Gas liquid chromatography through 5% FS-1265 on 80/100 mesh Diatoport S at 160° showed the product to be at least 98% pure. Preparative gas liquid chromatography on 3/8 in. by 11 ft. column of Ucon Water Soluble on 60/80 mesh Chromosorb W at 175° yielded an analytical sample: $\lambda_{max}^{CCl_4}$ 5.86 (Figure 7); n.m.r. spectrum (CCl_4), δ 0.87 (singlet, 3H), 1.15 (singlet, 3H), 0.95-1.80 (multiplet, 5H), 1.90-2.70 (multiplet, 3H), and 2.70-3.20 (multiplet, 2H); mass spectrum (Figure 8) m/e 152 (M^+, 5% of base) and 110 (loss of ketene, 26% of base).

Anal. Calcd. for $C_{10}H_{16}O$: C, 78.89; H, 10.59. Found: C, 78.82, H, 10.49.

Baeyer-Villiger oxidation of *cis*-5,5-dimethylbicyclo[4.2.0]octan-7-one[1]

A 50 ml. Erlenmeyer flask was charged with 15 ml. of methylene chloride and cooled in an ice bath. Trifluoroacetic anhydride (4.55 g., 21.6 mmoles) was added followed by dropwise addition of 0.75 ml. of cold 90% hydrogen peroxide. The addition of hydrogen peroxide took approximately 10 min. A 100 ml. three neck flask was charged with 1.10 g. (7.2 mmoles) of *cis*-5,5-dimethylbicyclo[4.2.0]octan-7-one, 15 ml. of methylene chloride, and 5.65 g. of disodium monohydrogen phosphate and cooled in an ice bath. The cold peroxide solution was added dropwise with stirring over a period of about 45 min. The reactions mixture was then refluxed at 50° for 1 hr. After cooling to room temperature, 60 ml. of methylene chloride and 60 ml. of water were added and the reaction mixture was shaken in a separatory funnel. The aqueous layer was re-extracted with 30 ml. of methylene chloride. The combined methylene chloride extracts were extracted twice with 5% sodium bicarbonate and twice with water. After drying over anhydrous sodium sulfate and checking for the presence of peroxides, the methylene chloride was removed by rotary evaporation. The γ-lactone, *cis*-2,2-dimethyl-9-oxabicyclo[4.3.0]nonan-8-one, was molecularly distilled at 0.05 mm., pot temperature 65 ± 5°, to yield 1.09 g. (90% yield). The product was at least 99% pure by gas liquid chroma-

---

[1]The procedure used for the Baeyer-Villiger oxidation was obtained from the Ph.D. thesis of T. A. Rettig (21).

tography on 5% Ucon Water Soluble on 80/100 mesh Chromosorb W. Prepara-
tive gas-liquid chromatography on 3/8 in. by 12 ft. column of 10% FS-1265
on 80/100 mesh Diatoport S (column A) at 175° yielded an analytical sample:
$\lambda_{max}^{CCl_4}$ 5.60 μ (Figure 7); n.m.r. spectrum (CCl$_4$), δ 0.95 (singlet, 3H),
1.07 (singlet, 3H), 0.90-1.80 (multiplet, 6H), 1.80-2.80 (multiplet, 3H),
and 3.87 (doublet, ^3J = 3 Hz., 1H); mass spectrum (Figure 8), m/e 168
(M^+, 8.5% of base), and 108 (base, m^*, 69.4, loss of acetic acid).

Anal. Calcd. for $C_{10}H_{16}O_2$: C, 71.39; H, 9.59. Found: C, 71.56;
H, 9.66.

Lithium aluminum hydride reduction of γ-lactone

Ether (60 ml.), refluxed with sodium metal for three hrs., was dis-
tilled directly into a 100 ml. three-neck flask equipped with condenser
and magnetic stirring mechanism. Freshly crushed lithium aluminum hydride
(0.354 g., 9.3 mmoles) was then added. With vigorous stirring 1.00 g.
(1.0 mmoles) of *cis*-2,2-dimethyl-9-oxabicyclo[4.3.0]nonan-8-one (γ-lactone)
was added dropwise. The reaction mixture was allowed to stir at room temp-
erature for 11 hrs. followed by 2 hrs. of refluxing. After cooling to
room temperature, 1.60 ml. of water was added dropwise, and the reaction
mixture was allowed to stir at room temperature for several hours. The
lithium and aluminum hydroxides were removed by vacuum filtration. The
ether filtrate was dried over magnesium sulfate, and the ether was re-
moved by rotary evaporation to yield 1.02 g. (100%) of white crystalline
product, m.p. 85-115°. Recrystallization from ether-pentane at -78°
yielded 0.724 g. (71% yield) of *cis*-2,2-dimethyl-6-(β-hydroxyethyl)-
cyclohexanol, m.p. 114-115°. An analytical sample, m.p. 115-115.5°, was

prepared by vacuum sublimation at 0.04 ± .01 mm. pressure, 65°: λ^{KBr}_{max}

305 μ (Figure 9); n.m.r. spectrum (dimethyl sulfoxide-d_6), δ 0.87

(singlet, 6H), 0.90-2.0 (multiplet, 9H), 3.02 (broadened doublet, ^3J =

6 Hz., 1H), 3.42 (slightly broadened quartet, 2H), 4.05 (doublet, ^3J =

6 Hz., 1H), and 4.21 (triplet, ^3J = 5.0 Hz., 1H); n.m.r. spectrum (di-

methyl sulfoxide-d_6 + deuterium oxide), δ 0.87 (singlet, 6H), 0.90-2.0

(multiplet, 9H), 3.03 (broadened singlet, 1H), and 3.43 (triplet, ^3J =

6.0 Hz., 2H); mass spectrum (Figure 10), m/e 172 (M^+, base), 154 (8.5%

of base, m^* 138), and 136 (5.2% of base, m^* 107.5).

Anal. Calcd. for $C_{10}H_{20}O_2$: C, 69.72; H, 11.70. Found C, 69.73;

H, 11.55.

Jones oxidation of *cis*-2,2-dimethyl-6-(β-hydroxyethyl)-cyclohexanol

Jones reagent (10 ml., 17.1 mequiv.), *cis*-2,2-dimethyl-6-(β-hydroxy-

ethyl)-cyclohexanol (0.407 g., 14.2 mequiv.), and water (10 ml.) were

stirred at room temperature for 2 hrs. The reaction mixture was then

extracted with four 25 ml. portions of ether. The combined ether ex-

tracts were extracted with 25 ml. of 5% sodium sulfite solution and 15

ml. of saturated salt solution. After drying over magnesium sulfate, the

ether was rotary evaporated to yield 0.278 g. of crude product mixture.

The crude product mixture was chromatographed on 28 × 143 mm. of Baker

silica gel packed in Skelly B. *Cis*-2,2-dimethyl-9-oxabicyclo[4.3.0]-

nonan-8-one (γ-lactone) and an unidentified product (total yield 0.159 g.,

77% γ-lactone, 23% unknown by g.l.p.c.) were eluted with 10% ether 90%

Skelly B. The γ-keto-acid, 2-keto-3,3-dimethylcyclohexyl acetic acid,

(0.067 g., 15%) was eluted with 50% ether 50% Skelly B. Pure γ-lactone

was obtained by preparative gas liquid chromatography on 3/8 in. by 12 ft. column of 10% FS-1265 on 80/100 mesh Diatoport S (column A) at 182°. The i.r. and n.m.r. spectra of the γ-lactone were identical with those of the γ-lactone obtained by Baeyer-Villiger oxidation of *cis*-5,5-dimethylbicyclo-[4.2.0]octan-7-one. The keto-acid was purified by fractional sublimation at 0.05 mm., 70° to yield 0.030 g. (6.7% yield) of 2-keto-3,3-dimethyl-cyclohexyl acetic acid, m.p. 93.5-95°: $\lambda_{max}^{CHCl_3}$ 2.8-4.5 and 5.87 μ (Figure 9); n.m.r. spectrum CDCl₃ (accumulated, 8 scans), δ 1.06 (singlet, 3H), 1.22 (singlet, 3H), 1.3-2.5 (multiplet, 7H), 2.5-3.5 (multiplet, 2H), and 11.32 (broad singlet, 1H); mass spectrum (Figure 10), m/e 184 (M^+, 15.6% of base).

Esterification of 2-keto-3,3-dimethylcyclohexyl acetic acid

The keto-ester was prepared by heating 0.0198 g. of 2-keto-3,3-dimethylcyclohexyl acetic acid with 60 ml. of absolute ethanol (distilled from sodium metal prior to use) and 1 drop of concentrated hydrochloric acid to 100° for 10 hrs. An atmosphere of prepurified nitrogen was maintained throughout the heating period. After cooling to room temperature the ethanol was removed by rotary evaporation of an ethanol-benzene azeotrope. The last traces of ethanol were removed by rotary evaporation of benzene. The last tracers of benzene were removed by rotary evaporation of dry ether to yield 0.0164 g. (72% yield) ethyl (2-keto-3,3-dimethyl-cyclohexyl)-acetate. The i.r. and n.m.r. (obtained by an 8 scan accumulation) spectra were identical to the spectra obtained from the synthetic keto-ester.

Synthesis of ethyl (2-keto-3,3-dimethylcyclohexyl)-acetate

A 100 ml. three neck flask, equipped with condenser, magnetic stirring apparatus, and nitrogen inlet tube, was charged with 0.386 g. (8.87 mmoles) of 55.1% sodium hydride oil dispersion. The oil was removed by washing with dry benzene several times under an atmosphere of prepurified nitrogen. The sodium hydride was then suspended in 30 ml. dry benzene. 2,2-Dimethylcyclohexanone (93) (1.00 g., 7.94 mmoles) was added, and the reaction mixture was refluxed under an atmosphere of nitrogen for 18 hrs. After cooling to room temperature, 30 ml. of benzene was added followed by 1.33 g. (7.95 mmoles) of ethyl bromoacetate dissolved in 5 ml. of benzene. The reaction mixture was refluxed under nitrogen atmosphere for 1.5 hrs. Ether (50 ml.) was added and the reaction solution was extracted with 15 ml. of water. After drying over magnesium sulfate, the ether-benzene was removed by rotary evaporation. The crude product mixture was chromatographed on 38 × 147 mm. of Baker silica gel packed in Skelly B. Unreacted 2,2-dimethylcyclohexanone (0.442 g., 44%) (identified by i.r. and g.l.p.c. retention time) was eluted with Skelly B. The keto-ester was eluted with 5% ether 95% Skelly B to yield 0.152 g. Molecular distillation at 0.1 mm., 75° yielded 0.101 g. (11% yield based on ketone reacted) of ethyl (2-keto-3,3-dimethylcyclohexyl)-acetate. Gas-liquid chromatography on 5% Ucon Water Soluble on 80/100 mesh Chromosorb W at 172° indicated the keto-ester to be 94% pure. Preparative gas liquid chromatography on 3/8 in. by 10 ft. column of 10% FS-1265 on 80/100 mesh Diatoport S at 182° yielded an analytical sample: $\lambda_{max}^{CCl_4}$ 5.75 and 5.85 (Figure 9); n.m.r. spectrum, CCl_4, δ 1.00 (singlet, 3H), 1.20 (singlet,

3H), 1.22 (triplet, ^3J = 7 Hz.), 1.40-2.40 (multiplet, 7H), 2.40-3.40

(multiplet, 2H), and 4.05 (quartet, ^3J = 7 Hz., 2H); mass spectrum (Figure

10), m/e 212 (M^+, 0.9% of base).

Anal. Calcd. for $C_{12}H_{20}O_3$: C, 67.89; H, 9.50. Found: C, 68.02,

H, 9.60.

Instruments and Methods for Quantitative Study

Rotating photochemical apparatus

A rotating photochemical apparatus (the "wheel") was constructed

for the simultaneous irradiation of eight samples, each sample receiving

the same amount of light per unit of time (± 2%). Differences in light

absorption were corrected by actinometric calibration prior to irradiation

(*vide infra*). The light source was a Rayonet photochemical reactor

(Southern New England Ultraviolet Co.) equipped with black lamps, λ_{max}

3500 Å. The rotating wheel consisted of a round steel table 7 in. in

diameter × 1/8 in. thick mounted on a central shaft of 1/2 in. steel rod.

The shaft was supported by ball bearings at the top and bottom. The lower

bearing was mounted in a brass block, the bottom of which was milled to

fit securely the reactor fan screen. The upper bearing was mounted in a

1/8 in. steel plate, connected to the reactor support rods. At the

periphery of the wheel were symmetrically mounted four Beckman DU cell

holders. The cell holder windows facing the shaft were covered with black

plastic tape. The wheel was rotated at 20 r.p.m. by a Minneapolis Honey-

well induction motor (13.5 watts, 40 r.p.m.) mounted on the top bearing

plate. Only the central two cell positions of each Beckman cell holder

were used. The equilibration temperature of the "wheel" depended upon

room temperature and varied between 39 and 47°.

Linear quantum yield apparatus I

A double-beam, linear quantum yield apparatus I[1] was constructed from the design of Moore and Ketchum (94) and is pictured in the Ph.D. thesis of T. A. Rettig (21). The apparatus employed a Westinghouse, 800 watt, short arc, high pressure, mercury lamp. The light was collimated by a 2.5 in. planoconvex lens (focal length 6.0 in.) and filtered with appropriate filter solutions and Corning glass filters. A Beckman DU cell holder was placed in the filtered light column such that the two central compartments received the same amount of light as indicated by a thermopile. The cell holder was positioned with the aid of a motor driven Eppley thermopile connected to a 1 mv. recorder. As the thermopile passed behind the cell holder, it intercepted the light passing through each cell compartment giving two peaks on the recorder. The cell holder position was adjusted until the peak heights were the same. To assure that both cells received the same amount of light, the cells were interchanged in the Beckman DU cell holder at the mid-time of each irradiation.

Linear quantum yield apparatus II

Absolute quantum yields were measured with linear quantum yield apparatus II. The apparatus used an Osram 200 watt, super pressure, mercury light source (Bausch and Lomb) powered with a DC power supply

---

(Ionics Corp.). The source was attached to a Bausch and Lomb high intensity monochromator with u.v.-visible grating and variable slits (0-6.0 mm.). The grating was blazed at 220 mμ with a dispersion of 7.4 mμ/mm. The entrance slit of the monochromator was equipped with Bausch and Lomb quartz collective lens #1. One of the central compartments of a Beckman DU cell holder was mounted in front of the exit slit of the monochromator. A rotating sector (to attenuate the light intensity for actionometry) was attached to the cell holder mount such that the sector passed between the exit slit and the cell holder. The sector, powered by an induction gear motor at 50 r.p.m., consisted of an 8 in. by 1/8 in. aluminum disc with a small sector removed. The attenuation of the average light intensity was dependent upon the angle of the sector. The entire quantum yield apparatus was mounted on a Cenco optical bench and enclosed in a dry box with plexiglass door and aluminum heat exchanger above the lamp housing. The monochromator was cooled by a fan inside the dry box and the lamp was cooled by a fan blowing across the heat exchanger outside the dry box. With cooling fans operating, the apparatus equilibrated at about 49° ± 3°. Quantum yields were measured with the monochromator set at 345 mμ, the power supply at 3.0 amps., and the entrance and exit slits at 6.10 mm. (band pass at base 323 to 367 mμ[1]).

Cells used for quantum yield measurements

Round cells (length, 50 mm., outside diameter 13.9 ± 0.05 mm.) were constructed from Pyrex tubing and equipped with standard taper 10/30

---

[1]The band pass is calculated by multiplying the exit slit width times the grating dispersion (7.4 mμ/mm.).

joints. Square cells (length, 50 mm.) were constructed from ACE square Pyrex tubing (inside dimension, 10 mm.) and equipped with standard taper 10/30 joints. Square and round Pyrex cells were used in the rotating photochemical apparatus, and square Pyrex cells were used in linear quantum apparatus II. Cells for linear quantum yield apparatus I consisted of 1.00 cm. spectrosil u.v. cells (Thermal American Fused Quartz Co.) equipped with graded quartz to Pyrex seals and 4 mm. Teflon needle valves.

Actinometry

Potassium ferrioxalate actinometry (95, 96) was used for quantum yield measurements in the rotating photochemical apparatus and linear quantum yield apparatus II. In the rotating photochemical apparatus, eight cells each containing 3.0 ml. of 0.13 M potassium ferrioxalate solution were irradiated for 4.0 min. For each cell a 1.00 ml. alliquot of the irradiated solution was added to a 50.0 ml. volumetric flask containing 8.0 ml. of 0.10%, 1.10-phenanthroline solution and 1.0 ml. of sodium acetate sulfuric acid buffer (95). After diluting to 50.0 ml, the solutions were allowed to stand for at least 1 hr. The optical density was measured with a Beckman DU spectrometer equipped with model 205 Gilford power supply, model 220 optical density converter (Gilford), and model 209 automatic absorbance meter (Gilford). Using an average quantum yield of 1.20, the quantum output of the rotating photochemical apparatus was approximately 2×10^{16} quanta/sec. The exact quantum output depended upon the cells and lamp age. The cells which were calibrated by actinometry were also used for the subsequent quantum yield experiment. In

linear quantum yield apparatus II approximately the same actinometry technique was used. Because of the high light intensity and random fluctuations of the super pressure lamp, a rotating sector was employed to attenuate the light beam for actinometry. With the 47° sector rotating, a cell containing 3.0 ml. of potassium ferrioxalate was irradiated for 18 min. Using a quantum yield of 1.22 for potassium ferrioxalate, the approximate light intensity was 3×10^{16} quanta/sec. For the rotating photochemical apparatus, the average of two actinometers for each cell (run prior to the quantum yield experiment) was used as a measure of the light intensity. For absolute quantum yields on linear quantum yield apparatus II, the average of four actinometers (two before and two after the quantum yield experiment) was used as a measure of the average light intensity. For absolute quantum yield experiments, the syringes employed in volumetric measurements were calibrated. No temperature correction for the actinometry was necessary. Over the wide band passes employed, the reported variations of ferrioxalate quantum yield with temperature (96) cancel.

Calibration of light intensity of linear quantum yield apparatus II

The linearity of light intensity of linear quantum yield apparatus II as a function of sector angle was determined. Three aluminum discs with 30.2, 47.0, and 61.5 degree sectors were used for the calibration. Actino-meter solutions (3.0 ml., 0.13 M ferrioxalute) in square Pyrex cells were irradiated with the 61.5, 47.0, and 30.2 degree sectors rotating for 13.8, 18.0, and 28.0 min., respectively. Two actinometers were run for each sector, and the average was used in the calculation of light intensity.

A plot of measured light intensity versus sector angle was linear (Figure 28). The calculated light intensities correcting for the sector angle were 3.34×10^{16}, 3.30×10^{16}, and 3.31×10^{16} quanta/sec. for the 61.5, 47.0, and 30.2 degree sectors, respectively.

Preparation of samples for quantum yield experiments

For all quantum yield measurements, a 3.00 ml. sample was used. In preparing the samples as described in the experimental, 1.00 ml. Becton Dickinson syringes were employed for volumetric measurements. Samples in square or round Pyrex cells were degassed by four freeze (liquid nitrogen), pump (pressure 10^{-5}mm.), thaw cycles and sealed with the torch under vacuum. The quartz cells for linear quantum yield apparatus I were degassed with argon for 3 min. including a 10 sec. period when argon was bubbled through the irradiation solution. After degassing the cells were sealed with Teflon needle valve stopcocks. A positive pressure of argon was maintained when the needle valves were closed. The degassed samples were irradiated to 5-10% completion unless otherwise specified.

The stability of Pyrex cells to freeze, pump, thaw cycles is a function of the solvent and technique. Non-polar solvents and *t*-butyl alcohol should be frozen slowly. Polar solvents except *t*-butyl alcohol should be frozen quickly. Isopropyl alcohol does not respond to either technique and must be teased. If isopropyl alcohol is allowed to freeze solid as a clear glass, the sample vessel will generally shatter sometime during the freeze. If the liquid nitrogen Dewar is periodically raised and lowered during the freeze, the isopropyl alcohol glass will crack and relieve the internal pressure. Quartz u.v. cells are only stable to

Figure 28. A calibration plot of linear quantum yield apparatus II;
           slope (9.20 ± 0.01) × 10^{13} quanta/sec./degree
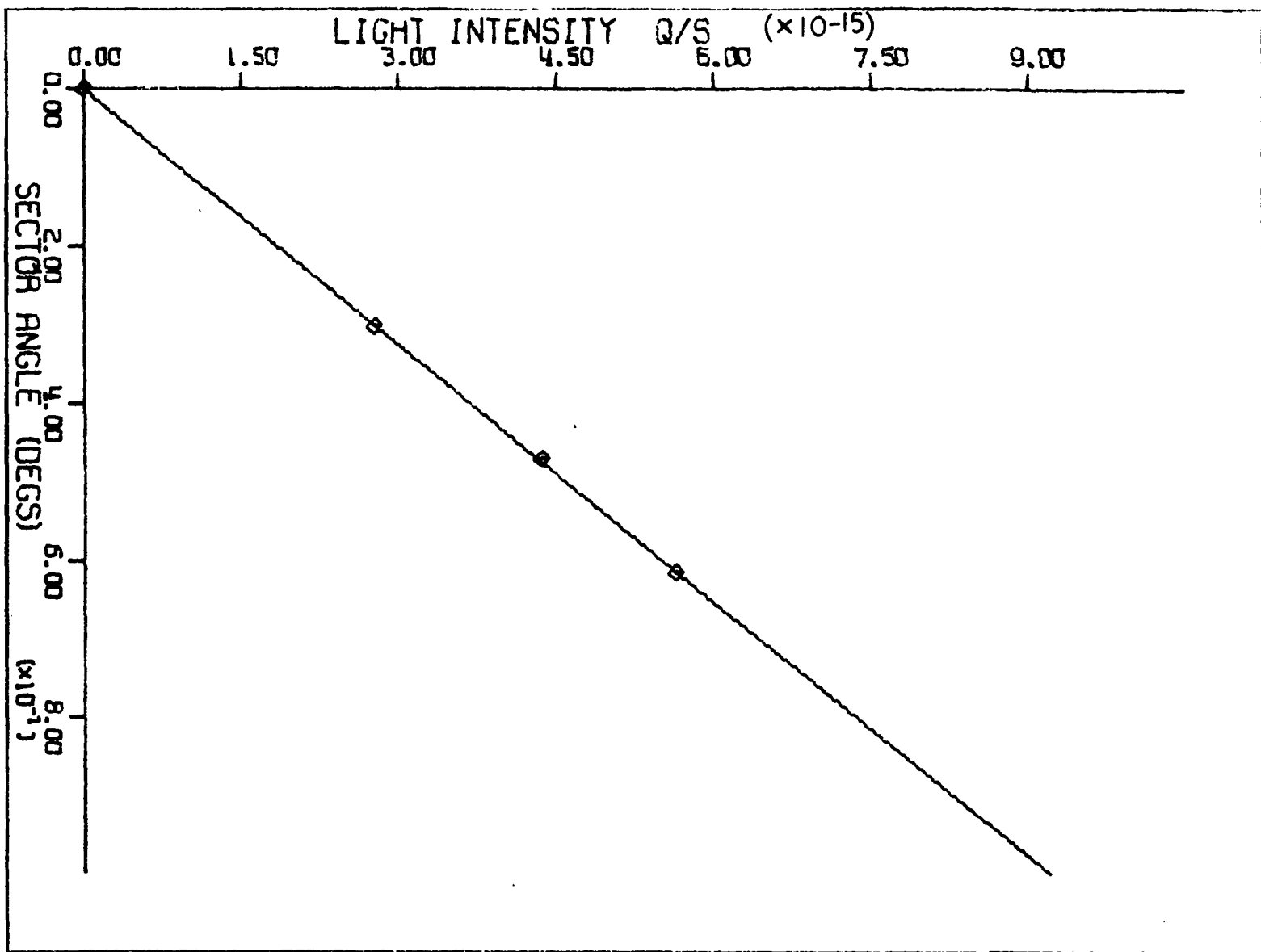
freeze thaw cycles when hexane is used as a solvent.[1]

Analytical procedure

An Aerograph model 1521 B gas chromatograph was used for product analysis of quantum yield experiments. The photocycloaddition products were analyzed relative to external piperonal on a 1/4 in. by 9 ft. column of 7% Dow Corning FS-1265, 0.5% Polyterg J-200 (Olin-Mathieson Chemical Co.), 92.5% 60/80 mesh Diatoport S (F & M Corp.) at 150°. The photo-rearrangement and photoreduction products were analyzed relative to external acetophenone on 1/4 in. by 9 ft. of 5% LAC-446, 0.5% Polyterg J-200, 94.5% non-acid wash 60/80 mesh Chromasorb P at 148°. On column injection was used for all analyses, and the injection temperature was maintained the same as the column temperature. The columns were eluted with helium at 80 cc/min. Relative areas were measured by disc integration and corrected for differences in thermal conductivity. The data reported is the average of two or three analyses. It was necessary to rebuild both analytical columns periodically to maintain peak efficiency. When analyzing for cycloadducts, it was sometimes necessary to evaporate as much as 3/4 of the solvent with a stream of prepurified nitrogen. Rearrangement products were analyzed without evaporation of solvent.

Symbols used in tables of data

The abbreviations and symbols used in the tables of quantum yield data are explained as follows: [K], concentration of 4,4-dimethyl-2-cyclo-

---

[1]The author wishes to thank Dr. Melvin Druelinger and Dr. Frank Klein for some of these observations about freeze thaw cycles.

hexenone; [O], concentration of 1,1-dimethoxyethylene; [Q], concentration

of quencher; [sens.], concentration of sensitizer; ϕ_o/ϕ_q, ratio of quantum

yield in the absence of quencher to the quantum yield in the presence of

quencher; ϕ_{sens}/ϕ_o, ratio of the quantum yield in the presence of sensi-

tizer to quantum yield in the absence of sensitizer.

Correction of data

The solutions irradiated in the rotating photochemical apparatus did

not absorb all the incident light because the band pass was too wide. The

experiments are still meaningful since the change in light absorption

during the irradiation period was very small. The data given in the

Experimental have been corrected to total absorption and corrected for any

light absorption by quencher. The corrected quantum yield for photocyclo-

addition in hexane obtained with the "wheel" compares favorably (within

2%) with the absolute quantum yield obtained with linear quantum yield

apparatus II.

The percent light absorbed by 4,4-dimethyl-2-cyclohexenone, di-*t*-

butyl nitroxide, and sensitizers was calculated from u.v. absorption

spectra and the lamp emission plot (97). The percent light absorbed by

0.20 M 4,4-dimethyl-2-cyclohexenone in benzene was calculated as follows.

The percent light emitted every 10 mμ from 410 to 310 mμ was calculated

from the lamp emission plot. The absorbance of 0.20 M 4,4-dimethyl-2-

cyclohexenone was determined every 10 mμ from 410 to 310 mμ. From the

absorbances the fraction of light absorbed every 10 mμ was calculated.

Adding the percent emission times fraction light absorbed every 10.mμ

over 11 wavelengths gave the percent light absorbed by 4,4-dimethyl-2-

cyclohexenone (93%). Stern-Volmer plots were corrected for quencher abosrption from a plot of percent light absorbed versus quencher concentration. The data for the plot was calculated as described above considering the absorption of both 4,4-dimethyl-2-cyclohexenone and di-*t*-butyl nitroxide. In calculating the percent light absorbed by sensitizers with fine structure in their absorption spectra, an estimated average absorbance over each 10 mμ was used.

Plots of quantum yield data

Least squares slopes and intercepts were calculated with the I.B.M. 360/65 computer for data which were represented by linear plots. The linear plots given in the figures were drawn by the simplotter from computer output tapes and represent the least squares lines.

Quantitative Study of Photocycloaddition and Photorearrangement

Absolute quantum yield of rearrangement in *t*-butyl alcohol

Two square Pyrex cells were each charged with 3.00 ml. of 0.301 M 4,4-dimethyl-2-cyclohexenone in *t*-butyl alcohol. The cells were freeze-thaw degassed, sealed, and irradiated individually in linear quantum yield apparatus II for 702 and 692 min., respectively. The absolute quantum yields of formation of 6,6-dimethylbicyclo[3.1.0]hexan-2-one and 3-isopropyl-2-cyclopentenone were 0.613×10^{-2} and 0.7373×10^{-2} (cell 1, temperature 218°) and 0.531×10^{-2} and 0.639×10^{-2} (cell 2, temperature 52°), respectively.

Effect of solvent on rearrangement

The data in Table 5 was obtained in three separate experiments. In each experiment rearrangement in t-butyl alcohol was used as a standard.

Experiment 1   Four square Pyrex cells [1, 2, 3, 4] were filled with 1.00 ml. of 0.906 M 4,4-dimethyl-2-cyclohexenone in 95% ethanol and the following quantities of 95% ethanol: cell 1, 2.00 ml.; cell 2, 1.56 ml.; cell 3, 1.43 ml.; cell 4, 1.29 ml. Enough twice distilled water was added to each cell to make the total volume 3.00 ml. Cell 6 was charged with 3.00 ml. of 0.304 M 4,4-dimethyl-2-cyclohexenone in methanol, and cell 7, with 3.00 ml of 0.301 M 4,4-dimethyl-2-cyclohexenone in t-butyl alcohol. The cells were freeze-thaw degassed, sealed, and irradiated in the "wheel" for 1329 min.

Experiment 2   Five square Pyrex cells [5, 7, 8, 13 and 14] containing 3.0 ml. quantities of 0.30 M 4,4-dimethyl-2-cyclohexenone in isopropyl alcohol, t-butyl alcohol, acetonitrile, benzene and hexane, respectively, were degassed and irradiated for 17.46 min.

Experiment 3   Six round Pyrex cells [7, 8, 9, 10, 11] containing 3.0 ml. quantities of 0.30 M 4,4-dimethyl-2-cyclohexenone in t-butyl alcohol, acetonitrile, N-methyl-2-pyrrolidone, 1,2-dimethoxyethane, ethyl acetate, and fluorobenzene, respectively, were degassed and irradiated for 1511 min.

Gas liquid chromatographic analysis gave the quantum yield ratios reported in Table 5. The two determinations of $\phi_{acetonitrile}/\phi_{t-butyl\ alcohol}$ (Experiments 2 and 3) differed by less than one percent. The

rearrangement product composition (46 ± 1% 6,6-dimethylbicyclo[3.1.0]-
hexane-2-one, 54 ± 1% 3-isopropyl-2-cyclopentenone) was independent of

solvent. In isopropyl alcohol formation of 4,4-dimethylcyclohexanone

accounted for 29% of the volatile products. Rearrangement occurred in

N-methyl-2-pyrrolidone; however, quantitative analysis was impossible

because the solvent overlapped badly with the products in the gas

chromatogram. In hexane and benzene a maximum relative quantum yield of

Table 5. Effect of solvent on photorearrangement[a]

cell	solvent	$\phi_{solvent}/\phi_{t\text{-butyl alcohol}}$	
1	70.8% ethanol, 29.2% water	1.45	
2	76.4% ethanol, 23.6% water	1.49	
3	81.5% ethanol, 18.5% water	1.57	
4	95% ethanol, 5% water	1.36	
5	isopropyl alcohol[b]	1.21	
6	methanol	1.02	
7	t-butyl alcohol	1.00	
8	acetonitrile	0.58	
9	N-methyl-2-pyrrolidone[c]	----	
10	1,2-dimethoxyethane	0.05	
11	ethyl acetate—	0.02	
12	fluorobenzene	0.02	
13	benzene	0.00	0.01[d]
14	hexane	0.00	0.01[d]

[a]Concentration of 4,4-dimethyl-2-cyclohexenone was 0.30 M.

[b]Photoreduction also occurs.

[c]Photorearrangement occurs.

[d]Relative quantum yield of destruction of 4,4-dimethyl-2-cyclo-
hexenone.

destruction of 4,4-dimethyl-2-cyclohexenone was determined.

Quenching of photorearrangement of 4,4-dimethyl-2-cyclohexenone by di-tertiarybutyl nitroxide

Eight calibrated round cells for the rotating photochemical apparatus were charged with 1.00 ml. of 0.906 M 4,4-dimethyl-2-cyclohexenone solution in t-butyl alcohol. One of the following quantities of 1.43 × 10^{-2} M di-t-butyl nitroxide was added to each vessel: 0 ml., 0.25 ml., 0.65 ml., 1.10 ml., 1.30 ml., 1.80 ml., 2.00 ml., 0 ml. Tertiary butyl alcohol was added to each vessel to make the total volume 3.00 ml. The vessels were degassed by four freeze-thaw cycles and sealed. Solutions 1, 2, and 8 were irradiated for 1344 min. and solutions 3, 4, 5, 6, and 7 were irradiated 1593 min. in the "wheel". Analysis of the solutions by quantitative gas-liquid chromatography on LAC-446 gave the results presented in Table 6 and plotted in Figure 16. The quantum yields, ϕ_o, for the two blank reactions were identical. Two of the samples were analyzed at 240° on 1/4 in. by 8.5 ft. of 10% Carbowax 20M. No significant high molecule weight peaks were observed which could be assigned to dimeric products.

A second quenching experiment was carried out in similar fashion. Six calibrated, round cells were each charged with 1.00 ml. of 0.912 M 4,4-dimethyl-2-cyclohexenone. The following quantities of 0.0918 M di-t-butyl nitroxide were added to cells 1, 2, 3, 4, 5, and 6, respectively: 0 ml., 0 ml., 0.50 ml., 1.02 ml., 1.50 ml., 2.00 ml. t-Butyl alcohol was added to each vessel to make the total volume 3.00 ml. After degassing, the cells were irradiated in the rotating photochemical apparatus as follows: cell 1, 2625 min.; cell 2, 1407 min.; cell 3, 3428 min.; cells

4, 5, and 6, 4178 min. The results from gas liquid chromatographic analysis are presented in Table 6 and plotted in Figure 16. The quantum yields, ϕ_o, for the two bland reactions differed by less than 1%. The final results were corrected for light absorption by di-t-butyl nitroxide.

Table 6.   Quenching photorearrangement by di-t-butyl nitroxide

[K]	[Q] $\times$ 10^3	% 6,6-dimethyl-bicyclo[3.1.0]hexan-2-one	% 3-isopropyl--2-cyclopentenone	ϕ_o/ϕ_q
0.302	1.18	46	54	1.01
0.302	3.09	46	54	1.08
0.302	5.24	47	53	1.16
0.302	6.17	45	54	1.17
0.302	8.55	46	54	1.20
0.302	9.51	46	54	1.27
0.304	15.3	47	53	1.38
0.304	30.6	47	53	1.83
0.304	45.9	47	53	2.16
0.304	61.3	45	55	3.00

Rearrangement in the presence of ferric dipivaloyl methane

A round Pyrex cell was charged with 1.00 ml. of 0.933 M 4,4-dimethyl-2-cyclohexenone in t-butyl alcohol and 2.00 ml. of 1.53 $\times$ 10^{-5} M ferric dipivaloyl methane in t-butyl alcohol. After freeze-thaw degassing, the cell was sealed and irradiated for 1429 min. in the "wheel". Gas chromatographic analysis gave ϕ_o/ϕ_q = 1.0 for 1.0 $\times$ 10^{-5} M ferric dipivaloyl methane.

<u>Data</u> <u>for</u> <u>plot</u> <u>of</u> <u>reciprocal</u> <u>quantum</u> <u>yield</u> <u>versus</u> <u>reciprocal</u> <u>of</u> <u>olefin</u>
<u>concentration</u> <u>for</u> <u>photocycloaddition</u> <u>in</u> <u>hexane</u>

Four round Pyrex cells were each charged with 1.00 ml. of 0.606 M
4,4-dimethyl-2-cyclohexenone in hexane and 1,1-dimethoxyethylene in
hexane as follows: cell 1, 2.00 ml. of 0.536 M; cell 2, 1.20 ml. of
0.536 M; cell 5, 0.75 ml. of 0.536 M; cell 6, 2.00 ml. of 0.147 M.
Enough hexane was added to each cell to make the total volume 3.00 ml.
After freeze-thaw degassing and sealing, the cells in numerical order
were irradiated in the rotating photochemical apparatus for 766, 474, 474,
and 372 min., respectively. Gas liquid chromatographic analysis gave the
quantum yields listed in Table 7 and plotted in Figures 12 and 13. The
product composition (42% oxetane, 27% *cis*-cyclobutane, 31% *trans*-cyclo-
butane) was independent of olefin concentration.

<u>Absolute</u> <u>quantum</u> <u>yield</u> <u>of</u> <u>photocycloaddition</u> <u>in</u> <u>hexane</u>

Four square Pyrex cells were charged with 1.00 ml. of 0.606 M 4,4-
dimethyl-2-cyclohexenone in hexane. To cells 3 and 4 was added 2.00 ml.
of 0.234 M 1,1-dimethoxyethylene in hexane and to cells 7 and 8 were
added 1.00 ml. of 0.234 M 1,1-dimethoxyethylene and 1.00 ml. of hexane.
After freeze-thaw degassing, cells 1, 2, 3, and 4 were irradiated in-
dividually in linear quantum yield apparatus II for 413, 488, 528, and
500 min., respectively. Gas-liquid chromatographic analysis gave the
absolute quantum yields of formation recorded in Table 7 and plotted in
Figures 12 and 13. The product composition (45% oxetane, 24% *cis*-cyclo-
butane, 31% *trans*-cyclobutane) was independent of olefin concentration.

Table 7. Photocycloaddition in hexane as a function of olefin concentration

cell	[O]	ϕ_{total} [a]	$1/\phi_{total}$	$1/\phi_{oxetane}$ [b]	$1/\phi_{cis}$ [b]	$1/\phi_{trans}$ [b]
1	0.357	0.0397	25.2	61.2	97.0	76.6
2	0.214	0.0239	41.8	97.6	159	133
3	0.149	0.0167	59.8	137	243	189
4	0.149	0.0173	57.8	128	242	191
5	0.134	0.0153	65.6	154	246	211
6	0.0982	0.0109	92.1	218	342	299
7	0.0747	0.0085	118	261	488	388
8	0.0747	0.0088	113	249	462	376

[a] Total quantum yield of formation.

[b] Reciprocal of quantum yield of formation for oxetane, cis-cyclobutane, and trans-cyclobutane.

Data for plot of reciprocal of quantum yield versus reciprocal of olefin concentration for photocycloaddition in benzene

The data for the plot of $1/\phi$ versus $1/[O]$ for photocycloaddition in benzene was obtained from three separate experiments. Ten calibrated round Pyrex cells were charged with 3.00 ml. of a benzene solution of 4,4-dimethyl-2-cyclohexenone and 1,1-dimethoxyethylene as indicated in Table 6. After freeze-thaw degassing and sealing, the solutions in numerical order were irradiated in the "wheel" for 685, 685, 926, 1127, 1127, 1127, 1500, 1500, 1500, 1500 min., respectively. Gas-liquid chromatographic analysis gave the reciprical of the quantum yields recorded in Table 8 and plotted in Figures 14 and 15. The product composition (13% oxetane, 35% cis-cyclobutane, 52% trans-cyclobutane) was independent of olefin concentration.

Table 8. Photocycloaddition in benzene as a function of olefin concentration

cell	[K]	[O]	1/[O]	ϕ_{total}	$1/\phi_{total}$[a]	$1/\phi_{oxetane}$[b]	$1/\phi_{cis}$[b]	$1/\phi_{trans}$[b]
1	0.200	0.772	1.37	0.0806	12.4	85.3	35.6	25.2
2	0.200	0.389	2.57	0.0445	22.5	152	65.0	44.2
3	0.203	0.264	3.79	0.0279	35.8	306	100	67.9
4	0.203	0.174	5.74	0.0184	54.5	467	152	104
5	0.203	0.132	7.57	0.0128	77.9	656	219	149
6	0.203	0.106	9.44	0.0102	96.7	738	277	187
7	0.20	1.0847	11.8	0.00870	115	930	327	219
8	0.206	0.0742	13.5	0.00752	133	986	384	253
9	0.206	0.0632	15.7	0.00662	151	1120	441	290
10	0.206	0.0529	18.9	0.00515	194	1700	550	365

[a]Reciprocal of total quantum yield of formation.

[b]Reciprocal of quantum yield of formation for oxetane, *cis*-cyclobutane, and *trans*-cyclobutane.

<u>Photocycloaddition</u> <u>and</u> <u>photorearrangement</u> <u>as</u> <u>a</u> <u>function</u> <u>of</u> <u>olefin</u> <u>con-</u>
<u>centration</u> <u>in</u> <u>t-butyl</u> <u>alcohol</u>

Eight, calibrated, square, Pyrex cells were each charged with 1.00

ml. of 0.756 M 4,4-dimethyl-2-cyclohexenone in t-butyl alcohol. A solution

of 1,1-dimethoxyethylene in t-butyl alcohol (0.298 M) was added to the

cells as follows: cell 1, 0.55 ml.; cell 2, 0.60 ml.; cell 3, 0.65 ml.;

cell 4, 0.70 ml.; cell 5, 0.90 ml.; cell 6, 1.10 ml.; cell 7, 1.45 ml.;

cell 8, 2.00 ml. Enough t-butyl alcohol was added to each cell to make

the total volume 3.00 ml. The cells were freeze-thaw degassed, sealed,

and irradiated in the "wheel" for 2165, 2165, 1530, 1530, 1066, 1066, 788,

and 357 min., respectively. Gas-liquid chromatographic analysis gave the

data listed in Table 10 and plotted in Figures 22 and 23. The solutions

were irradiated (40°) to 1-7% destruction of 4,4-dimethyl-2-cyclohexenone

and 20-35% destruction of 1,1-dimethoxyethylene. The cis-cyclobutane to

trans-cyclobutane product ratio (0.59) was independent of olefin concen-

tration.

Table 9. Photocycloaddition and photorearrangement in t-butyl alcohol as
a function of olefin concentration

cell	[K]	[0]	Photocycloaddition			Photorearrangement	
			$\phi \times 10^3$	$1/\phi_{cis}$	$1/\phi_{trans}$	$\phi \times 10^3$	$1/\phi$
1	0.252	0.0545	8.77	304	182	13.0	77.1
2	0.252	0.595	9.43	286	169	13.0	77.1
3	0.252	0.0645	16.7	160	94.7	12.5	80.0
4	0.252	0.0695	20.4	131	78.6	12.5	80.0
5	0.252	0.0893	43.5	62.5	36.4	11.4	88.0
6	0.252	0.109	59.5	45.2	26.7	11.0	90.6
7	0.252	0.144	95.2	28.1	16.8	10.6	94.2
8	0.252	0.199	176	15.1	9.1	8.06	123

Quenching of photocycloaddition in hexane by di-*t*-butyl nitroxide

Eight calibrated, round cells were each charged with 1.00 ml. of 0.606 M 4,4-dimethyl-2-cyclohexenone in hexane and 1.00 ml. of 0.303 M 1,1-dimethoxyethylene in hexane. Di-*t*-butyl nitroxide in hexane solution was added to the cells as follows: Cell 1, 0.50 ml. of .0152 M; cell 2, 1.00 ml. of .0152 M; cell 3, 0.50 ml. of 0561 M; cell 4, 1.00 ml. of .0561 M; cell 5, 0.75 ml. of 0.1296 M; cell 6, 1.00 ml. of .1296 M. Hexane was added to make the total volume in each cell 3.00 ml. Each cell was degassed by four freeze-thaw cycles and sealed. The solutions were irradiated in the rotating photochemical apparatus for the following periods: cells 1 and 2, 889 min.; cell 3, 1190 min.; cells 4, 5, and 6, 2381 min.; cells 7 and 8, 716 min. The blank solutions 7 and 8 were irradiated in the time interval 936 min. to 1652 min. to assure that they received an average quantity of light (assuming that the lamp intensity decreases with age). Gas liquid chromatographic analysis yielded the data recorded in Table 10 and plotted in Figures 19 and 20. The relative quantum yield of the two blank reactions differed by approximately 3%. The average value was used in computing ϕ_o/ϕ_q. The data was corrected for light absorption by di-*t*-butyl nitroxide.

In a second quenching experiment, two round Pyrex cells were each charged with 1.00 ml. of 0.612 M 4,4-dimethyl-2-cyclohexenone in hexane and 1.00 ml. of 0.303 M 1,1-dimethoxyethylene in hexane. To cell 1 was added 1.00 ml. of 0.251 M di-*t*-butyl nitroxide in hexane and to cell 2, 1.00 ml. of hexane. Both cells were freeze-thaw degassed, sealed, and irradiated in the "wheel" for 1166 min. Gas-liquid chromatographic

analysis gave (ϕ_o/ϕ_q) oxetane = 1.47, $(\phi_o/\phi_q)_{cis}$ = 2.34, and $(\phi_o/\phi_q)_{trans}$ = 1.61. The data is included in Table 10 and Figure 19 and 20.

Table 10.   Quenching photocycloaddition in hexane by di-t-butyl nitroxide

$[Q] \times 10^3$	total ϕ_o/ϕ_q	oxetane ϕ_o/ϕ_q	cis-cyclobutane ϕ_o/ϕ_q	$trans$-cyclobutane ϕ_o/ϕ_q
2.54	1.09	1.07	1.25	1.02
5.08	1.33	1.25	1.59	1.25
8.36	1.68	1.47	2.34	1.61
9.34	1.81	1.67	2.31	1.66
18.70	2.65	2.29	3.71	2.52
32.40	4.08	3.56	6.06	3.81
43.20	5.19	4.44	7.75	4.82

Quenching photocycloaddition in hexane by oxygen

Two quartz quantum yield cells were each charged with 2.00 ml. of 0.301 M 4,4-dimethyl-2-cyclohexenone and 1.00 ml. of 0.303 M 1,1-dimethoxyethylene. One cell was degassed with argon, and the other was flushed with oxygen using the same technique. The cells were irradiated for 1320 min. in linear quantum yield apparatus I equipped with a Corning CS-7-60 filter.[1] Gas-liquid chromatographic analysis gave $(\phi_o/\phi_q)_{total}$ = 3.74, $(\phi_o/\phi_q)_{oxetane}$ = 3.16, $(\phi_o/\phi_q)_{cis}$ = 5.37, $(\phi_o/\phi_q)_{trans}$ = 3.65.

Photocycloaddition in the presence of biacetyl

Two quartz quantum yield cells were charged with 1.00 ml. of 0.615 M 4,4-dimethyl-2-cyclohexenone in benzene and 1.00 ml. of 0.318 M 1,1-di-

[1]CS-7-60 filter transmits from 300 to 405 mμ at base, λ_{max} 355 mμ.

methoxyethylene in benzene. Benzene (1.00 ml.) was added to cell 1 and

0.0909 M biacetyl (1.00 ml.) in benzene was added to cell 2. After de-

gassing with argon, the cells were sealed with the Teflon needle valves

and irradiated simultaneous for 1440 min. in the double-beam linear

quantum yield apparatus I equipped with Corning CS-7-37 filter.[1] Analysis

of the solution containing biacetyl at 422 mμ indicated that 19% of the

biacetyl was destroyed during irradiation. Gas liquid chromatographic

analysis after approximately 3% reaction gave a value of ϕ_o/ϕ_q equal to

1.27 for cycloaddition to 1,1-dimethoxyethylene (total adduct formation).

One new product was observed in the chromatogram of the solution contain-

ing biacetyl. A control reaction indicated that this product probably

resulted from reaction of biacetyl with 1,1-dimethoxyethylene. The

presence of biacetyl did not change the normal cycloadduct composition.

Photocycloaddition in the presence of 1,3-cyclohexadiene

Six calibrated cells for the rotating photochemical apparatus were

each charged with 1.00 ml. of 0.609 M 4,4-dimethyl-2-cyclohexenone in

benzene and 1.00 ml. of 0.309 M 1,1-dimethoxyethylene. One of the follow-

ing quantities of 0.193 M 1,3-cyclohexadiene (Columbia, pure by g.l.p.c.)

in benzene was added to four of the cells: 1.00 ml., 0.75 ml., 0.50 ml.,

0.25 ml. Benzene was added to each of the cells to make the total volume

3.00 ml. After degassing by four freeze-thaw cycles, the samples were

irradiated for 1440 min. in the rotating photochemical apparatus. Gas-

liquid chromatographic analysis on FS-1265 gave the results listed in

---

[1]CS-7-37 filter transmits from 315 to 390 mμ at base, λ_{max} 360 mμ.

Table 11. One new product was observed for those solutions containing 1,3-cyclohexadiene. Control experiments and g.l.p.c. retention time (4.8 min. after *trans*-cyclobutane) indicated that the new product was a cycloadduct of 1,3-cyclohexadiene with 4,4-dimethyl-2-cyclohexenone. The amount of this new cycloadduct was dependent upon 1,3-cyclohexadiene concentration and was the predominant product at 0.0644 M 1,3-cyclohexadiene.

Table 11. Photocycloaddition in the presence of 1,3-cyclohexadiene

[K]	[O]	[Q]	ϕ_o/ϕ_q [a]
0.203	0.103	0.0644	1.12
0.203	0.103	0.0483	1.08
0.203	0.103	0.0322	1.04
0.203	0.103	0.0161	1.07

[a]Formation of normal cycloadducts.

Photocycloaddition in the presence of naphthalene

Two quartz cells were charged with 1.00 ml. of 0.609 M 4,4-dimethyl-2-cyclohexenone in hexane and 1.00 ml. of 0.303 M 1,1-dimethoxyethylene in hexane. To cell 1 was added 1.00 ml. of 0.152 M naphthalene in hexane and to cell 2, 1.00 ml. of hexane. After degassing with argon, the solutions were irradiated for 1420 min. in linear quantum yield apparatus I equipped with CS-7-60 filter and a 2.0 cm., 0.50 M naphthalene in benzene filter solution. Gas-liquid chromatographic analysis gave $(\phi_o/\phi_q)_{total}$ = 1.37, $(\phi_o/\phi_q)_{oxetane}$ = 1.44, $(\phi_o/\phi_q)_{cis}$ = 1.36, and $(\phi_o/\phi_q)_{trans}$ = 1.32.

Photocycloaddition in the presence of 1-methylnaphthalene

Two quartz cells were charged with 1.00 ml. of 0.612 M 4,4-dimethyl-2-cyclohexenone in benzene and 1.00 ml. of 0.306 M 1,1-dimethoxyethylene in benzene. To cell 1 was added 1.00 ml. of 0.0885 M 1-methylnaphthalene (Rutgerswerke-Aktiengesellschaft) and to cell 2, 1.00 ml. of benzene. After argon degassing, the cells were irradiated in linear quantum yield apparatus I equipped with CS-7-60 filter and a 2.0 cm., 0.50 M naphthalene in benzene filter solution. Gas chromatographic analysis gave $(\phi_o/\phi_q)_{total}$ = 1.14. The presence of 1-methylnaphthalene did not affect the product composition.

Photocycloaddition in the presence of p-terphenyl

A 10 ml. volumetric flask was charged with 0.507 g. of 4,4-dimethyl-2-cyclohexenone and 0.186 g. of 1,1-dimethoxyethylene and diluted to 10.0 ml. with benzene. A quartz cell was charged with 1 50 ml. of the enone-olefin solution and 1.50 ml. of benzene. A second 10 ml. volumetric flask was filled with 0.0709 g. of p-terphenyl and 5.00 ml. of enone-olefin solution. After diluting to 10.0 ml., 3.00 ml. was added to a second quartz cell. Both cells were degassed with argon and irradiated for 1440 min. in linear quantum yield apparatus I equipped with CS-7-60 filter and 2.0 cm. of 0.02 M p-terphenyl in benzene filter solution. Gas-liquid chromatographic analysis gave $(\phi_o/\phi_q)_{total}$ = 1.00. The presence of p-terphenyl did not change the product composition. The p-terphenyl (0.0174 g., 82%) was recovered by vacuum filtration after most of the solvent had been evaporated, m.p. 209-210°.

Quenching photocycloaddition and rearrangement by di-t-butyl nitroxide
in t-butyl alcohol

Eight, calibrated, square, Pyrex cells were charged with 1.00 ml. of

0.606 M 4,4-dimethyl-2-cyclohexenone in t-butyl alcohol and 1.00 ml. of

0.210 M 1,1-dimethoxyethylene in t-butyl alcohol. A t-butyl alcohol

solution of di-t-butyl nitroxide was added to the cells as follows: cell 3,

1.00 ml. of 0.150 M; cell 4, 0.80 ml. of 0.150 M; cell 5, 0.60 ml. of

0.150 M; cell 6, 1.00 ml. of 0.0582 M; cell 7, 0.50 ml. of 0.0582 M; cell

8, 0.25 ml. of 0.0582 M. Enough t-butyl alcohol was added to each to make

the total volume 3.00 ml. The cells were freeze-thaw degassed, sealed,

and irradiated in the "wheel" at 83° (cooling fan off). Cells 1 and 2

were irradiated for 839 min.; cells 3 and 4, 1450 min.; cells 5 and 6, 1236

min.; and cells 7 and 8, 1053 min. Gas chromatographic analysis gave the

results recorded in Table 12 and plotted in Figure 21. The two determi-

nations (cells 1 and 2) of ϕ_o for photocycloaddition differed by less than

3%, and the average was used in calculating ϕ_o/ϕ_q. Only solution 1 was

analyzed for rearrangement products and was used in calculating ϕ_o/ϕ_q.

Table 12. Quenching photocycloaddition and photorearrangement by di-t-
butyl nitroxide in t-butyl alcohol

[K]	[O]	[Q]	Rearr. ϕ_o/ϕ_q	cis-cyclobutane ϕ_o/ϕ_q	$trans$-cyclobutane ϕ_o/ϕ_q
0.202	0.0735	0.0049	1.18	1.59	1.28
0.202	0.0735	0.0097	1.34	2.00	1.46
0.202	0.0735	0.0194	1.51	2.10	1.32
0.202	0.0735	0.0301	1.42	2.89	1.67
0.202	0.0735	0.0401	1.75	3.96	2.22
0.202	0.0735	0.0501	1.98	5.16	2.74

Sensitization of photocycloaddition by triphenylamine and phenanthrene

Four calibrated, round cells were each charged with 1.00 ml. of 0.300 M 4,4-dimethyl-2-cyclohexenone in benzene and 1.00 ml. of 0.318 M 1,1-dimethoxyethylene in benzene. To cell 1 was added 1.00 ml. of 0.300 M triphenylamine in benzene; to cell 2, 1.00 ml. of 0.300 M phenanthrene in benzene; and to cells 3 and 4, 1.00 ml. of benzene. After freeze-thaw degassing, the solutions were irradiated in the rotating photochemical apparatus for 824 min. Gas-liquid chromatographic analysis gave the results recorded in Table 13. The product ratios were the same (± 1%) in the sensitized and unsensitized reactions.

Sensitization of photocycloaddition by triphenylene and thioxanthone

Three 10 ml. volumetric flasks were charged as follows: flask 1, 0.0914 g. 1,1-dimethoxyethylene, 0.1233 g. 4,4-dimethyl-2-cyclohexenone, 0.0693 g. triphenylene; flask 2, 0.0894 g. 1,1-dimethoxyethylene, 0.1269 g. 4,4-dimethyl-2-cyclohexenone, 0.0429 g. thioxanthone; flask 3, 0.0898 g. 1,1-dimethoxyethylene, 0.1358 g. 4,4-dimethyl-2-cyclohexenone. The solutions were diluted to 10.0 ml. with benzene. Two, calibrated, square, Pyrex cells were each filled with 3.00 ml. of solution from flask 1; two cells, with 3.00 ml. of solution from flask 2; and two cells, with 3.00 ml. of solution from flask 3. After freeze-thaw degassing, the cells were sealed and irradiated in the "wheel" for 1013 min. Gas-liquid chromatographic analysis gave the average data presented in Table 13. The two determinations of ϕ_o and $\phi_{thioxanthone}$ differed by less than one percent and the two determinations of $\phi_{triphenylene}$ differed by 14%. The product ratios were the same (± 1%) for the triphenylene sensitized and the un-

sensitized reactions.

Table 13. Sensitization of photocycloaddition[a]

Sensitizer	[sens.]	ϕ_{sens}/ϕ_o	E_T (kcal.)	% light absorbed by sensitizer
Triphenylamine	0.100	1.00	71	80
Triphenylene	0.0304	1.04	66	71
Thioxanthone	0.0202	0.261	65	98
Phenanthrene	0.100	0.601	62	65
Michler's ketone	0.0109	0.10[b]	61	99[c]

[a]The concentrations of 4,4-dimethyl-2-cyclohexenone and 1,1-dimethoxyethylene were both 0.10 M.

[b]For normal product formation.

[c]Initial light absorption.

Sensitization of photocycloaddition by Michler's ketone

Two round, Pyrex cells were each charged with 1.00 ml. of 0.312 M 1,1-dimethoxyethylene in benzene. To cell 1 was added 2.00 ml. of 0.303 M 4,4-dimethyl-2-cyclohexenone in benzene and to cell 2, 1.00 ml. of 0.303 M 4,4-dimethyl-2-cyclohexenone and 1.00 ml. of 0.0327 M 4,4'-bis-(dimethyl-amino)-benzophenone (Michler's ketone) in benzene. After freeze-thaw degassing, the cells were sealed and irradiated in the wheel for 932 min. The results of gas-liquid chromatographic analysis are reported in Table 13. The presence of Michler's ketone did not affect the normal product composition, however, two new products were formed (rention times 3.3 and 4.2 min. longer than *trans*-cyclobutane). The new products were the major products and were spectroscopically identified as the *meso-* and *dl*-pinacols.

One pinacol shows an O-H stretching vibration at 2.83 μ in the infrared

spectrum (CCl_4). The n.m.r. spectrum ($DCCl_4$) has methyl singlets at 0.95

(6H) and 1.03 δ (6H), a complex multiplet (8H) from 1.20 to 2.00 δ, a

singlet (2H) at 2.40 δ which disappears upon addition of deuterium oxide,

and an AB pattern (4H) at 5.77 and 5.80 δ ($^3J_{AB}$ = 10.0 Hz.). The mass

spectrum has a weak parent ion at m/e 250 and strong fragments at m/e 232

(m/e 250 - H_2O) and m/e 214 (m/e 232 - H_2O). The other pinacol has a

strong O-H stretching vibration at 2.92 μ in the infrared spectrum (CCl_4).

The n.m.r. spectrum shows two methyl singlets at 0.90 (6H) and 1.00 δ (6H),

a complex multiplet (8H) from 1.20 to 1.90 δ, a broad singlet (2H) at

2.15 δ which disappears upon addition of deuterium oxide, and a singlet

(4H) at 5.65 δ. The mass spectrum has a weak parent ion a m/e 250 and

major fragments at m/e 232 (m/e 250 - H_2O) and m/e 214 (m/e 232 - H_2O).

The effect of temperature on photocycloaddition and photorearrangement

The effect of temperature on photocycloaddition and photorearrangement

is presented in Tables 14 and 15. The data for these tables was compiled

from quantum yield experiments using the three instruments described. The

"wheel" provided data at 39-47° and 83°; linear quantum yield apparatus I,

at 28°; linear quantum yield apparatus II, at 47-52°.

Relative sensitized quantum yields of photocycloaddition of 1,1-dimethoxyethylene to isophorone and 4,4-dimethyl-2-cyclohexenone

Two quartz cells were each charged with 1.00 ml. of 0.300 M tri-

phenylamine in benzene and 1.00 ml. of 0.309 M 1,1-dimethoxyethylene in

benzene and 1.00 ml. of 0.309 M 1,1-dimethoxyethylene in benzene. To one

Table 14. Effect of temperature on cycloadduct composition[a]

temperature	solvent	% oxetane	% *cis*	% *trans*
28°	hexane	37	27	36
43°	hexane	42	27	31
47°	hexane	45	24	31
28°	benzene	9	35	57
43°	benzene	13	35	52

[a]The data is for 0.20 M 4,4-dimethyl-2-cyclohexenone, 0.10 M 1,1-dimethoxyethylene.

Table 15. Effect of temperature on quantum yield of photorearrangement

temperature	$\phi \times 10^2$
28°	1.71[a]
39°	1.67
43°	1.50
47°	1.30
47°	1.38
48°	1.35
52°	1.17
83°	0.94

[a]From the Ph.D. thesis of T. A. Rettig (21).

cell was added 1.00 ml. of 0.30 M 4,4-dimethyl-2-cyclohexenone and to the other cell was added 1.0 ml. of 0.30 M isophorone. After degassing with argon, the solutions were irradiated 1806 min. in linear quantum yield apparatus I equipped with a CS-7-37 filter. Gas-liquid chromatographic analysis gave $\phi_{isophorone}/\phi_{4,4-dimethyl-2-cyclohexenone}$ = 2.17.[1]

---

[1]The author wishes to thank Dr. Frank Klein for analysis of the isophorone sample.

Determination of the stability of di-t-butyl nitroxide

Two square, Pyrex cells were each charged with 1.00 ml. of 0.606 M

4,4-dimethyl-2-cyclohexenone in hexane and 1.00 ml. of 0.299 M 1,1-dimeth-

oxyethylene in hexane. To cell 1 was added 1.00 ml. of 0.0738 M di-t-

butyl nitroxide in hexane, and to cell 2, 1.00 ml. of hexane. After freeze-

thaw degassing, the cells were sealed and irradiated in the "wheel" (cell 1,

1320 min.; cell 2, 1013 min.).

Di-t-butyl nitroxide follows Beer's Law from 0.004 M to 0.074 M in

hexane solution between 500 and 430 mμ. The absorbances used in the Beer's

Law plot were the average absorbances for eight wavelengths between 500

and 430 mμ. The concentration of di-t-butyl nitroxide in cell 1 after

irradiation was determined by the average absorbance between 500 and 430

mμ and the Beer's Law plot. Only 2.4% of the di-t-butyl nitroxide was

destroyed during the irradiation.

Gas-liquid chromatographic analysis of the products from both cells

gave $(\phi_o/\phi_q)_{total} = 3.53$, $(\phi_o/\phi_q)_{cis} = 4.94$, $(\phi_o/\phi_q)_{trans} = 3.26$, and

$(\phi_o/\phi_q)_{oxetane} = 3.17$.

Determination of cycloadduct stability

To each of four, square, Pyrex cells was added 2.00 ml. of a hexane

solution containing 0.0282 M oxetane, 0.0292 M cis-cyclobutane, and 0.0293

M trans-cyclobutane. To cells 1 and 2 was added 1.00 ml. of hexane, and

to cells 3 and 4, 1.00 ml. of 0.125 M di-t-butyl nitroxide in hexane. All

the irradiation vessels were freeze-thaw degassed and sealed. Cells 1 and

3 were irradiated in the rotating photochemical apparatus for 1441 min.

Cells 2 and 4 were used as controls for the g.l.p.c. analysis. Analysis

of solution 1 and 2 indicated that 1.0% of the oxetane, 10.6% of the *cis*-cyclobutane, and 9.4% of the *trans*-cyclobutane were destroyed by irradiation. Analysis of solutions 3 and 4 indicated that 2.3% of the oxetane, 7.0% of the *cis*-cyclobutane, and 5.9% of the *trans*-cyclobutane were destroyed by irradiation in the presence of 0.0416 M di-*t*-butyl nitroxide.

Absence of ground state complexing

The u.v. spectrum of 4,4-dimethyl-2-cyclohexenone (0.0198 M in benzene) was observed with a Carey 14 spectrophotometer. The spectrum of 0.0198 M 4,4-dimethyl-2-cyclohexenone in the presence of 0.100 M 1,1-dimethoxyethylene in benzene showed no change in the extinction coefficient or the appearance of the n-π^* transition (λ_{max} 338 mμ) of 4,4-dimethyl-2-cyclohexenone.

BIBLIOGRAPHY

1. P. E. Eaton. Journal of the American Chemical Society 84: 2454. 1962.

2. E. J. Corey and S. Nozve. Journal of the American Chemical Society 86: 1652. 1964.

3. R. W. Guthrie, A. Philipp, Z. Valenta, and K. Wiesner. Tetrahedron Letters 1965: 2954. 1965.

4. P. E. Eaton. Journal of the American Chemical Society 84: 2344. 1962.

5. P. E. Eaton and W. S. Hurt. Journal of the American Chemical Society 88: 5671. 1966.

6. J. L. Ruhlen and P. A. Leermakers. Journal of the American Chemical Society 88: 5671. 1966.

7. J. L. Ruhlen and P. A. Leermakers. Journal of the American Chemical Society 89: 4944. 1967.

8. P. deMayo, J. P. Pete, and M. Tchir. Journal of the American Chemical Society 89: 5713. 1967.

9. E. Y. Y. Lam, D. Valentine, and C. S. Hammond. Journal of the American Chemical Society 89: 3482. 1967.

10. O. L. Chapman, P. J. Nelson, R. W. King, D. J. Trecker, and A. A. Griswold. Record of Chemical Progress 28: 167. 1967.

11. P. Yates, S. N. Ege, G. Büchi, and D. Knutsen. Canadian Journal of Chemistry 45: 2927. 1967.

12. S. N. Ege and P. Yates. Canadian Journal of Chemistry 45: 2933. 1967.

13. H. Ziffer, N. E. Sharpless, and R. O. Kan. Tetrahedron 22: 3011. 1966.

14. E. J. Corey, J. D. Bass, R. LeMahien, and R. B. Mitra. Journal of the American Chemical Society 86: 5570. 1964.

15. O. L. Chapman, T. H. Koch, F. Klein, P. J. Nelson, and E. L. Brown. Journal of the American Chemical Society 90: 1657. 1968.

16. P. deMayo, J. -P. Pete, and M. Tchir. Canadian Journal of Chemistry 46: in press. 1968.

17. P. Eaton. Tetrahedron Letters 1964: 3695. 1964.

18. P. Eaton and K. Lin. Journal of the American Chemical Society 86: 2087. 1964.

19. P. Eaton and K. Lin. Journal of the American Chemical Society 87: 2052. 1965.

20. E. J. Corey, M. Tada, R. LeMahieu, and L. Libit. Journal of the American Chemical Society 87: 2051. 1965.

21. T. A. Rettig. The photochemistry of some 2-cyclohexenones. Unpublished Ph.D. thesis. Ames, Iowa, Library, Iowa State University of Science and Technology. 1966.

22. E. Paterno and G. Chieffi. Gazzetta Chimica Italiana 39: 341. 1909.

23. G. Büchi, C. G. Inman, and E. S. Lipinski. Journal of the American Chemical Society 76: 4327. 1954.

24. N. C. Yang. Pure and Applied Chemistry 9: 591. 1964.

25. D. R. Arnold, R. L. Hinman, A. H. Glick. Tetrahedron Letters 1964: 1425. 1964.

26. N. C. Yang, J. I. Cohen, and A. Shani. Journal of the American Chemical Society 90: 3264. 1968.

27. G. Porter and P. Suppan. Transactions of the Faraday Society 62: 3375. 1966.

28. D. J. Patel and D. I. Schuster. Journal of the American Chemical Society 89: 184. 1967.

29. N. D. Yang, R. Loeschen, and D. Mitchell. Journal of the American Chemical Society 89: 5465. 1967.

30. N. C. Yang and R. Loeschen. Tetrahedron Letters 1968: 2571. 1968.

31. N. J. Turro, P. Wriede, J. C. Dalton, D. Arnold, and A. Glick. Journal of the American Chemical Society 88: 159. 1966.

32. O. L. Chapman, T. A. Rettig, A. A. Griswold, A. I. Dutlon, and P. Fitton. Tetrahedron Letters 1963: 2049. 1963.

33. H. E. Zimmerman, R. G. Lewis, J. J. McCullough, A. Padwa, S. W. Staley, and M. Semmelhack. Journal of the American Chemical Society 88: 159. 1966.

34. H. E. Zimmerman, R. G. Lewis, J. J. McCullough, A. Padwa, S. W. Staley, and M. Semmelhack. Journal of the American Chemical Society 88: 1965. 1966.

35. O. L. Chapman, J. B. Sieja, and W. J. Welstead, Jr. Journal of the American Chemical Society 88: 161. 1966.

36. H. E. Zimmerman and D. J. Sam. Journal of the American Chemical Society 88: 4905. 1966.

37. H. E. Zimmerman and J. Wilson. Journal of the American Chemical Society 86: 4036. 1964.

38. H. E. Zimmerman, R. D. Rieke, and J. R. Scheffer. Journal of the American Chemical Society 89: 2033. 1967.

39. H. E. Zimmerman and G. E. Samuelson. Journal of the American Chemical Society 89: 5973. 1967.

40. W. G. Dauben and W. A. Spitzer. Journal of the American Chemical Society 90: 802. 1968.

41. A. Butenandt, L. K. Posehmann, G. Failer, U. Schiedt, and E. Biekert. Justus Liebig's Annalen der Chemie 575: 123. 1952.

42. B. Nann, D. Gravel, R. Schorta, H. Wedrli, K. Schaffner, and O. Jeger. Helvetica Chimica Acta 46: 2473. 1963.

43. M. Pfau, R. Dulvo, and M. Vilkas. Academie des Sciences Comptes rendus 254: 1817. 1962.

44. I. A. Williams and P. Blandon. Tetrahedron Letters 1964: 257. 1964.

45. I. A. Williams and P. Blandon. Journal of the Chemical Society C: 2032. 1967.

46. T. Matsuura and K. Ogura. Journal of the American Chemical Society 88: 2602. 1966.

47. B. J. Ramey and P. D. Gardner. Journal of the American Chemical Society 89: 3949. 1967.

48. H. Nozaki, M. Kurita, and R. Noyori. Tetrahedron Letters 1968: 2025. 1968.

49. N. J. Turro. Molecular photochemistry. New York, New York, W. A. Benjamin. 1965.

50. P. deMayo, J. -P. Pete, and M. Tchir. Journal of the American Chemical Society 89: 5712. 1967.

51. S. L. Murov, R. S. Cole, and G. S. Hammond. Journal of the American Chemical Society 90: 2957. 1968.

52. R. S. Cooke and G. S. Hammond. Journal of the American Chemical Society 90: 2958. 1968.

53. R. S. H. Liu and J. R. Edman. Journal of the American Chemical Society 90: 213. 1968.

54. R. S. H. Liu and D. M. Gale. Journal of the American Chemical Society 90: 1897. 1968.

55. R. S. H. Liu. Journal of the American Chemical Society 90: 1899. 1968.

56. R. Kellogg. Journal of Chemical Physics 44: 411. 1966.

57. R. G. Bennett and P. J. McCartin. Journal of Chemical Physics 44: 1969. 1966.

58. D. F. Evans. Journal of the Chemical Society 1960: 1735. 1960.

59. S. Hosaka and S. Wakamatsu. Tetrahedron Letters 1968: 219. 1968.

60. G. S. Hammond, J. Saltiel, A. A. Lamola, N. J. Turro, J. S. Bradshaw, D. O. Cowan, R. C. Counsell, V. Vogt, and C. Dalton. Journal of the American Chemical Society 86: 3197. 1964.

61. D. F. Evans. Journal of the Chemical Society 1957: 1351. 1957.

62. D. R. Kearns, R. A. Hollins, A. U. Khan, R. W. Chambers, and P. Radlick. Journal of the American Chemical Society 89: 5455. 1967.

63. D. R. Kearns, R. A. Hollins, A. U. Khan, and P. Radlick. Journal of the American Chemical Society 89: 5457. 1967.

64. O. L. Chapman and R. W. King. Journal of the American Chemical Society 86: 1256. 1964.

65. A. S. Hussey and R. H. Baker. Journal of Organic Chemistry 25: 1434. 1960.

66. E. B. Reid and T. E. Gompf. Journal of Organic Chemistry 18: 661. 1953.

67. W. G. Herkstroeter, A. A. Lamola, and G. S. Hammond. Journal of the American Chemical Society 86: 4536. 1964.

68. H. E. Zimmerman and R. L. Morse. Journal of the American Chemical Society 90: 954. 1968.

69. P. Debye. Transactions of the Electrochemical Society 82: 265. 1942.

70. A. A. Lamola and G. S. Hammond. Journal of Chemical Physics 43: 2129. 1965.

71. F. Wilkinson and J. T. Dubois. Journal of Chemical Physics 39: 377. 1963.

72. P. D. Bartlett and P. S. Engel. Journal of the American Chemical Society 90: 2960. 1968.

73. G. Porter and F. Wilkinson. Proceedings of the Royal Society A264: 1. 1961.

74. National Research Council of the United States of America. International Critical Tables of Numerical Data, Physics, Chemistry and Technology 7: 211. 1930.

75. A. L. Buchachenko, M. S. Khloplyankina, and S. N. Dobryakov. Optics and Spectroscopy 22: 304. 1967.

76. A. P. Marchetti and D. R. Kearns. Journal of the American Chemical Society 89: 768. 1967.

77. P. J. Wagner. Journal of the American Chemical Society 89: 5715. 1967.

78. P. J. Wagner and I. Kochevar. Journal of the American Chemical Society 90: 2232. 1968.

79. L. A. Singer and G. A. Davis. Journal of the American Chemical Society 89: 158. 1967.

80. L. A. Singer and G. A. Davis. Journal of the American Chemical Society 89: 598. 1967.

81. A. K. Hoffman, A. M. Feldman, E. Gelblum, and W. G. Hodgson. Journal of the American Chemical Society 86: 639. 1964.

82. V. J. Shiner and C. R. Wasmuth. Journal of the American Chemical Society 1960: 2746. 1960.

83. G. M. Badger and R. W. L. Kimber. Journal of the Chemical Society 1960: 2746. 1960.

84. R. Huisgen, J. Sauer, and A. Hauser. Berichte der Deutsche Chemische Gesellschaft 91: 2366. 1958.

85. W. Tadros, A. B. Sakla, and M. S. Ishak. Journal of the Chemical Society 1958: 2631. 1958.

86. F. Scardiglia and J. D. Roberts. Journal of Organic Chemistry 23: 629. 1958.

87. W. Pelletier and D. M. Locke. Journal of Organic Chemistry 23: 131. 1958.

88. C. Hansch and C. F. Geiger. Journal of Organic Chemistry 23: 477. 1958.

89. H. Gilman and J. W. Diehl. Journal of Organic Chemistry 26: 2132. 1961.

90. H. K. Hall, Jr. Journal of the American Chemical Society 80: 6428. 1958.

91. C. F. H. Allen. Journal of the American Chemical Society 52: 2955. 1930.

92. Huang-Minlon. Journal of the American Chemical Society 68: 2487. 1946.

93. W. S. Johnson and H. Posvic. Journal of the American Chemical Society 69: 1361. 1947.

94. W. M. Moore and M. Ketchum. Journal of the American Chemical Society 84: 1368. 1962.

95. C. A. Parker. Proceedings of the Royal Society A220: 104. 1953.

96. C. G. Hatchard and C. A. Parker. Proceedings of the Royal Society A235: 518. 1956.

97. Southern New England Ultraviolet Co. Rayonet photochemical chamber reactor. Middletown, Conn., author. 1965.

ACKNOWLEDGMENTS

The author wishes to express his gratitude to his parents, Dr. and Mrs. Justin L. Koch, for their continuing interest and assistance in his education and development. They have given much that he might succeed.

The author wishes to thank Professor Paul Gassman for guidance during his undergraduate education. Professor Gassman initiated the author's interest in organic chemistry.

The author wishes to express his gratitude to Professor Orville Chapman for his encouragement and guidance during his graduate career. Professor Chapman provided the stimulating atmosphere necessary for the pursuit of creative research.

The author would also like to thank the other faculty members and his colleagues for their assistance and stimulating discussions throughout his graduate career.

The author wishes to acknowledge Mr. Ray Seymour and Mr. Lael Smith for the construction of the quantum yield instruments and Mrs. Marie Seastrand for her excellent typing of the manuscript.

The author acknowledges the National Science Foundation for their financial support of his graduate education from July 1964 to July 1968.

A publication originating in part from the research presented here is:

O. L. Chapman, T. H. Koch, F. Klein, P. J. Nelson, E. L. Brown. Journal of the American Chemical Society 90: 1657. 1968.

APPENDIX

Rate constants k_r and k_d' were calculated from equations 18.3 and 18.4 (Figure 18) as follows.

$$\phi_{rearrangement} = 0.014 = \frac{1.0 \times k_r}{k_r + k_d'}$$

$$\text{Stern-Volmer slope} = 30.1 = \frac{4.5 \times 10^9}{k_r + k_d'}$$

$$0.014 \ (k_r + k_d') = k_r$$

$$30.1 \ (k_r + k_d') = 4.5 \times 10^9$$

$$k_r = 2.1 \times 10^6 \ \text{sec.}^{-1} \qquad k_d' = 1.5 \times 10^8 \ \text{sec.}^{-1}$$

The rate constants and intersystem crossing efficiencies for photo-cycloaddition in hexane were calculated from equations 25.2, 25.3, 25.4, 25.7, 25.8, and 25.9 and definitions 25.10, 25.11, and 25.12 as follows.

For *cis*-cyclobutane

$$\phi_{cis} = 0.00142 = \frac{k_c [0.149] \phi_{ic}'}{k_d'' + k_c [0.149]}$$

$$\text{slope (Figure 13)} = 35.4 = \frac{k_d''}{\phi_{ic}' k_c}$$

$$\text{Stern-Volmer slope} = 157 = \frac{2.5 \times 10^{10}}{k_d'' + k_c [0.10]}$$

$$\phi_{ic}' = \frac{k_d''}{35.4 \ k_c}$$

$$0.00412 \ (k_d'' + k_c [0.149]) = k_c [0.149] \phi_{ic}'$$

$$0.00412 \ k_d'' \ + \ 0.00614 \ k_c \ = \ \frac{0.149 \ k_d''}{35.4}$$

$$0.000614 \ k_c \ = \ 0.00010 \ k_d''$$

$$6.14 \ k_c \ = \ k_d''$$

$$157 \ k_d'' \ + \ 15.7 \ k_c \ = \ 2.5 \times 10^{10}$$

$$964 \ k_c \ + \ 16 \ k_c \ = \ 2.5 \times 10^{10}$$

$$k_c \ = \ 2.6 \times 10^7 \ \ell/\text{mole/sec.} \qquad k_d'' \ = 1.6 \times 10^8 \ \text{sec.}^{-1} \quad \phi_{ic}' \ = \ 0.17$$

For *trans*-cyclobutane and oxetane

$$\phi_{\text{oxetane}} \ = \ 0.00756 \ = \ \frac{k_o[0.149]\phi_{ic}''}{k_d''' + (k_o + k_t)[0.149]}$$

$$\phi_{trans} \ = \ 0.00526 \ = \ \frac{k_t[0.149]\phi_{ic}''}{k_d''' + (k_o + k_t)[0.149]}$$

$$\text{slope (Figure 13)} \ = \ 18.6 \ = \ \frac{k_d'''}{\phi_{ic}'' \ k_o}$$

$$\text{Stern-Volmer slope} \ = \ 85.6 \ = \ \frac{2.5 \times 10^{10}}{k_d''' + (k_o + k_t)[0.10]}$$

$$\phi_{ic}'' \ = \ \frac{k_d'''}{18.6 \ k_o} \qquad\qquad \phi_{ic}'' \ = \ \frac{k_d'''}{28.9 \ k_t}$$

$$\frac{k_d'''}{18.6 \ k_o} \ = \ \frac{k_d'''}{28.9 \ k_t}$$

$$k_t \ = \ \frac{18.6 \ k_o}{28.9}$$

$$0.00756 \ k_d''' \ + \ 0.00113 \ k_o \ + \ 0.00113 \ k_t \ = \ 0.149 \ k_o \phi_{ic}''$$

$$0.0756 \ k_d''' \ + \ 0.00113 \ k_o \ + \ 0.00113 \ k_t \ = \ 0.00801 \ k_d'''$$

$$0.00113 \ k_o \ + \ 0.00113 \ k_t \ = \ 0.00045 \ k_d'''$$

$$k_o \ + \ k_t \ = \ 0.398 \ k_d'''$$

$$k_o \ + \ \frac{18.6 \ k_o}{28.9} \ = \ 0.398 \ k_d'''$$

$$4.13 \ k_o \ = \ k_d'''$$

$$85.6 \ k_d''' \ + \ 9.56 \ (k_o + k_t) \ = \ 2.5 \times 10^{10}$$

$$85.6 \times 4.13 \ k_o \ + \ 14.7 \ k_o \ = \ 2.5 \times 10^{10}$$

$$k_o \ = \ 6.8 \times 10^7 \ \ell/\text{mole}/\text{sec.} \qquad k_d''' \ = \ 2.8 \times 10^8 \ \text{sec.}^{-1}$$

$$k_t \ = \ 4.4 \times 10^7 \ \ell/\text{mole}/\text{sec.} \qquad \phi_{ic}'' \ = \ 0.22$$

The expression for reciprocal of total quantum of photocycloaddition was calculated for the mechanism in Figure 24 as follows.

By definition $\quad \phi_{total} \ = \ \dfrac{\text{rate of product formation}}{\text{intensity of the light}}$

$$\phi_{total} \ = \ \frac{(k_t + k_o)[0][^3K'] + k_c[0][^3K]}{I}$$

The steady state expressions for triplet states K^*, K, and K' are

$$[^3K^*] \ = \ \frac{I \ \phi_{ic}}{k_d' + k_{it} + k_{it}'} \qquad\qquad [^3K] \ = \ \frac{k_{it}[^3K^*]}{k_d'' + k_c[0]}$$

$$[^3K'] \ = \ \frac{k_{it}'[^3K^*]}{k_d''' + (k_o + k_t)[0]}$$

Hence $[^3K] = \dfrac{\phi'_{ic} I}{k''_d + k_c[0]}$ $[^3K'] = \dfrac{\phi''_{ic} I}{k'''_d + (k_o + k_t)[0]}$

Then $\phi_{total} = \dfrac{(k_t + k_o)[0]\phi''_{ic}}{k'''_d + (k_o + k_t)[0]} + \dfrac{k_c[0]\phi'_{ic}}{k''_d + k_c[0]}$

$$\phi_{total} = \dfrac{\left[(k_t + k_o)[0]\phi''_{ic}\right]\left[k''_d + k_c[0]\right] + \left[k_c[0]\phi'_{ic}\right]\left[k'''_d + (k_o + k_t)[0]\right]}{\left[k'''_d + (k_o + k_t)[0]\right]\left[k''_d + k_c[0]\right]}$$

$$1/\phi_{total} = \dfrac{1}{[0]}\left[\dfrac{k'''_d k''_d + k'''_d k_c[0] + k_o k''_d[0] + k_o k_c[0]^2 + k_t k''_d[0] + k_t k_c[0]^2}{k_t k''_d \phi''_{ic} + k_o k_d \phi''_{ic} + k_c k_d \phi'_{ic} + (\phi'_{ic} + \phi''_{ic})(k_o k_c[0] + k_c k_t[0])}\right]$$

$$1/\phi_{total} \sim \dfrac{1}{[0]} \times \left[\dfrac{k'''_d k''_d}{k_t k''_d \phi''_{ic} + k_o k''_d \phi''_{ic} + k_c k''_d \phi'_{ic}}\right]$$

Substituting for the known physical constants

$$1/\phi_{total} \sim 8.65 \times \dfrac{1}{[0]}$$

The calculated slope deviates from the experimental slope by approximately 1%.

The linearity of the Stern-Volmer plot for total photocycloadduct formation (Figure 19) was verified as follows.

$(\phi_o/\phi_q)_{cis} = 1 + \tau k_q[Q]$

$(\phi_o)_{cis} = (\phi_q)_{cis} + (\phi_q)_{cis}\,\tau k_q[Q]$

$(\phi_o/\phi_q)_{trans} = 1 + \tau' k_q[Q]$

$(\phi_o)_{trans} = (\phi_q)_{trans} + (\phi_q)_{trans}\,\tau' k_q[Q]$

$$(\phi_o/\phi_q)_{oxetane} = 1 + \tau'k_q[Q]$$

$$(\phi_o)_{oxetane} = (\phi_q)_{oxetane} + (\phi_q)_{oxetane} \, \tau'k_q[Q]$$

$$\frac{(\phi_o)_{cis} + (\phi_o)_{trans} + (\phi_o)_{oxetane}}{(\phi_q)_{cis} + (\phi_q)_{trans} + (\phi_q)_{oxetane}} = (\phi_o/\phi_q)_{total} =$$

$$1 + \frac{\left[(\phi_q)_{cis}\,\tau + (\phi_q)_{trans}\,\tau' + (\phi_q)_{oxetane}\,\tau'\right]k_q[Q]}{(\phi_q)_{cis} + (\phi_q)_{trans} + (\phi_q)_{oxetane}}$$

$$(\phi_o/\phi_q)_{total} \sim 95.5 \; [Q]$$

The slope calculated assuming the three triplet mechanism (Figure 24) deviates from the experimental slope by 2.5%.